GENETIC MANIPULATION OF THE MURINE CHOLINE TRANSPORTER

By

Mihaela H. Bazalakova

Dissertation

Submitted to the Faculty of the

Graduate School of Vanderbilt University

in partial fulfillment of the requirements

for the degree of

DOCTOR OF PHILOSOPHY

in

Neuroscience

May 2008

Nashville, Tennessee

Approved:

Professor Randy D. Blakely

Professor P. Jeffrey Conn

Professor Michael P. McDonald

Professor David Robertson

ACKNOWLEDGEMENTS

I would first like to extend sincere gratitude to my Ph.D. advisor, Dr. Randy Blakely, for his enthusiasm, mentorship, support, and encouragement. Thank you, Randy, for being an unwavering advocate for my scientific and professional development, and expecting me to do my best, always. I would also like to thank the members of my committee, Dr. Jeff Conn, Dr. Mike McDonald, and Dr. David Robertson for their time and insightful suggestions: Dr. Conn, for his involvement in my progress as the chair of my thesis committee, Dr. McDonald for his expertise and helpful commentary on behavioral experiments, and Dr. Robertson, not only for his knowledgeable input on cardiovascular experiments, but also for that early morning intercontinental phone call extending an offer of acceptance to Vanderbilt's M.D./Ph.D. program.

Several members of the Blakely lab deserve special thanks for their contributions to experimental design, techniques, data, and manuscript editing: Shawn Ferguson, Jane Wright, Valentina Savchenko, David Lund, and Alicia Ruggiero. My gratitude also to Uhna Sung for being a great "desk" mate – whether providing scientific advice, patiently tolerating my music, or being there for late night scientific and otherwise discussions. I have enjoyed getting to know all other members of the Blakely lab and thank them for making my time in the lab fun and productive.

Some of the most exciting findings of my Ph.D. thesis research are the product of collaborations. None of the cardiovascular studies would have been possible without the impressive expertise and enthusiasm of Martin Appalsamy. Nancy Keller, Laura Miller and Brett English have all contributed ideas and data on the project. John Allison is

always of great help and fun to chat with at the Behavioral core. Chris Olsen from Danny Winder's lab has enabled the cocaine addiction studies, while Yu Dong from John Dani's lab contributed dopamine microdyalisis data. My thanks to Allan Levey and Craig Heilman for expert advice and data generation on muscarinic receptors, and Ray Johnson for neurotransmitter measurements.

My sincere gratitude to Vanderbilt's Medical Scientist Training Program for providing me with the opportunity and financial support to pursue the M.D. and Ph.D. degrees.

Finally, I dedicate this thesis to my parents, Ivanka Bazalakova and Hristo Bazalakov, and my husband, Alesksandar Stanic, for their love, belief in me, and never-ending enthusiasm.

TABLE OF CONTENTS

LIST OF FIGURES

LIST OF ABBREVIATIONS

-/-	Homozygous knockout
+/-	Heterozygous
ACh	Acetylcholine
AChE	Acetylcholinesterase
ChAT	Choline acetyltransferase
CHT	Choline Transporter
DA	Dopamine
HACU	High-affinity choline uptake
HC-3	Hemicholinium-3
i.p.	Intraperitoneal
KRH	Kreb's-Ringer's-HEPES buffer
mAChR	Muscarinic acetylcholine receptor
nAChR	Nicotinic acetylcholine receptor
NAc	Nucleus accumbens
NMJ	Neuromuscular junction
SCG	Superior cervical ganglia
SNP	Single nucleotide polymorphism
Tg	Transgenic
TRF	Transferrin receptor
UTR	Untranslated region
VAChT	Vesicular acetylcholine transporter

CHAPTER I

THE HIGH-AFFINITY CHOLINE TRANSPORTER – A CRITICAL PROTEIN FOR SUSTAINING CHOLINERGIC SIGNALING

CHT Function and Regulation

Cholinergic Neuroanatomy

The presynaptic high-affinity choline transporter (CHT) derives its physiological importance from its support of the synthesis of the neurotransmitter acetylcholine (ACh). ACh plays an important role in both central and peripheral nervous systems, where it maintains vital biological functions such as motor function, attention, memory, reward, and autonomic regulation (Dani, 2001; Fink-Jensen et al., 2003; Kitabatake et al., 2003; Misgeld et al., 2002; Perry et al., 1999b; Sarter and Bruno, 1997; Wess, 2004; Winkler et al., 1995). Major cholinergic nuclei and their neuroanatomical connections include (Fig. 1): septo-hippocampal projections, supporting learning and memory processes; basal forebrain – cortical projections, supporting attention and arousal; large aspinal cholinergic interneurons, which modulate striatal function and are increasingly implicated as modulators of movement, attention, and reward processes; medial habenula – interpeduncular nucleus projections; and mesopontine tegmental nuclei, including the pedunculopontine (PPT) and laterodorsal (LDT) tegmental nuclei, projecting to various brain structures, including the basal forebrain and the ventral tegmental area (VTA), the latter connections being strongly implicated in reward and addiction. In addition, brainstem and spinal cord cholinergic motor neurons support movement, while

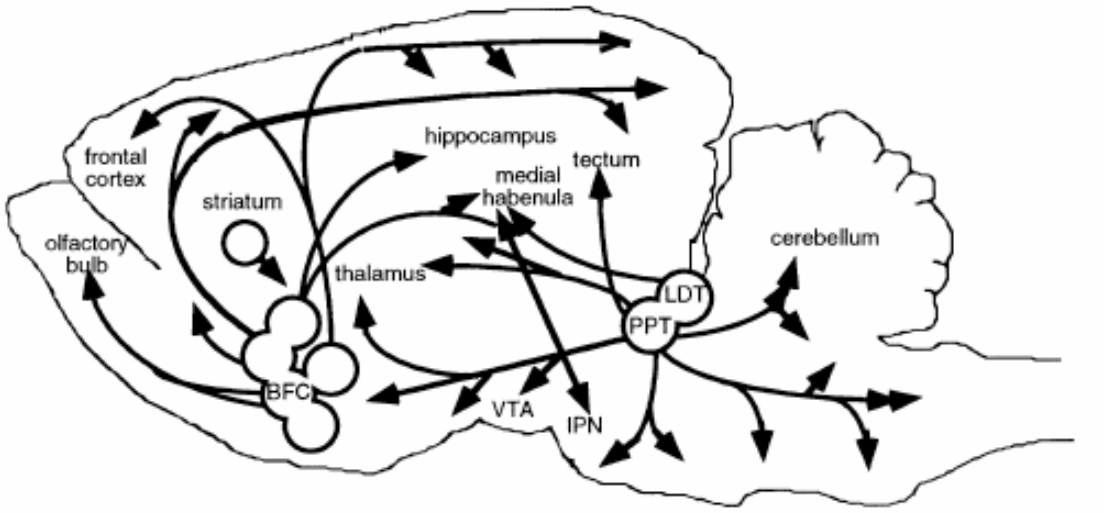

Figure 1. Cholinergic pathways in the brain. The basal forebrain complex includes the diagonal band nuclei, nucleus basalis, substantia inominata, and magnocellular preoptic nucleus and provides cholinergic innervation to the cortex. The medial septum, habenula, and mesopontine tegmentum (LDT, PPT) originate major cholinergic projections to the hippocampus, IPN, and midbrain (VTA) respectively. Cholinergic interneurons are found in the striatum, nucleus accumbens, olfactory tubercle, and the islands of Calleja. BFC, basal forebrain complex; IPN, interpeduncular nucleus; LDT, laterodorsal tegmental nucleus; PPT, pedunculopontine tegmental nucleus; VTA, ventral tegmental area. Adapted from Piccioto et al. (2002).

cholinergic cells in the intermediolateral column of the spinal cord participate in autonomic nervous system regulation.

The Cholinergic Synapse

The turnover of ACh in cholinergic neurons involves a well-studied cycle of synthesis, release, hydrolysis, and reuptake (Fig. 2). The enzyme choline acetyltransferase (ChAT) synthesizes ACh in the axoplasm from the precursors choline and acetyl coenzymeA (acetyl-CoA). ChAT is not believed to be saturated with the substrate choline, as presynaptic levels of choline are significantly lower than ChAT Km. ACh is packaged into synaptic vesicles by the vesicular ACh transporter (VAChT), and released into the synaptic cleft upon depolarization of the neuron by an action potential. Once released in the synaptic cleft, ACh interacts with pre and post-synaptic nicotinic (nAChR) and muscarinic (mAChR) receptors and is inactivated enzymatically, through hydrolysis, into acetate and choline by the enzyme acetylcholinesterase (AChE). The choline released by hydrolysis is recycled at the presynaptic terminal via a distinct, carrier-mediated mechanism of high-affinity choline uptake (HACU). Low affinity choline uptake (LACU) transporters are found in all cell types, are not enriched in nerve terminals, and take up choline to be used in phosphatidylcholine synthesis in order to support cellular membrane maintenance and repair needs (Bussiere et al., 2001). Cholinergic neurons have an added requirement, elaborated in the presynaptic terminal, for choline, which they cannot synthesize de novo, but need as a substrate for ACh synthesis. This need is supported by the HACU mechanism.

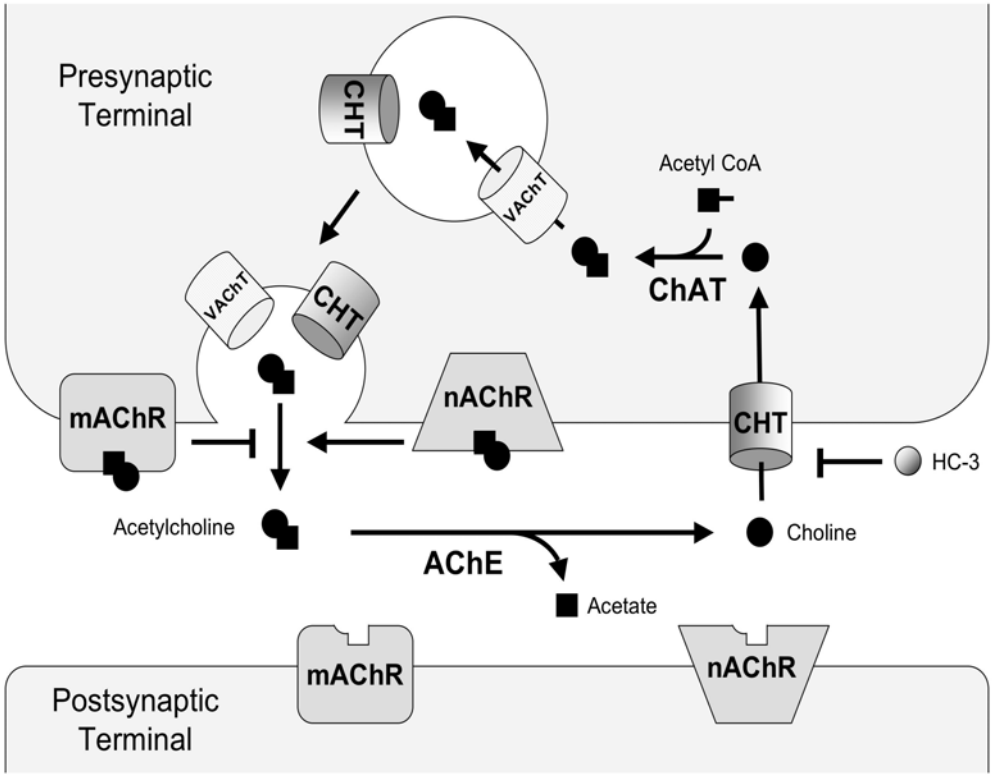

Figure 2. The cholinergic synapse. The enzyme choline acetyltransferase (ChAT) synthesizes ACh in the axoplasm from the precursors choline and acetyl coenzymeA (acetyl-CoA). ACh is then packaged into synaptic vesicles by the vesicular ACh transporter (VAChT), and released into the synaptic cleft upon neuronal depolarization. In the synaptic cleft, ACh interacts with pre- and post-synaptic nicotinic (nAChR) and muscarinic (mAChR) receptors. Presynaptic mAChRs exert an autoinhibitory effect on ACh release, whereas presynaptic nAChR activation increases ACh release. Synaptic ACh is hydrolyzed into acetate and choline by the enzyme acetylcholine esterase (AChE). Choline is then transported into the presynaptic terminal by the HC-3 sensitive, high-affinity choline transporter (CHT), in the rate-limiting step of subsequent ACh synthesis.

High-Affinity Choline Uptake (HACU) and Cholinergic Neurotransmission

Selective blockade or genetic ablation of the rate-limiting step in ACh synthesis - CHT-mediated HACU - reduces ACh synthesis and release *in vitro* (Fig. 3), and impairs cholinergic transmission at central and peripheral synapses *in vivo* (Ferguson et al., 2004; Guyenet et al., 1973; Macintosh et al., 1956; Maire and Wurtman, 1985). Breakdown of cholinergic signaling at the neuromuscular junction (NMJ) due to CHT dysfunction leads to lethal respiratory paralysis and demonstrates the essential physiological role of CHT (Ferguson et al., 2004; Schueler, 1955).

The HACU process was described as early as 1961 (Birks and McIntosh, 1961). Subsequent work showed it is present primarily in cholinergic nerve terminals (Kuhar and Murrin, 1978a; Kuhar et al., 1973), where it takes up choline specifically for the biosynthesis and replenishment of ACh pools (Blusztajn, 1998; Bussiere et al., 2001; Haga and Noda, 1973; Kuhar et al., 1973; Yamamura and Snyder, 1972). HACU displays affinity for choline in the lower micromolar range (K_m^{HACU} =1-5 µM, versus K_m^{LACU}=50 µM) is a Na^+- and Cl^--dependent process (versus Na^+/Cl^-independent LACU), and is inhibited by the selective and competitive antagonist hemicholinium-3 (HC-3) (K_i^{HACU} = 10-100 nM, versus Ki^{LACU}=50 µM) (Kuhar and Murrin, 1978a; Simon and Kuhar, 1976; Yamamura and Snyder, 1972; Yamamura and Snyder, 1973). Studies described below with CHT knockout (-/-) mice demonstrate that HACU is mediated by CHT, whereas earlier studies demonstrated that CHT provides the rate-limiting step in ACh synthesis (Holden et al., 1975; Jope, 1979b; Kuhar and Murrin, 1978a; Simon and Kuhar, 1975; Tucek, 1985a). Consequently, specific inhibition of CHT by HC-3 impairs ACh synthesis

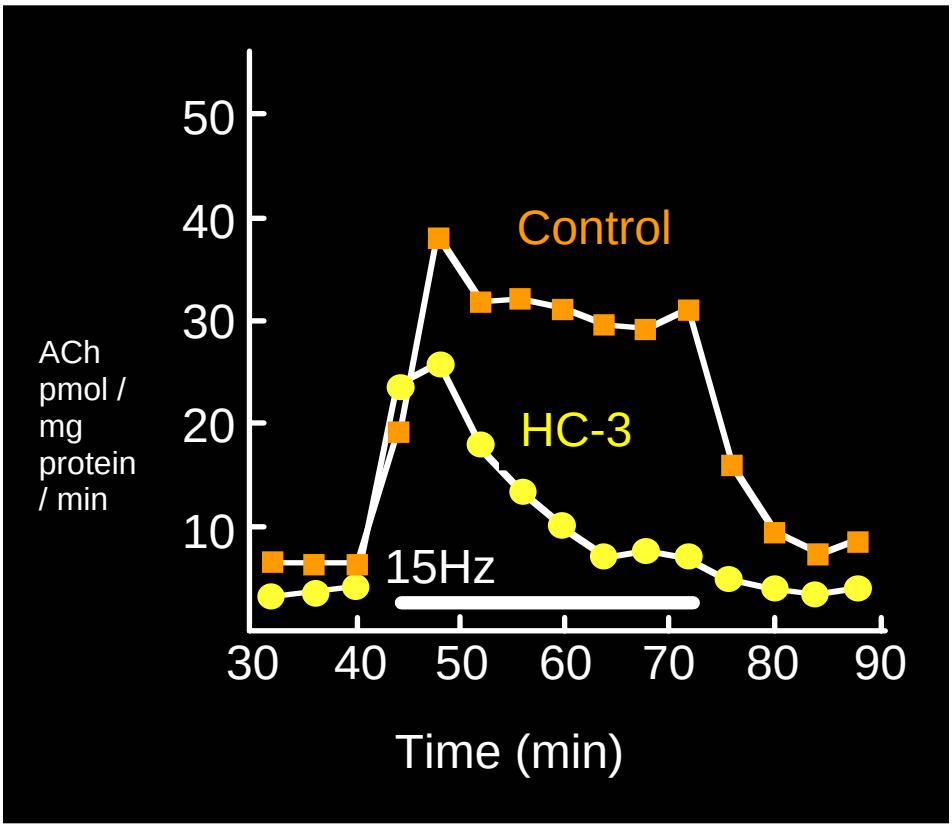

Figure 3. High affinity choline uptake is essential to maintain evoked ACh synthesis and release. Rat striatal slices were incubated in the presence (HC-3) or absence (control) of 5 μM HC-3, a specific inhibitor of CHT-mediated high affinity choline uptake. In the presence of HC-3, ACh release could not be sustained during a 15Hz electrical stimulation. Adapted from Maire et al. (1983).

and release, thus compromising cholinergic neurotransmission (Guyenet et al., 1973; Murrin et al., 1977).

Pharmacological and Behavioral Modulation of HACU

CHT-mediated HACU is highly regulated by neuronal activity (Simon and Kuhar, 1975), but the molecular mechanisms of this regulation remained unclear until recently. Traditionally, [^{3}H]HC-3 ligand binding assays have been used to quantitatively determine CHT levels in sealed nerve terminal preparations (synaptosomes) or tissue sections (Sandberg and Coyle, 1985b; Vickroy et al., 1985; Vickroy et al., 1984). Using uptake and binding techniques, studies have shown that CHT-mediated HACU is regulated by neuronal activity *in vitro* and *in vivo* (Murrin and Kuhar, 1976). Accordingly, *in vivo* administration of drugs that affect the turnover and release of ACh (both indices of cholinergic activity) results in altered HACU and [^{3}H]HC-3 binding measured *in vitro*. For example, intraperitoneal (i.p.) administration of the muscarinic antagonist atropine, which induces cholinergic firing and ACh release, leads to increases in HACU V_{max} and [^{3}H]HC-3 binding in synaptosomes from rat striatum and hippocampus (Goldman and Erickson, 1983; Lowenstein and Coyle, 1986). In contrast, treatment with agents that inhibit cholinergic signaling, such as pentobarbital, result in lower ACh turnover, HACU, and [^{3}H]HC-3 binding (Lowenstein and Coyle, 1986).

Additional studies have employed behavioral stimuli, such as training to criterion in a T maze or an 8 arm radial maze, to activate cholinergic neurons and assess CHT response in the whole animal (Burgel and Rommelspacher, 1978; Wenk et al., 1984). The data demonstrate increases in synaptosomal HACU V_{max} from behaviorally trained versus

non-trained animals, remarkably lasting more than 20 days beyond the final training or testing session (Wenk et al., 1984). In a modern refinement of these studies, Apparsundaram and colleagues have examined CHT-mediated HACU in a behavioral paradigm that specifically taxes attentional effort and therefore depends on intact cortical cholinergic circuits (Apparsundaram et al., 2005; McGaughy et al., 1996). The authors trained rats in a cognitive vigilance task (CVT), which required the animals to detect the presence or absence of a light stimulus and respond by making the correct choice between two levers. Control animals were either not subjected to the behavioral paradigm (non-performing (NP) rats) or were trained in a simple reaction time task (SRTT), where only the correct lever was present, thus decreasing demands on attentional processing. HACU V_{max} in synaptosomes from the right medial prefrontal cortex (mPFC), but not striatum, was accelerated in CVT compared to SRTT and NP control rats (Apparsundaram et al., 2005). These results support a coupling of cholinergic signaling, demonstrated by increased extracellular ACh release in the mPFC of CVT-performing rats, and CHT capacity (Arnold et al., 2002).

Two explanations for a mechanism underlying activity-dependent changes in HACU V_{max} have been proposed: a change in the intrinsic rate of CHT activity (catalytic activation) or a change in the number of CHTs at the plasma membrane (altered trafficking). Although changes in [^{3}H]HC-3 binding have commonly been interpreted in the literature as an index of changing CHT protein levels, several studies suggest that alterations in [^{3}H]HC-3 binding may reflect not only changes in the number of binding sites (B_{max}) but also affinity for the ligand (K_D) (Lowenstein and Coyle, 1986). Studies have shown Ca^{2+}-dependent, ATP-induced changes in [^{3}H]HC-3 binding in membrane

preparations, which appear to be primarily due to changes in K_D (Chatterjee and Bhatnagar, 1990; Saltarelli et al., 1990). This interpretation is supported by the use of membrane preparations which, unlike synaptosomal sealed nerve terminals, do not contain intracellular reserve pools of CHT that can be trafficked to the plasma membrane (Chatterjee and Bhatnagar, 1990; Saltarelli et al., 1990). Therefore, any differences in [^{3}H]HC-3 binding in membrane preparations are likely the result of conformational changes of the CHT protein already present in the plasma membrane, due to phosophorylation or other protein modifications. The cloning and characterization of CHT have provided new tools, such as CHT-specific antibodies, which can be used to affect a more direct and reliable quantification of CHT protein levels at the plasma membrane.

Cloning the CHT Gene

CHT genes have now been identified in *Caenorhabditis elegans* (Cho-1) (Okuda et al., 2000a), torpedo (CTL1) (O'Regan et al., 2000), rat (CHT1) (Okuda et al., 2000a), human (hCHT) (Apparsundaram et al., 2000; Okuda and Haga, 2000), and mouse (mCHT) (Apparsundaram et al., 2001b). The mCHT cDNA encodes a protein of 580 amino acids, with a molecular mass of approximately 63 kDa. Sequence analysis of mCHT demonstrates a 93% and 98% amino acid identity with the human and rat orthologs (Apparsundaram et al., 2001b), and identifies the gene as a member of the Na^+/glucose solute carrier superfamily 5 (SLC5). Analysis of the amino acid sequence predicts a topology of thirteen transmembrane domains, an extracellular consensus site for N-linked glycosylation, and several cytoplasmic protein kinase A (PKA) and protein

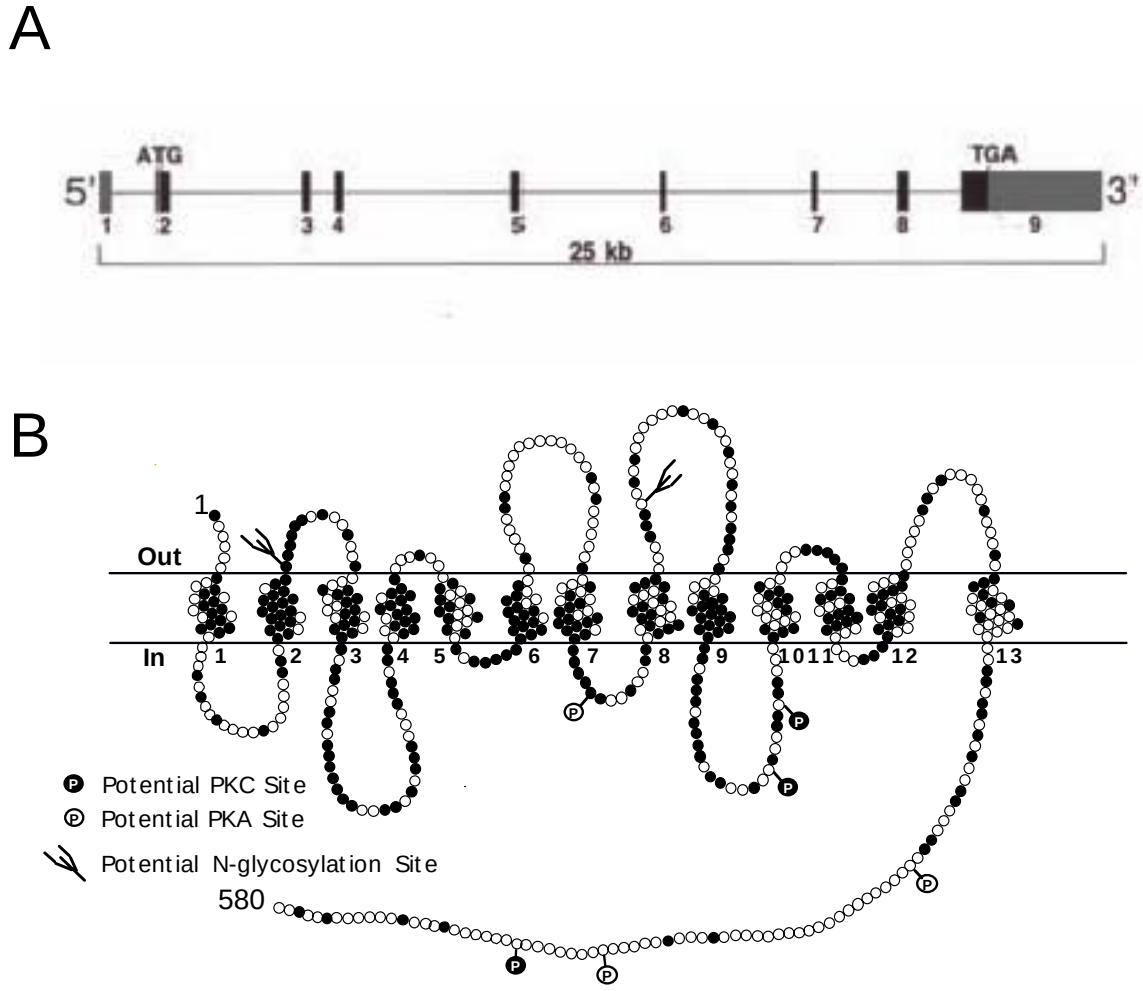

Figure 4. CHT gene and protein structures. (A) The hCHT gene is located on chromosome 2 and contains 9 exons. (**B)** The mCHT cDNA encodes a protein of 580 amino acids, with a molecular mass of approximately 63 kDa. Analysis of the amino acid sequence predicts a topology of thirteen transmembrane domains, an extracellular consensus site for N-linked glycosylation, and several cytoplasmic protein kinase A (PKA) and protein kinase C (PKC) phosphorylation sites (Apparsundaram et al. 2001a). Adapted from Ferguson and Blakely (2004).

kinase C (PKC) phosphorylation sites (Fig. 4) (Apparsundaram et al., 2001a); for review see (Ferguson and Blakely, 2004). Electron microscopy (EM) immunogold labeling studies, using antibodies directed towards COOH-terminal epitopes, support a cytoplasmic localization of this domain (Ferguson et al., 2003), whereas epitope-tagging efforts confirm an extracellular localization of the N-terminus (Ribeiro et al., 2005). In addition to the generation of polyclonal and monoclonal CHT-specific antibodies, the cloning of mCHT has led to the generation of a CHT knockout mouse (Ferguson et al., 2004) – both useful new tools for the study of *in vivo* CHT function and regulation.

CHT Provides the Molecular Basis of HACU Regulation

Prior to the availability of antibodies, [3H]HC-3 autoradiography in brain slices or binding in brain membrane preparations was used to assess HACU localization. These techniques demonstrated significant overlap between HACU and known cholinergic terminals, such as striatum, cortex, and hippocampus (Sandberg and Coyle, 1985a; Vickroy et al., 1984). Zahalka et al. (1993) showed that [3H]HC-3 binding in the rat cerebral cortex, striatum, and hippocampus generally reached adult levels around the 5th to 6th postnatal week (Zahalka et al., 1993).

The generation of CHT-specific antibodies allowed for the first detailed characterization of CHT expression and subcellular localization. Several studies utilizing immunoblotting and immunofluorescence have demonstrated that CHT is expressed predominantly in cholinergic terminals (Ferguson et al., 2003; Kus et al., 2003; Lips et al., 2002; Misawa et al., 2001), although CHT mRNA and protein expression have also been detected in human keratinocytes, rat tracheal epithelia, lung bronchial epithelial

cells, and human T lymphocytes (Fujii et al., 2003; Kawashima and Fujii, 2003; Pfeil et al., 2003b; Proskocil et al., 2004).

Within cholinergic terminals, where HACU activity predominates and the transported choline is specifically targeted for ACh synthesis (Bussiere et al., 2001), CHT is localized in at least two distinct pools: an intracellular vesicular pool and a plasma membrane pool (Ferguson and Blakely, 2004; Ferguson et al., 2003). Immunogold labeling and EM analysis in striatal cholinergic terminals and the NMJ reveal that the majority of CHT is present on intracellular small, clear synaptic vesicles (Ferguson et al., 2003; Nakata et al., 2004). At the NMJ, less than 5% of CHT immunoreactivity is associated with the plasma membrane (Nakata et al., 2004). Parallel biochemical approaches utilizing subcellular fractionation and velocity gradient purification confirm an enrichment of CHT in synaptic vesicles that are also enriched for synaptic vesicle proteins such as synaptophysin and VAChT, and can be demonstrated to contain ACh (Ferguson et al., 2003).

The pattern of synaptic vesicle CHT enrichment lends strong support to the hypothesis that CHT activity may be regulated, at least in part, by trafficking of CHT intracellular reserves to the plasma membrane under conditions of demand on cholinergic neurotransmission. Indeed, high potassium *in vitro* depolarization of striatal synaptosomal preparations (which leads to ACh release and hence mimicks *in vivo* neuronal activity) results in increased HACU V_{max}, mediated largely, but not entirely, by redistribution of CHT from the intracellular reserve pool (Ferguson et al., 2003). Interestingly, while all CHT-positive synaptic vesicles also contain VAChT, only CHT appears to be retained at the plasma membrane for a period of time following synaptic

terminal depolarization (Ferguson et al., 2003). The presence of dileucine-like internalization motifs in the cytoplasmic C-terminus of CHT and the transporter's largely intracellular localization suggest that specific mechanisms must exist to allow stabilization of CHT at the plasma membrane for prolonged enhancements of HACU. Indeed, experimental evidence from site-directed mutagenesis followed by *in vitro* biochemical studies in transfected cell lines, as well as primary neuronal cultures, points to clathrin-mediated endocytosis as a highly efficient mechanism for CHT trafficking (Ribeiro et al., 2003; Ribeiro et al., 2005). Gates and colleagues have used immunoprecipitation, immunoblotting and synaptosomal biotinylation techniques to reveal that PKC and protein phosphatase 2A (PP2A) induced alterations in CHT trafficking are paralleled by changes in CHT phosphorylation, although specific mechanisms linking phosphorylation with trafficking capacity are as yet unclear (Gates et al., 2004).

Finally, the Sarter and Apparsundaram labs elegantly combined *in vivo* behavioral paradigms (specifically taxing attentional cholinergic circuits) with *in vitro* synaptosomal subcellular fractionation (allowing quantification of CHT in the plasma membrane), in order to provide an explanation for the changes in HACU Vmax observed following behavioral modulation of cholinergic activity (Apparsundaram et al., 2005). The authors observed significantly increased density of CHT, but not VAChT or other synaptic protein, at the plasma membrane in response to cholinergic activity, but not a control behavioral paradigm, that did not challenge cholinergically-supported attentional processes specifically. The above studies provide strong evidence for CHT trafficking from intracellular reserves to the plasma membrane as the mechanism of CHT regulation

currently understood best. Additional studies will be needed to describe the molecular detail of possible alternative modes of CHT regulation, including catalytic activation of plasma membrane resident CHT proteins. Of note, activation of biogenic amine transporters by p38 mitogen-activated protein kinase has recently been described, and may provide a model for non-trafficking-based activation of CHT (Apparsundaram et al., 2001c; Zhu et al., 2004).

CHT and Genetic Mouse Models of Cholinergic Dysfunction

Genetic approaches have been used to generate mice with over-expression or knockouts of various components of the system that supports ACh neurotransmitter turnover, including CHT itself, the ChAT and AChE enzymes, and various muscarinic and nicotinic receptor subtypes. These mouse models of cholinergic dysfunction have provided new evidence for a dynamic role of CHT as a critical modulator of cholinergic neurotransmission (for review see Bazalakova and Blakely, 2006).

CHT is Upregulated in the AChE Knockout (AChE-/-) Mouse

AChE hydrolysis of ACh in the synaptic cleft terminates cholinergic neurotransmission. Therefore, a genetically-induced loss of AChE may be viewed as a hypercholinergic state, where diminished ACh metabolism leads to sustained cholinergic receptor stimulation. While such prolonged receptor activation can be lethal, AChE-/- mice survive to adulthood, although they are unable to eat solid food and their lifespan is reduced due to fatal seizures (Duysen et al., 2002; Xie et al., 2000). The survival of these

animals raises two questions: what parameters change to compensate for a state of ACh hypometabolism and which genes show the most plastic response?

Whereas butyrylcholinesterase activity and mRNA levels of muscarinic receptors in these mice are not changed, [^{3}H]quinuclinyl benzilate ([^{3}H]QNB) binding studies, immunofluorescence, and immunoblotting with specific antibodies demonstrate 50 to 80% reduced expression of M1, M2, and M4 receptors in AChE-/- cortex and hippocampus homogenates, as well as decreased cell surface and increased internalization of the muscarinic receptors (Li et al., 2003; Li et al., 2000; Mesulam et al., 2002; Volpicelli-Daley et al., 2003a). Consequently, AChE-/- mice display reduced sensitivity to mAChR stimulation such as oxotremorine-induced hypothermia, tremor, salivation, and analgesia, but dose-dependent heightened sensitivity to mAChR inhibition, namely scopolamine-induced increases in locomotor activity (Volpicelli-Daley et al., 2003b).

Intriguingly, immunoblotting for CHT reveals a 60% increase in CHT expression in striatal homogenates, in the absence of changes in ChAT activity or VAChT expression (Volpicelli-Daley et al., 2003b). This compensatory change may reflect an attempt by the presynaptic terminal to increase substrate availability in a cholinergic system deprived of choline derived from ACh hydrolysis, which thus appears critical for the sustained re-synthesis of releasable neurotransmitter. Apparently, although micromolar choline levels are present in blood and CSF, levels at cholinergic terminals may be more limited due to efficient clearance mechanisms (including both HACU and LACU). Regardless, AChE-/- phenotypes complement findings in CHT+/- mice which, in contrast to AChE-/- animals, have approximately 50% less CHT protein compared to

CHT wild type (CHT+/+) siblings, are hypo-sensitive to scopolamine challenge, and are hyper-responsive to oxotremorine-induced tremor (Bazalakova et al., 2007). The above studies suggest that CHT upregulation and muscarinic receptor downregulation and internalization act in concert to provide a mechanism of compensation for decreased ACh metabolism in AChE-/- mice. These data also indicate that a mechanism must be in place to transduce changes in extracellular levels of ACh to CHT. This feedback mechanism could be mediated by presynaptic receptors or a retrograde signal that has yet to be identified.

CHT is Also Upregulated in the Acetylcholinesterase (AChE) Transgenic Mouse

Interestingly, increased CHT protein expression is present in another model of cholinergic dysfunction – AChE transgenic (AChE-Tg) mice. Autoradiography in brain sections reveals a higher than twofold increase in [^{3}H]HC-3 binding in the striatum of AChE-Tg mice compared to wild type controls (Beeri et al., 1997). These findings correlate with observations of approximately 70% higher HACU in striatal and hippocampal, but not cortical synaptosomal preparations from AChE transgenics (Erb et al., 2001). Whereas microdialysis revealed normal basal levels of extracellular ACh in the hippocampi of freely moving AChE-Tg mice, halothane anaesthesia reduced both ACh levels and synaptosomal HACU to significantly lower levels in AChE transgenics compared to wild type controls. In addition, administration of the AChE inhibitor physostigmine (i.p.) normalized the higher HACU observed in AChE transgenics to control levels (Erb et al., 2001). Although it may appear paradoxical that CHT is upregulated in both AChE-Tg and AChE-/- mice, CHT upregulation in the AChE-Tg

brain may serve as an attempt to compensate for overall cholinergic hypofunction caused by hypermetabolism of ACh.

Whereas initial studies reported unchanged tritiated ligand-binding for nAChRs and mAChRs in brain sections (Beeri et al., 1997), subsequent studies detected increased [^{3}H]cytosine (α4 nAChR subunit) and [^{3}H]AF-DX-384 (M2 mAChR subtype) binding in homogenates from AChE transgenic striata. No changes were observed in [^{125}I]α-bungarotoxin (α7 nicotinic receptor subunit) or [^{3}H]pirenzepine (M1 muscarinic receptor subtype) binding (Svedberg et al., 2003). The specific changes in CHT, mAChR, and nAChR expression suggest that these proteins work concurrently to overcome insults on cholinergic signaling in AChE transgenics, a strategy for compensation comparable to that observed in AChE-/- mice.

Altered expression of CHT and cholinergic receptors may underlie differences in behavior and sensitivity to pharmacological challenges by the AChE-Tg mice. Similarly to AChE-/- animals, AChE transgenics are resistant to muscarinic (oxotremorine) agonist-induced hypothermia, as well as nicotinic (nicotine) agonist-induced hypothermia, but retain their ability to thermoregulate as evidenced by normal responses to noradrenergic agents and exposure to cold (Beeri et al., 1995). AChE transgenics display normal motor behavior in familiar environments (repeated exposure to open field paradigm), but increased motor activity in novel environments (initial exposure to open field chambers) (Erb et al., 2001), and are impaired in an age-dependent manner in both visible and hidden versions of the water maze (Beeri et al., 1995).

In summary, the findings of increased [^{3}H]HC-3 binding and HACU in AChE transgenics suggest that CHT upregulation provides one compensatory mechanism in a

hypocholinergic state due to excess ACh metabolism, possibly in conjunction with altered muscarinic and/or nicotinic receptor expression.

CHT Upregulation Provides Mechanism of Compensation in Choline Acetyltransferase Heterozygous (ChAT+/-) Mice

Upregulation of CHT protein expression and function have also been observed in ChAT+/- mice. While ChAT activity is reduced by almost 50% in the ChAT+/- brain, both bulk ACh levels in the striatum, frontal cortex, and hippocampus, as well as high potassium depolarization-induced ACh release from ChAT+/- hippocampal slices, are normal. Not surprisingly, ChAT+/- performance in the water maze paradigm is indistinguishable from that of ChAT+/+ controls (Brandon et al., 2004).

How, then, is functional compensation achieved in the ChAT+/- animals? The authors report that AChE activity is comparable between ChAT+/- and ChAT+/+ mice, and while they do not investigate muscarinic or nicotinic receptor expression, reverse-transcriptase polymerase chain reaction and immunoblotting reveal 70% and 150% increases in CHT mRNA (septum) and protein (striatum, cortex, hippocampus, spinal cord) respectively. In addition, *in vitro* [^{3}H]ACh synthesis in hippocampal slices pre-loaded with [^{3}H]choline substrate was approximately 60% higher in ChAT+/- tissues compared to ChAT+/+ controls (Brandon et al., 2004). The above studies point to CHT upregulation as an essential, compensatory response to the reduction in ChAT activity, sustaining wild type levels of AChE activity, as well as ACh content and depolarization-evoked ACh release. Clearly, cholinergic neurons place a significant responsibility on CHT to balance deficits elsewhere in cholinergic signaling.

CHT Downregulation in α3 Nicotinic Receptor Knockout (α3-/-) Mice

The α3-/- mice provide the first illustration of CHT regulation as a compensatory response to altered cholinergic receptor function (Rassadi et al., 2005). Electrophysiological recordings from cholinergic sympathetic superior cervical ganglia in α3-/- mice demonstrate that absence of postsynaptic α3 receptors completely disrupts fast excitatory synaptic transmission. Immunofluorescence, confocal microscopy, and EM analyses demonstrate unaltered terminal localization of various synaptic proteins, including ChAT, VAChT, synaptobrevin, syntaxin 1a, and synaptotagmin, as well as the morphologic integrity of the cholinergic synapses under investigation, including normal levels of small clear synaptic vesicles, large dense core vesicles, docked vesicles, synaptic cleft width, etc. Instead, the authors identify the basis of the electrophysiological phenotype as a deficit in presynaptic ACh release.

Electrophysiological recordings reveal that repeated stimulation results in faster depletion of neurotransmitter in α3-/- terminals compared to α3+/+ controls. Remarkably, HC-3 blockade has no effect on α3-/- ACh release, whereas it significantly reduces α3+/+ ACh output, providing further support for the hypothesis that CHT downregulation provides a compensatory mechanism at α3-/- sympathetic ganglia synapses (Rassadi et al., 2005). It will be informative to use choline uptake, immunoblotting, and immunofluorescence approaches to assess potential loss of CHT function and expression as a conclusive mechanism by which ACh release capacity is lost in α3-/- mice. The findings in α3-/- synapses again point to the likely existence of a retrograde signal, whose ultimate target is regulation of CHT function and expression.

In summary, studies in various genetic mouse models of cholinergic dysfunction

point to CHT as a predominant presynaptic modulator of functional compensation. For example, while VAChT and ChAT function and expression are unaltered, CHT is functionally upregulated to sustain cholinergic transmission in AChE Tg mice. CHT upregulation is the only biochemical variable that is different between ChAT+/+ and ChAT+/- mice, while CHT downregulation in α3 knockouts stands in stark contrast to wildtype expression and localization of various other presynaptic proteins, including ChAT, VAChT, synaptobrevin, syntaxin 1a, and synaptotagmin. Thus, studies of CHT function and regulation, including characterization of CHT knockout and heterozygous mice, are expected to provide valuable insight into mechanisms of signaling and compensation at the cholinergic synapse, cholinergic transmission in the whole organism, and a valuable new model of cholinergic dysfunction.

Significance

ACh is a neurotransmitter of key importance in both central and peripheral nervous systems (Iversen et al., 1975). ACh maintains vital biological functions such as motor function, memory, cognition, and autonomic regulation. Selective blockade of the rate-limiting step in ACh synthesis - CHT-mediated HACU - reduces ACh synthesis and release in vitro (Maire and Wurtman, 1985) and impairs cholinergic function in vivo (Schueler, 1955) demonstrating the essential physiological role of CHT. CHT-mediated HACU is highly regulated by neuronal activity (Simon and Kuhar, 1975), but the molecular mechanisms of this regulation are not clear. The recent cloning of CHT has allowed our lab to generate new, valuable tools, including specific anti-CHT antibodies and a CHT knockout mouse. The studies described here use these tools towards a first

direct demonstration of requirements for CHT *in vivo*, both under basal conditions and in response to behaviorally-activated cholinergic neurotransmission. The outlined experiments also extend previous studies, which have used less direct ligand-binding approaches to study CHT trafficking in pharmacologically-activated cholinergic signaling. The experimental results address the possibility of a pre-synaptic, CHT-mediated, molecular plasticity mechanism, regulated by and needed to sustain *in vivo* cholinergic activity.

In addition, characterizations of basal or induced phenotypes in CHT+/- mice suggest and will continue to direct new insights into the possible role of CHT in human disorders of known cholinergic dysfunction such as Alzheimer's disease (Coyle et al., 1983), Parkinson's disease (Calabresi et al., 2000), schizophrenia (Tandon, 1999), Huntington's disease (Lange et al., 1992), and dysautonomia (Baron and Engler, 1996). Furthermore, these studies can help identify disorders where CHT contributions have not been recognized so far. Better understanding of CHT function and regulation will allow manipulation of cholinergic signaling *in vivo* and suggest approaches to CHT as a target for therapy in disease.

Thesis Objectives

We have developed CHT-/- and CHT+/- mice which offer the valuable opportunity to study CHT in a whole animal model and provide a more physiologically relevant environment than *ex vivo* systems. Therefore, the experiments proposed here use CHT-/-, CHT+/-, and CHT+/+ animals and combine biochemical, pharmacological, and behavioral approaches to directly test the **central hypothesis: CHT is essential for ACh**

synthesis and release in response to sustained demands on cholinergic signaling, and in turn supports behaviors dependent on cholinergic signaling. Three specific aims were pursued to test the central hypothesis:

Specific Aim 1. Establish the physiological importance and the consequences of genetic ablation of CHT *in vivo*. *Hypothesis:* *As the rate-limiting step of ACh synthesis, CHT is essential for cholinergically-supported physiological processes.* To test this hypothesis I characterized morphological and biochemical phenotypes of CHT knockout (-/-) mice.

Specific Aim 2. **Assess dependence of ACh turnover and CHT regulation on CHT expression. *Hypothesis:*** *Diminished intracellular reserve pools of CHT, the rate-limiting step of ACh synthesis, will alter ACh synthesis and/or release in response to sustained cholinergic neurotransmission.* To test this hypothesis I evaluated ACh and choline levels in brain homogenates from CHT+/+, CHT+/-, and CHT-/- mice, and used biochemical approaches (HC-3 binding, synaptosomal biotinylation, AChE and ChAT activities, and muscarinic receptor immunoblotting) to investigate the mechanisms of CHT regulation and compensation in the CHT+/- brain.

Specific Aim 3. **Investigate the role of CHT in animal behavior dependent on cholinergic signaling. *Hypothesis:*** *Reduced CHT pools likely result in cholinergic dysfunction and compromise behavior dependent on cholinergic signaling in CHT+/- mice.* To test this hypothesis I compared basal and/or challenge-induced performances of CHT+/- and CHT+/+ siblings in sensory-motor, anxiety, cognitive, cardiovascular, addiction, and circadian rhythms behavioral paradigms.

CHAPTER II

GENETIC ABLATION OF CHT IS LETHAL – STUDIES IN CHT KNOCKOUT (CHT-/-) MICE

Introduction

Acetylcholine (ACh) serves important roles as a neurotransmitter of both the central and peripheral nervous systems. ACh is released at the neuromuscular junction (NMJ), as well as at autonomic synapses, and also modulates a variety of central circuits that support arousal, attention, reward, learning, and memory (Dani, 2001; Laviolette and van der Kooy, 2004; Wess, 2004; Winkler et al., 1995). Lethal deficits in cholinergic function occur with exposure to irreversible acetylcholinesterase (AChE) inhibitors (Hardman and Limbird, 2001). Genetic and autoimmune impairments in ACh synthesis or responsiveness at the NMJ trigger myasthenic syndromes (Engel et al., 2003), whereas degeneration of basal forebrain cholinergic neurons occurs in Alzheimer's disease and may contribute to dementia (Whitehouse et al., 1982). In turn, both myasthenias and symptoms of dementia are relieved by reversible AChE inhibitors (Doody, 2003).

Within presynaptic terminals, ACh is synthesized from choline and acetyl-CoA by the enzyme choline acetyltransferase (ChAT) (Brandon et al., 2003; Misgeld et al., 2002), and this ACh synthesis is thought to be limited by choline availability (Jope, 1979a; Tucek, 1985b). With respect to sources of choline, pathways exist within the brain for the de novo synthesis of phosphatidylcholine from phosphatidylethanolamine (Blusztajn and Wurtman, 1981), and the release of choline by the action of phospholipase D can support ACh synthesis (Lee et al., 1993). However, cytoplasmic synthesis of ACh is believed to

depend predominantly on the acute uptake of extracellular choline across the presynaptic plasma membrane (Birks and MacIntosh, 1961; Jope, 1979a). Two major neuronal transport mechanisms for choline have been described: a Na-dependent, hemicholinium-3 (HC-3)-sensitive, high-affinity choline uptake (HACU; Km = 1–5 μM) process associated with cholinergic presynaptic terminals and a more ubiquitous mechanism of HC-3-insensitive, Na-independent, choline transport having a lower affinity for choline (Km = 100 μM) (Haga, 1971; Yamamura and Snyder, 1972). High-affinity HC-3-sensitive choline transport is believed to sustain ACh synthesis in presynaptic terminals (Birks and MacIntosh, 1961; Guyenet et al., 1973; Haga, 1971). Indeed, the dynamic regulation of HACU in response to changes in cholinergic neuronal activity appears to match presynaptic ACh synthesis to the rate of ACh release (Kuhar and Murrin, 1978b).

Despite several decades of research on presynaptic cholinergic mechanisms, the identity of the choline transporter (CHT) has only recently become clear (Ferguson and Blakely, 2004). Okuda and coworkers (Okuda et al., 2000b), as well as our own group (Apparsundaram et al., 2001b; Apparsundaram et al., 2000), have shown that the transfection of cloned CHT cDNAs elicits Na/Cl -dependent HC-3-sensitive HACU in cultured cells. Additionally, in rodents (Ferguson et al., 2003; Misawa et al., 2001) and humans (Kus et al., 2003), CHT proteins are found in all major cholinergic nuclei and colocalize with the vesicular ACh transporter (VAChT) at presynaptic terminals (Ferguson et al., 2003). In conjunction with evidence that HC-3 treatment of animals suppresses ACh synthesis (Freeman et al., 1979; Schueler, 1955), CHT's synaptic localization argues that the transporter plays a critical role in sustaining cholinergic signaling.

To evaluate the in vivo contributions of CHT to cholinergic neurotransmission, we targeted the CHT gene in mice by homologous recombination in embryonic stem (ES) cells. CHT-/- mice exhibited deficits in cholinergic function and died neonatally. In contrast, CHT+/- mice maintain wild-type levels of HC-3-sensitive presynaptic choline uptake despite a significant reduction in CHT protein levels (Chapter III). Our results demonstrate that CHT plays an essential and regulated role in sustaining cholinergic neurotransmission.

Materials and Methods

Gene Targeting

Approval was obtained from our respective Institutional Animal Care and Use Committees for experiments involving mice. A portion of the mouse CHT gene beginning at the start codon in exon 2 and extending into intron 4 was deleted by homologous recombination in embryonic stem cells. To generate genomic fragments suitable for a CHT-targeting vector, we used PCR with Platinum Pfx DNA polymerase (Invitrogen) or the Expand long Template PCR System (Roche, Indianapolis, IN) and 129SvEvTacBr genomic DNA to amplify a 3-kb segment (short arm) extending from the CHT promoter region to the start codon in exon 2 and a 5-kb fragment (long arm) beginning in intron 4 from mouse genomic DNA. The DNA encoding enhanced green fluorescent protein (EGFP), including 3' untranslated region, was amplified from the plasmid pEGFP-N2 (BD Biosciences, San Jose, CA). The oligonucleotide primers used in the PCRs included the addition of restriction enzyme cutting sites and/or loxP sites to

facilitate subsequent subcloning, targeting vector construction, and marker excision. The ligation of the PCR products into the vector pFLP-NTK (courtesy of Mark Magnuson, Department of Molecular Physiology and Biophysics, Vanderbilt University) yielded the final targeting construct that included loxP sites flanking the EGFP and FLP recognition target (FRT) sites flanking the phosphoglycerol kinase promoter-driven neomycin (NEO) gene cassette (Fig. 5A). This targeting construct also included a 3' thymidine kinase gene driven by a phosphoglycerol kinase promoter to allow for negative selection.

For targeting of the mouse CHT (mCHT) gene, the linearized targeting vector was electroporated into TL-1 129SvEvTacBr embryonic stem (ES) cells and recombination was selected for with G418 and ganciclovir (Vanderbilt Transgenic Mouse/ES Cell Shared Resource). Southern blotting was used to screen » 380 surviving ES cell colonies, and 1 positive recombined clone was identified. The selected ES cells were injected into C57BL/6 blastocysts and after transfer into a surrogate mother, seven chimeric animals were born. The amount of chimerism ranged from 20% up to 95% and two lines have been established from the most chimeric animals. The results described in this report derive from experiments on mice carrying NEO and EGFP at the CHT locus on a mixed 129SvEvTacBr × C57BL/6 genetic background. Each replication of an individual experiment involved littermates of the reported genotypes to minimize differences in genetic variability.

To improve EGFP expression that could be limited by the adjacent NEO transgene (Pham et al., 1996), and rule out any toxic effects of NEO expression at this locus, we also excised the NEO cassette by breeding one line to FLP transgenic mice (Rodriguez et al., 2000). Studies on lines with excised markers yielded initial results that

appear identical to those of our studies with the nonexcised lines. Finally, the EGFP expression is also unlikely to contribute our phenotypes as much higher, directly detectable levels of transgenic EGFP expression have been reported in motor neurons without causing neuronal dysfunction (Feng et al., 2000).

Mouse Genotyping

For Southern blotting, mouse tail DNA was digested with EcoRV (New England Biolabs), separated on 0.9% agarose gels, and transferred to Zetaprobe nylon membranes (Bio-Rad). A 5' external probe was generated by PCR with 5'-CCAGGATCTAGACCAACTCG-3' and 5'-TGAAAGACGACCTGAGGTAG-3' as oligonucleotide primers, followed by EcoRV digestion and random-priming 32P labeling of the resulting 1-kb fragment (Fig. 5B) Genotyping by PCR was performed using a common WT and KO sense oligonucleotide primer: (96 bp 5' of ATG of CHT, 5'-AGTGCGTGGCTGCTTAAT-3'), a WT antisense primer (841 bp from above primer in WT allele, 5'-AGATGATGGCCTGTGAATTC-3'), and a KO reverse primer (401 bp from sense primer in EGFP of the KO allele, 5'-TTGAAGAAGATGGTGCGCTC-3') (Fig. 5C) and Taq DNA polymerase (Promega) with extracted tail DNA as template.

Immunofluorescence and Histochemical Analyses

Immunofluorescent labeling of floating brain sections and neuromuscular junction preparations was based on previously described protocols (Schroeter et al., 2000). We have previously characterized the anti-CHT antibodies used in this study (Ferguson et al., 2003). Commercially available antibodies and fluorescent probes included mouse

monoclonal neurofilament antibody (Sternberger Monoclonals, Lutherberg, MA), goat anti-ChAT polyclonal antibody (Chemicon, Temecula, CA), rabbit polyclonal anti-GFP, Alexa-660-phalloidin and Alexa-488-a -bungarotoxin (BgTx) (Molecular Probes). Secondary antibodies were obtained from Jackson ImmunoResearch. Acetylcholinesterase histochemistry was performed by the method of Karnovsky and Roots (Karnovsky and Roots, 1964). Bright-field images were captured on an Olympus BX50WI microscope with Kodak Elite 160 film. Confocal analysis was performed with an Axioplan 2 confocal imaging system equipped with internal He/Ne and external Ar/Kr lasers with output at 488, 568, and 660 nm (Vanderbilt University Medical Center Cell Imaging Core Resource). Z-series were collected by optical sectioning at an interval of 1 um. Quantitative analyses of digital images were performed with METAMORPH software (Universal Imaging).

Immunoblot Analysis

Freshly dissected brain tissue was homogenized in 0.32M sucrose-5mM Hepes-NaOH pH 7.4 supplemented with a protease inhibitor cocktail (Sigma, St. Louis, MO) with a Potter Elvejhem homogenizer (8 strokes at 500 rpm). After determining and adjusting protein concentration, the homogenate was diluted with sample buffer to yield 1% sodium dodecyl sulfate (SDS), 31.25 mM TRIS pH 6.8, 5% glycerol, 200mM 2-mercaptoethanol). The samples were then resolved by SDS-polyacrylamide gel electrophoresis (PAGE), transferred to polyvinylidine difluoride membranes and subjected to immunoblot analyses with CHT-specific monoclonal and polyclonal anti-CHT antibodies (Kus et al., 2003). Anti-VAChT immunoblots employed a goat

polyclonal antibody from Chemicon (Temecula, CA).

Transport Assays

Crude synaptosomes (P2 fraction) from the brains of newborn mice were prepared as previously described for adult mice (Ferguson et al., 2003). All comparisons made between CHT genotypes were performed using male littermates. Assays of choline transport activity in the brains of newborn mice were performed for 5 minutes at 37 °C in Kreb's Ringer's Hepes buffer (KRH, 130mM NaCl, 3mM KCl, 2.2mM $CaCl_2$, 1.2mM $MgSO_4$, 1.2mM KH_2PO_4, 10 mM glucose, 10mM HEPES, pH 7.4) with a final [choline] of 100 nM (specific activity: 83 Ci/mmol, Amersham). 1 μM HC-3 was used to define CHT-mediated choline uptake. For γ-aminobutyric acid (GABA) uptake assays, samples were incubated in parallel with 50 nM [^{3}H]-GABA at either 37ºC or 4°C ([^{3}H]-GABA, 93 Ci/mmol, NEN Perkin Elmer Life Science, Boston, MA). Assays were terminated by aspiration and washing onto polyethyleneimine coated glass fiber filters using a Brandel Cell Harvester (Gaithersburg, MD). The low yield of tissue from the newborn mouse brain precluded analysis of saturation kinetics in these samples. Analysis of saturation kinetics for choline uptake in whole brain synaptosomes from the adult CHT+/- and +/+ littermates was performed as previously described (Ferguson et al., 2003).

HC-3 Binding Assays

Membrane preparations were prepared by lysing crude synaptosomes in the P2 fraction with a Potter Elvejhem homogenizer (5 strokes at 900 rpm) in 5mM Hepes-

NaOH pH 7.4. Membranes were collected by centrifugation at 15 000 x g for 20 minutes and resuspended in 50mM Tris, 200mM NaCl pH 8 (TRIS-NaCl). The membranes were washed by centrifugation at 15 000 x g and resuspension in TRIS-NaCl. The binding assay used 250-400 µg protein per sample and was performed for 45 minutes at room temperature in TRIS-NaCl in the presence of 10nM [^{3}H]-HC-3 (128 Ci/mmol, NEN Perkin Elmer Life Science) as per a previously described protocol (Sandberg and Coyle, 1985a). This concentration of [^{3}H]-HC-3 exceeds the K_d for binding to mCHT (Apparsundaram et al., 2001b) and thus represents a measure of the number of HC-3 binding sites in the preparation. Specific binding to CHT was defined by parallel assays that included 1 µM unlabeled HC-3 or 2 mM choline as competitors of [^{3}H]-HC-3 binding.

ChAT Activity

Activity of the choline acetyltransferase (ChAT) enzyme in brain tissue homogenates was measured by the synthesis of [^{14}C] acetylcholine (ACh) from [acetyl-1-^{14}C]-acetyl-coenzyme A and choline. The newly synthesized [^{14}C] acetylcholine was separated from the precursor [acetyl-1-^{14}C]-acetyl-coenzyme A by sodium tetraphenylboron extraction (Frick et al., 2002).

Analysis of ACh Levels

ACh levels in brain tissue were quantified using a liquid chromatography/mass spectrometry (LC/MS) approach. The internal standard propionylcholine was added to brain tissue microwaved for AChE inactivation (Bertrand et al., 1994), followed by

homogenization in acetonitrile, heptane lipid removal, and vacuum drying. The samples were resuspended in mobile phase and ACh was quantified using standard LC/MS protocols described previously (Koc et al., 2002) (Vanderbilt Mass Spectrometry Core Resource). Additional assays were performed using high pressure liquid chromatography (HPLC) methods (Damsma et al., 1985) with electrochemical detection and achieved similar results.

For the analysis of ACh synthesis in brains of P0 mice, 400 µm slices from the whole brain were preincubated for 10 minutes at 37°C in KRH with or without 10 µM HC-3 prior to the addition of [^{3}H]-choline (final concentration 100 nM). After 30 minutes the slices were washed and the newly synthesized [^{3}H]-ACh was extracted by sonication in acetonitrile. The samples were centrifuged to pellet cellular debris and the supernatant was collected. This ACh containing supernatant (1 ml) was further purified by adding 500 µl heptane, mixing and centrifuging for 15 minutes at 15,000 x g. The resulting heptane layer (upper) was discarded. The remaining acetonitrile layer was vacuum-dried and resuspended in 100 µl 50 mM H_sPo_4. 50 µl were subjected to HPLC in order to separate ACh from choline, as defined by preinjected standards. 20x500 µl fractions (flow rate 1ml/min) were collected and subjected to liquid scintillation spectrometry.

Results

Confirmation of Targeting Strategy

Using our previous elucidation of the mCHT coding sequence as a reference point (Apparsundaram et al., 2001b) we searched the Celera Discovery System and GenBank databases to define the organization of the mCHT gene, including exon and intervening intronic sequences. The mCHT gene is encoded by nine exons and spans a 27-kb interval on chromosome 17 (GenBank accession no. for genomic contig containing the mCHT gene: NT_039656). Our targeting strategy (Fig. 5A) resulted in the deletion of an » 5-kb segment of the CHT gene, originating at the start codon in exon 2 and extending into intron 4. This deleted sequence was replaced with an EGFP-NEO cassette, with the EGFP reporter placed in frame with the endogenous CHT start codon to drive EGFP expression in cholinergic neurons and the NEO cassette in the opposite orientation. Southern blotting and PCR analyses indicate the successful completion of this targeting strategy (Fig. 5 B and C).

Further confirmation of successful CHT gene disruption is evident with the loss of CHT protein from whole-brain extracts (Fig. 5D). The CHT immunoreactivity present in distinct cholinergic neurons and fibers is also abolished in the CHT–/– CNS (Fig. 5 E and F, respectively). We observe comparable losses of CHT expression by using previously characterized polyclonal and monoclonal anti-CHT antibodies (Ferguson et al., 2003). Because the anti-CHT antibodies used in these experiments detect epitopes in the distal C terminus of the CHT protein, the absence of CHT immunoreactivity also indicates an absence of truncated CHT protein.

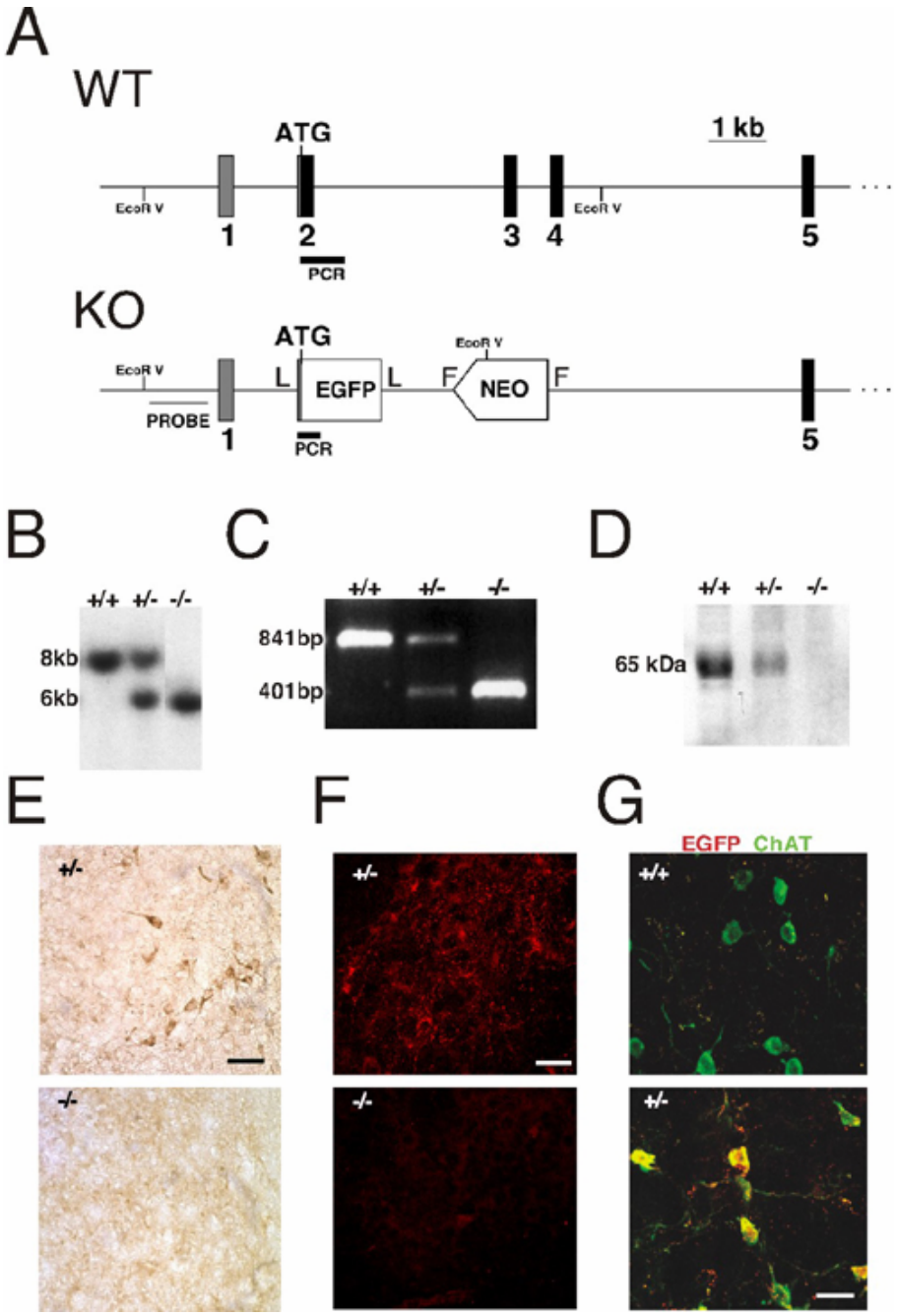
A
WT
ATG
1 kb
EcoR V
EcoR V
1
2
3
4
5
PCR
KO
ATG
EcoR V
EcoR V
L
EGFP
L
F
NEO
F
PROBE
1
PCR
5
B
+/+ +/- -/-
8kb
6kb
C
+/+ +/- -/-
841bp
401bp
D
+/+ +/- -/-
65 kDa
E
+/-
-/-
F
+/-
-/-
G
EGFP ChAT
+/+
+/-

Fig. 5. CHT targeting construct and expression. (**A)** The mouse CHT gene was disrupted by replacing the coding region of exons 2–4 with EGFP and NEO cassettes. The EGFP coding sequence is in frame with the endogenous CHT start codon and is flanked by loxP sites (L). The NEO cassette is flanked by FRT sites (F). Also indicated are the locations of the Southern blotting probe and the PCR products used in the genotyping of mice. This diagram depicts five of the nine exons comprising the mouse CHT gene. **(B)** Southern blot detection of the 8- and 6-kb WT and KO alleles, respectively. **(C)** Our PCR-based genotyping strategy detects a WT product of 841 bp and a KO product of 401 bp. **(D)** Immunoblot detection of CHT protein in extracts from the whole brains of newborn mice reveals a reduction of CHT protein levels in the +/– mice and an absence of CHT immunoreactivity in the –/– mice. **(E**) Immunohistochemistry demonstrates loss of CHT immunoreactivity from cholinergic striatal interneurons in CHT–/– mice at birth. **(F)** CHT immunoreactivity is present in facial nucleus motor neuron somata and fibers in a CHT+/– brain (E19) but not in the facial nucleus of a CHT–/– littermate. **(G)** EGFP immunoreactivity (red) overlaps (yellow) with ChAT-positive (green) cholinergic neurons in the basal forebrain of an adult CHT+/– mouse but is not detected in a +/+ littermate. (Scale bars = 40 μ m in *E*–*G*.). Shawn Ferguson, Valentina Savchenko, and Jane Wright contributed to this figure.

Furthermore, our strategy resulted in the expression of EGFP in cholinergic neurons, as demonstrated by colocalization of EGFP with ChAT in cholinergic neurons of the basal forebrain of an adult CHT+/– mouse (Fig. 5G). EGFP levels are not sufficiently high in these cholinergic neurons to allow direct visualization of EGFP fluorescence, but reporter expression is clearly detected by using indirect immunofluorescence approaches. Our targeting strategy also flanked the EGFP sequence with loxP sites and the NEO cassette by FRT sites, to allow for their subsequent removal by Cre and Flp recombinase, respectively. In the offspring arising from the mating of CHT+/– mice and Flp mice the only difference that we have observed resulting from the removal of the NEO cassette is an increase in the expression of EGFP as detected by immunofluorescence analysis (data not shown). This may reflect a recognized effect of the NEO cassette in suppressing the expression of neighboring genes (Pham et al. 1996) and confirms that the phenotypes we observe are most likely due to the loss of CHT expression rather than a toxic effect arising from the NEO cassette.

CHT Is Essential for Neonatal Viability

Validation of our successful disruption of the mouse CHT gene is included in Fig. 5. In 35 litters produced from the mating of CHT+/- mice, we obtained the expected Mendelian ratios in the genotypes of the 242 pups analyzed at E19 or the day of birth (55 CHT+/+, 117 CHT+/-, and 70 CHT-/-, P=0.35 by $\chi 2$ analysis). Newborn CHT-/- pups were morphologically normal (Fig. 6A) and equal in weight compared with their healthy CHT+/+ and CHT+/- littermates (1.22 ± 0.02 g versus 1.20 ± 0.03 g, n = 10 and 13, respectively). Further gross analysis of various organs, including brain, heart, stomach,

liver, and kidney, revealed no significant differences in weights or morphologies between genotypes. For example, at E19 we observed brain weights of 68 ± 5 mg, 65 ± 4 mg, and 74 ± 3 mg for (n = 6), (n = 9), and (n = 5) pups (ANOVA $P > 0.05$). We did not observe the hunched back or other symptoms of flaccid paralysis reported for newborn ChAT-/- mice (Brandon et al., 2003; Misgeld et al., 2002). With respect to the CNS, Nissl staining of brain sections did not reveal any obvious defects in brain development (data not shown).

In the minutes following birth, CHT-null mice became distinguishable from their littermates as they were immobile and could only respond with a limited contraction when touched. Breathing was sporadic and occurred as single gasps separated by bouts of prolonged apnea. These pups became visibly cyanotic and did not often survive beyond the first hour (Fig. 6A). Histological examination of the lungs of the CHT-/- pups revealed fewer aerated alveoli compared with +/+ littermates (Fig. 6B). The diminished aeration of alveoli in lungs from CHT-/- mice affected their buoyancy such that whereas CHT+/+ or +/- lungs floated, the CHT-/- lungs sank when placed in aqueous solutions (data not shown). These findings support the hypothesis that CHT-/- mice die as a result of hypoxia arising from a failure of neurotransmission at the NMJs of the diaphragm and intercostal muscles that support respiration. In our analysis of hematoxylin- and eosin-stained sections of CHT-/- embryos and pups we did not observe any other differences in gross organ development or morphology. For example, unlike the ChAT-/- mice (Misgeld et al., 2002), the CHT knockouts did not exhibit herniation of the diaphragm.

We attempted to rescue the CHT knockouts by enriching the diets of the pregnant dams throughout gestation with choline-supplemented chow (4 g/kg or 10 g/kg versus the

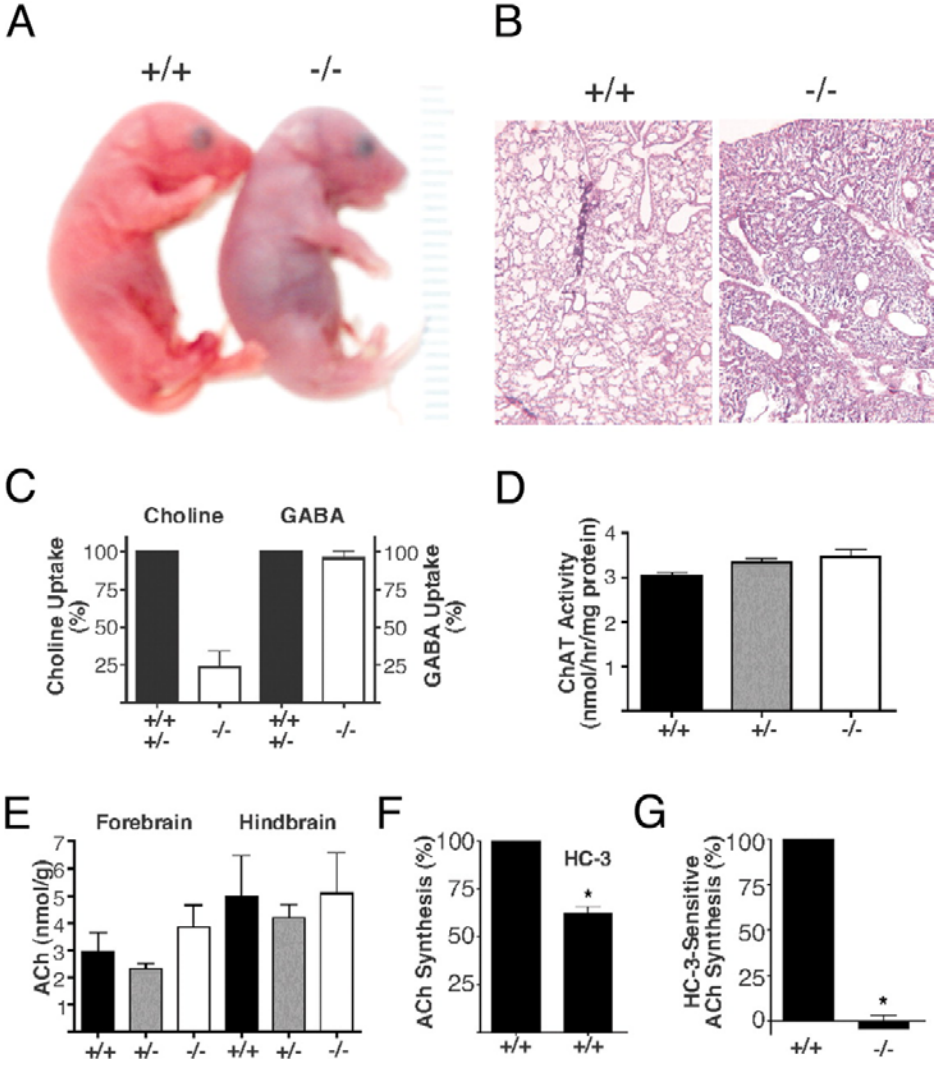
A
+/+
-/-
B
+/+
-/-
C
Choline
GABA
Choline Uptake (%)
GABA Uptake (%)
100
75
50
25
+/+ +/-
-/-
+/+ +/-
-/-
D
ChAT Activity (nmol/hr/mg protein)
4
3
2
1
+/+
+/-
-/-
E
Forebrain
Hindbrain
ACh (nmol/g)
7
6
5
4
3
2
1
+/+
+/-
-/-
+/+
+/-
-/-
F
ACh Synthesis (%)
100
75
50
25
HC-3
*
+/+
+/+
G
HC-3-Sensitive ACh Synthesis (%)
100
75
50
25
0
*
+/+
-/-

Fig. 6. CHT mediated choline uptake is essential for postnatal viability. (A) Although the two pups are equal in size, the CHT–/– pup is visibly cyanotic compared with its CHT+/+ littermate (photo taken 30 min after birth). (B) Consistent with the breathing defect in CHT–/– mice, lungs from these animals contain fewer inflated alveoli than their +/+ littermates. (C) HC-3-sensitive choline uptake (inhibited by 1 μM HC-3) is lost in synaptosomes from CHT–/– mice compared with healthy littermates (mean ± SEM of measurements made in triplicate). The HC-3-sensitive choline uptake for three CHT–/– mice (from separate litters) was compared with eight healthy littermates (six CHT+/– and two CHT+/+). The remaining HC-3-sensitive uptake in the CHT–/– mice was not significantly different from 0 (t test, $P = 0.2$). In contrast, uptake of [3H]GABA was unimpaired in synaptosomes from the CHT–/– mice. (D) No significant difference (ANOVA, $P > 0.05$) in whole-brain ChAT activity was observed between CHT genotypes (mean ± SEM of assays performed in triplicate on samples from 8 +/+,16 +/–, and 11–/– mice). (E) ACh levels as detected by LC/MS were not different (ANOVA, $P > 0.05$) in either forebrain or hindbrain extracts for any of the CHT genotypes (mean ± SEM, n = 4 +/+, 5+/–, and 5–/–). (F) HC-3-sensitive synthesis of [3H]ACh from [3H]choline is detected in CHT+/+ brain slices (E19 or newborn, n = 3, *, $P < 0.05$, Student's t test). (G) The HC-3-senstive component of ACh synthesis is absent from CHT–/– brain slices (n = 3 mice for each genotype, *, $P < 0.05$, Student's t test). Shawn Ferguson contributed to this figure.

normal 1 g/kg, Testdiet, Richmond, IN) alone or in combination with choline-supplemented water (25 mM or 125 mM plus 50 mM saccharin). Similar choline supplementation of diets during pregnancy has been reported to have an impact on the developing cholinergic system (Cermak et al., 1998; Garner et al., 1995). However, these dietary manipulations failed to enhance the survival of the CHT-knockout pups (data not shown). We also attempted to rescue newborn CHT pups by limiting the degradation of ACh. Newborn mice were injected sequentially with physostigmine (500 g/kg i.p.) and neostigmine (5 mg/kg intramuscular). Signs of cholinergic hyperactivity (splay posture and urination) were evident in the control littermates (n = 4) but not in the CHT-/- mice (n = 3), yet these treatments failed to noticeably prolong survival of the knockouts (data not shown).

Loss of HC-3-Sensitive Choline Uptake and ACh Synthesis in CHT CNS

To test whether CHT is solely responsible for HC-3-sensitive HACU in the brain, we measured rates of [3H]choline uptake into synaptosomes prepared from whole newborn mouse brains. As shown in Fig. 6C, CHT-/- synaptosomes failed to accumulate [3H]choline in a HC-3-sensitive manner, but they were otherwise normal, as they did not differ from samples prepared from littermates with respect to the uptake of [3H]GABA (Fig. 6C). The loss of CHT expression also did not appear to affect the viability of cholinergic neurons as revealed by assays of forebrain ChAT activity (Fig. 6D). Surprisingly, measurements of bulk tissue ACh levels, in either hindbrain or forebrain extracts from E19 mice, did not reveal a difference between any of the three genotypes (Fig. 6E). We hypothesized that CHT-/- mice may acquire these ACh stores under

conditions of low demand on the cholinergic system during development, but might not be able to rapidly synthesize ACh via synaptic pathways overseen by CHT. To monitor de novo synthesis and storage of ACh, we tested the ability of CHT-/- brain slices to synthesize [3H]ACh from [3H]choline in vitro. We observed an HC-3-sensitive pool of ACh synthesis in the CHT+/+ samples (Fig. 6F) but not in the slices from the CHT-/- mice (Fig. 6G). These results reveal a specific deficit in HC-3-sensitive ACh synthesis in CHT mice.

CHT-/- NMJs Cannot Sustain ACh Release

The lethal phenotype in CHT-/- is consistent with a deficit in ACh release at NMJs as a result of the elimination of presynaptic choline uptake. To directly test this hypothesis, cholinergic neurotransmission was assessed by using in vitro preparations of the sternomastoid muscle of newly born CHT-/- mice and their CHT+/+ littermates. Although comparable evoked and spontaneous responses were initially detected by intracellular recordings from muscle fibers in the two genotypes, the ACh release in the CHT-/- mice was not sustainable (Fig. 7, 8). After 2–3 h of perfusion, failures predominated in the CHT-/- tissue, whereas the amplitude of evoked EPPs remained robust and reliable in the CHT+/+ tissue (Fig. 8B, 8D). By 4 h, evoked responses were no longer obtained in the CHT-/- muscle fibers, although the resting membrane potential remained stable at 52 mV (Fig. 7A). This decline in evoked responses between 1 and 4 h of perfusion is paralleled by a decrease in the amplitude and frequency of miniature EPPs from a level that is initially indistinguishable from the CHT+/+ control (Fig. 7B). The loss of this functional measure of ACh release over time parallels the decline in

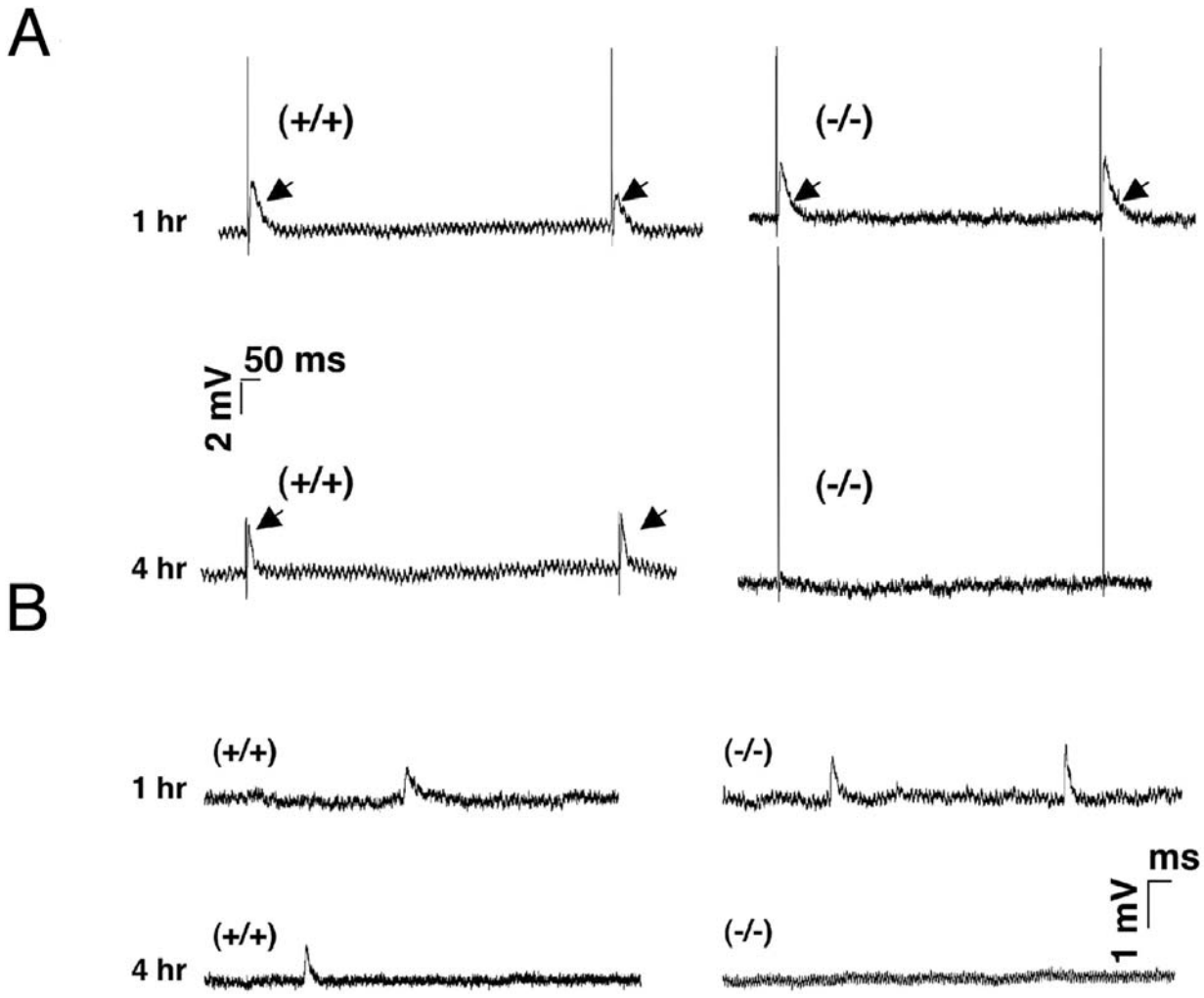

Fig. 7. Electrophysiological characterization of ACh release at CHT–/– NMJs. (A) Examples of evoked EPP traces (arrows) from CHT+/+ (left) and CHT–/– (right) sternomastoid NMJs 1 or 4 h after birth. Note the absence of evoked EPPs after 4 h in the CHT–/– muscles. Stimulation ranged from 1 to 15 V at 1 Hz with 1-ms pulse duration. **(B)** Examples of spontaneous miniature EPPs recorded in the absence of *d*-tubocurarine from CHT+/+ and CHT–/– muscle fibers 1 and 4 h after birth. Data obtained through collaborative effort with Joshua Sanes lab. This figure was contributed by Carlos Tapia.

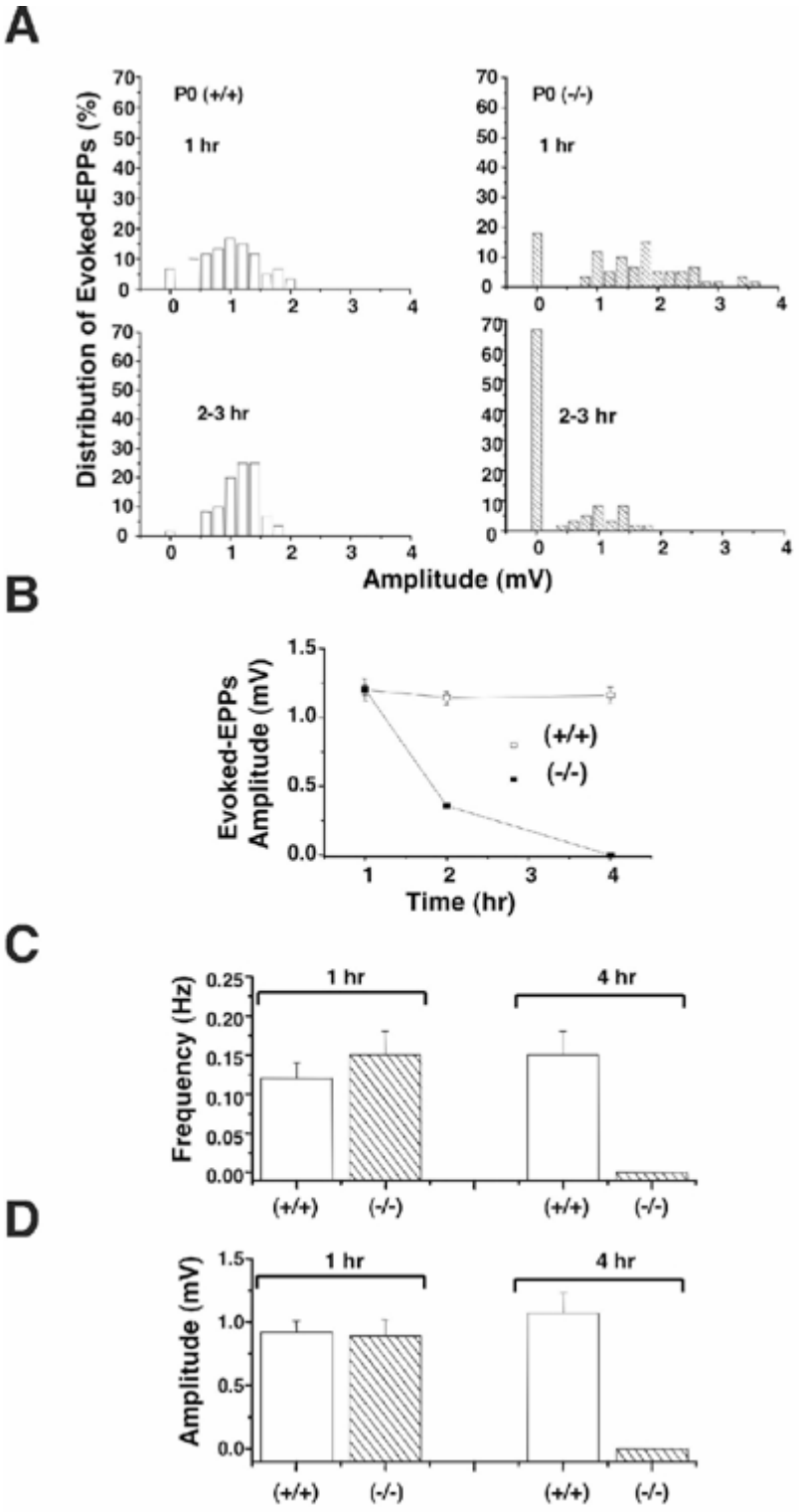
A
P0 (+/+)
1 hr
P0 (-/-)
1 hr
2-3 hr
2-3 hr
Distribution of Evoked-EPPs (%)
Amplitude (mV)
B
Evoked-EPPs Amplitude (mV)
(+/+)
(-/-)
Time (hr)
C
Frequency (Hz)
1 hr
4 hr
(+/+)
(-/-)
(+/+)
(-/-)
D
Amplitude (mV)
1 hr
4 hr
(+/+)
(-/-)
(+/+)
(-/-)

Fig. 8. Summary of ACh release defects at CHT–/– NMJs. (A) Evoked-EPP amplitude histograms, including failures from +/+ (*Left*) and –/– (*Right*) NMJs after 1 and 2–3 hr of birth. Failures predominate at the CHT–/– NMJs after 2–3 hr but responses are still reliably evoked in the CHT+/+ samples. **(B)** Graphical summary of the temporal mean evoked-EPP amplitude after birth from CHT+/+ and CHT–/– muscles. **(C and D)** Bar graphs showing the mean frequency **(C)** and amplitude **(D)** of miniature EPPs from +/+ and –/– in the hours after birth. Data were obtained from at least three junctions per condition for CHT+/+ and CHT–/– muscles. Data obtained through collaborative effort with Joshua Sanes lab. This figure was contributed by Carlos Tapia.

movement and progressive cyanosis seen in the CHT-/- pups after birth. Both of these findings indicate the presence of an initial limited supply of choline and ACh that becomes depleted in the absence of CHT.

Alterations in NMJ Morphology Are Consistent with Diminished ACh Release

ACh plays a role in utero in the development and maturation of both presynaptic and postsynaptic aspects of the NMJ (Sanes and Lichtman, 1999). ChAT-/- mice cannot synthesize ACh, and the resulting lack of neurotransmission impairs proper development of neuromuscular junctions (Brandon et al., 2003; Misgeld et al., 2002). Therefore, we examined several aspects of NMJ morphology to investigate whether the loss of CHT function significantly diminished ACh availability during NMJ development. In ChAT-/- mice, the loss of ACh synthesis during development resulted in an abnormally broad band of nicotinic ACh receptor (nAChR) clusters along intramuscular nerve trunks innervating the diaphragm (Brandon et al., 2003; Misgeld et al., 2002). We observed a similar phenotype in the CHT-/- mice at E19 (Fig.9 B versus E). To quantify this difference, measurements were made at 30- m intervals to assess the maximum diameter (perpendicular to axis of band) occupied by nAChR clusters. The mean band diameter was 124 ± 22 μm compared with 194 ± 24 μm for CHT+/+ and -/- samples, respectively (data not shown). These results represent the average of measurements made from multiple fields of Alexa-488-α-bungarotoxin-labeled whole-mount diaphragms from five pairs of E19 littermates (640 μm X 640 μm fields, 20 measurements per field, > 3 fields per animal, $P < 0.005$, paired t test). Increases in endplate area were reported in the ChAT-/- mutants (Misgeld et al., 2002), and we also observed that individual nAChR

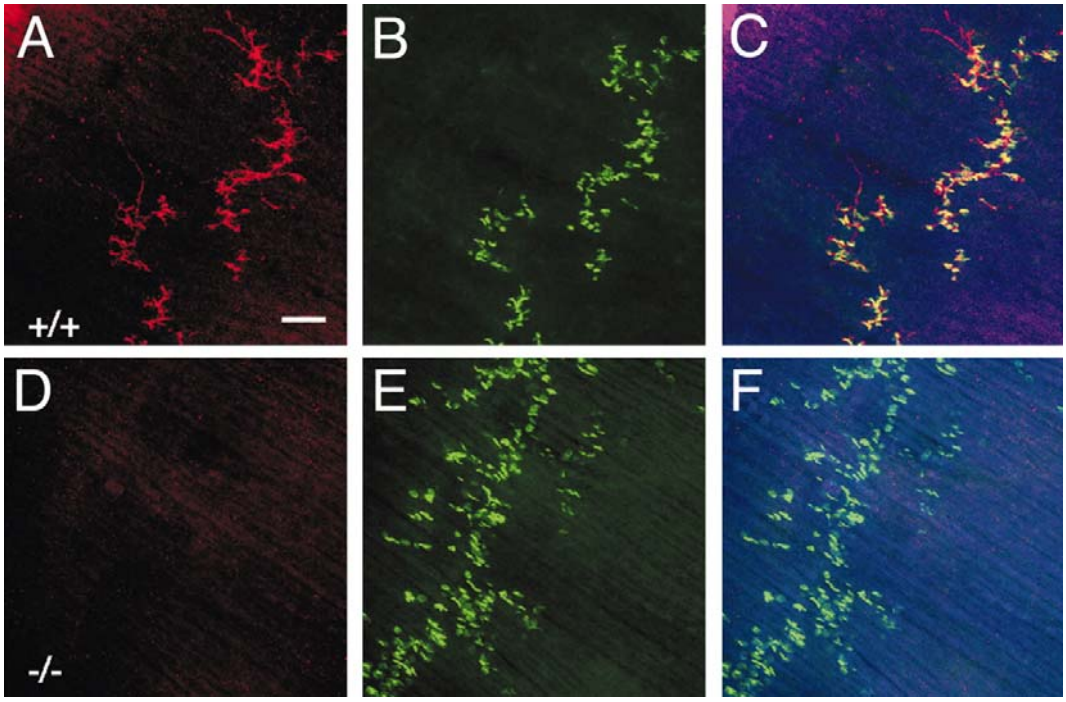
A
B
C
+/+
D
E
F
-/-

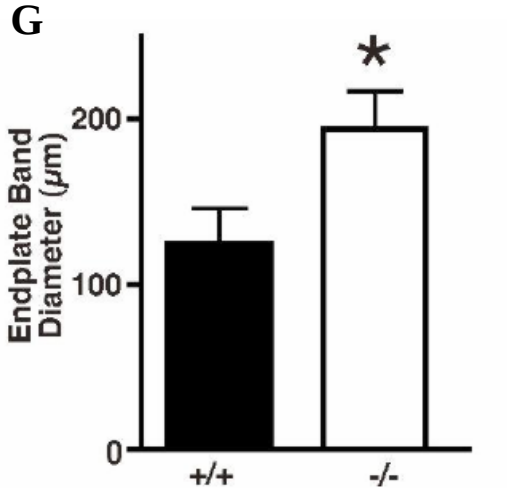
G
Endplate Band Diameter (μm)
200
100
0
*
+/+
-/-

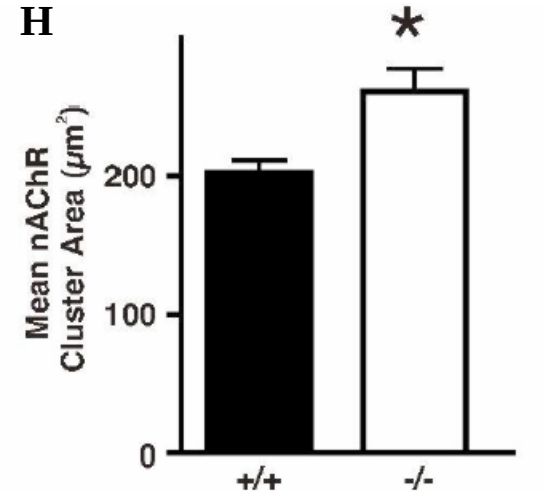
H
Mean nAChR Cluster Area (μm²)
200
100
0
*
+/+
-/-

Fig. 9. Alterations in nAChR distribution at CHT–/– NMJs. (A) CHT immunoreactivity is found in the axons and presynaptic terminals of motor neurons at CHT+/+ NMJs of the diaphragm (age = E19; scale bar = 80 μm). **(B)** Alexa-488--bungarotoxin labels clusters of postsynaptic nAChR clusters that form a band across the diaphragm. **(C)** The CHT-positive presynaptic terminals overlap the nAChRs on the muscle. Alexa-660-phalloidin labeling of actin reveals a regular pattern of muscle fibers. **(D)** CHT immunoreactivity is absent from motor neuron axons and terminals of the CHT–/– littermate. **(E)** The central band of nAChR clusters is wider in the CHT–/– diaphragm. **(F)** The loss of CHT–/– expression does not alter the morphology of the muscle fibers. **(G)** The diameter of the central band is greater at the CHT-/- diaphragm. Measurements were made at 30 μm intervals to assess the maximum diameter (perpendicular to axis of band) occupied by nAChR clusters.This data represents the average of measurements made from multiple fields of alexa-488-BgTx labeled whole mount diaphragms from 5 pairs of E19 littermates (640 μm x 640 μm fields, 20 measurements per field, >3 fields per animal, $p<0.005$, paired t test). **(H**) The area occupied by each individual Alexa488-α-bungarotoxin labeled nAChR cluster is also increased. This data represents the average area measured from a total of 4621 CHT+/+ and 4209 CHT-/- individual alexa488-BgTx labeled nAChR clusters on whole mount diaphragm preparations analyzed for 5 pairs of CHT+/+ and -/- littermates (E19, $p<0.005$, paired t test). Figure contributed by Valentina Savchenko.

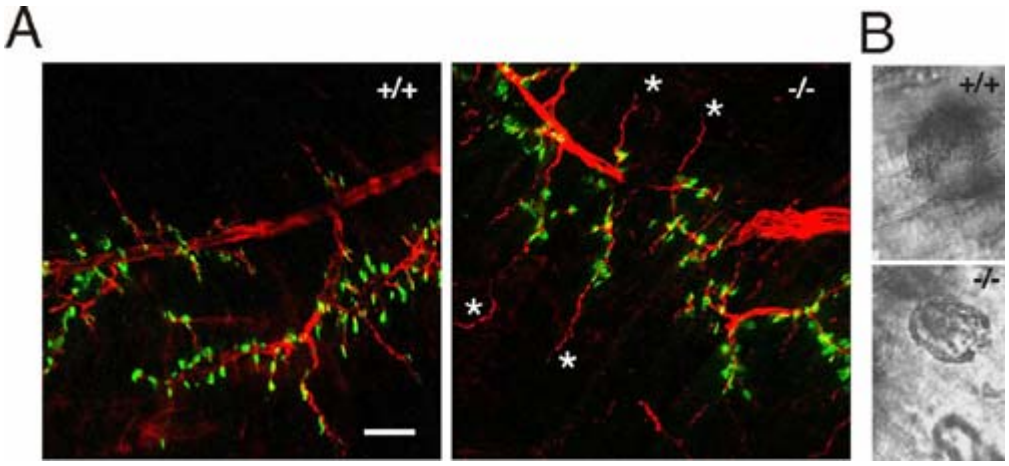

Fig. 10. CHT–/– NMJs are characterized by increased axonal sprouting and decreased acetylcholinesterase (AChE) activity. (**A)** Labeling of motor neuron axons for neurofilament immunoreactivity (red) and postsynaptic nAChR clusters by Alexa-488-α-BgTx (green) shows colocalization at the CHT+/+ diaphragm muscle. (Scale bar = 80 μm.) Although nAChR clusters colocalize with CHT–/– axons, these axons also frequently extend processes beyond the area occupied by nAChR clusters (asterisks). **(B)** Histochemical assays reveal a decrease in AChE activity (revealed by dark precipitate) at individual E19 CHT–/– motor neuron terminals compared with CHT+/+ synapses. Figure contributed by Valentina Savchenko.

clusters are on average larger in the CHT-/- mice compared with wild-type littermates (261 ± 17 μm^2 versus 202 ± 9 μm^2). These data represent the average area measured from a total of 4,621 CHT+/+ and 4,209 CHT+/- individual Alexa-488-α-bungarotoxin-labeled nAChR clusters on whole-mount diaphragm preparations analyzed for five pairs of CHT-/- and +/+ littermates (E19, $P < 0.005$, paired t test).

The morphology of the motor neuron axons at the diaphragm was examined by labeling for neurofilament immunoreactivity (Fig. 10A). There is a close overlap between CHT+/+ motor axons and underlying nAChR clusters, whereas motor axons in the CHT mice frequently extend processes beyond areas occupied by nAChRs. Finally, we have observed reduced AChE activity at individual synapses in the CHT knockouts relative to +/+ littermates (Fig. 10B). These alterations in NMJ morphology parallel, but are perhaps less severe than, those reported in the ChAT-knockout mice that are incapable of ACh synthesis (Brandon et al. 2003; Misgeld et al. 2002).

Discussion

Previous work has identified HACU as a major regulator of ACh synthesis (Freeman et al., 1979; Guyenet et al., 1973; Haga, 1971). The lethal effects and spectrum of cholinergic deficits arising from in vivo HC-3 administration support the physiological importance of this mechanism (Schueler, 1955). Nonetheless, work in cultured cells of neuroendocrine origin has demonstrated the feasibility of ACh synthesis and vesicular release (Bauerfeind et al., 1993) in the absence of detectable CHT expression (Apparsundaram et al., 2001b; Ferguson et al., 2003). Studies in neuroblastoma cells have also indicated pathways for the release of choline from membrane

phosphatidylcholine by phospholipase D (Lee et al., 1993) and low-affinity choline uptake mechanisms as sources of choline for ACh synthesis (Richardson et al., 1989). Even in neuronal preparations where CHT is present, such as the perfused superior cervical ganglia and striatal synaptosome preparations, there are reports of a small fraction (20%) of ACh synthesis that is independent of HC-3-sensitive choline uptake (Birks and MacIntosh, 1961; Guyenet et al., 1973).

A Lethal Phenotype Arising from Loss of CHT Expression

At the outset of our current studies, we envisioned several possible major phenotypes for CHT-/- mice. Because ACh synthesis and release are absolutely required for postnatal survival but are not necessary for viability in utero (Brandon et al., 2003; Misgeld et al., 2002), one prediction was that the loss of CHT-mediated presynaptic choline uptake might result in neonatal lethality. Alternatively, given the evidence for the existence of CHT-independent sources of choline for ACh synthesis, there was a possibility that these mechanisms could be up-regulated during development to compensate for the lack of CHT. A third possibility was that CHT could have as-yet unknown functions during development that could cause embryonic lethality for the CHT-/- mice.

In this study, we show that the CHT-/- mice are born in expected Mendelian ratios from the mating of heterozygous parents. However, they fail to survive their first hours of life, and their phenotype indicates an impaired ability to sustain the synthesis of adequate releasable pools of ACh. Unlike what is observed in the ChAT-/- mice (Brandon et al., 2003; Misgeld et al., 2002), the normal posture and capacity for movement observed in

CHT-/- mice at birth indicate the presence of limited stores of ACh produced in the absence of CHT. Indeed, our electrophysiological studies of cholinergic neurotransmission indicate the presence of a releasable pool of ACh that becomes depleted over time unless CHT is available to recapture choline back into the presynaptic terminal. Similarly, although we confirmed that CHT is uniquely responsible for both HC-3-sensitive HACU and HC-3-sensitive ACh synthesis, we also found evidence for HC-3-insensitive ACh synthesis in brain slices from the -/- mice. These latter findings are paralleled by observations of ACh synthesis in the c*aenorhabditis elegans* CHO-/-, likely supported by LACU mechanisms (Matthies et al., 2006). Overall, our studies confirm a unique role for CHT in sustaining cholinergic neurotransmission and indicate that although other pathways can supply choline that contributes to ACh synthesis, they are not sufficiently robust to compensate for the loss of the CHT-mediated transport activity in active cholinergic terminals.

It seems reasonable to conclude that the phenotypes of the CHT-null mice arise from a defect in ACh synthesis at the NMJ, because the only known function of CHT is to transport choline into cholinergic neurons, and cholinergic neurotransmission at the NMJs of the diaphragm and intercostal muscles controls breathing. Although the presence of limited movement and early time point recordings from CHT-/- NMJs indicate that some ACh is synthesized and released in the absence of CHT, the CHT-/- NMJs exhibit morphological changes that are similar to, but less severe than, the effects reported for ChAT-/- mice that completely lack ACh synthesis (Brandon et al., 2003; Misgeld et al., 2002). As ChAT and CHT are proposed to act sequentially in ACh synthesis and the two knockouts yield similar phenotypes, the most direct explanation is

that the diminished cholinergic function at the NMJ of the CHT-/- mice is sufficiently severe to reproduce some of the developmental effects previously attributed to total ACh loss. Because the CHT-/- mice recapitulate some, but not all, of the phenotypes of ChAT -/- animals, we propose that these findings reveal different quantitative thresholds for cholinergic signaling, particularly during development.

CHT Sustains Synaptically Releasable Pools of ACh

The similar total ACh levels in the brains of newborn CHT-/- compared with CHT+/+ mice (Fig. 6E) suggest that low levels of neuronal activity and ACh turnover in the newborn brain might not place a large demand on ACh synthesized from CHT-independent supplies of choline. At birth, the CNS cholinergic system is not well developed, particularly in the forebrain (Coyle and Yamamura, 1976). However, ACh levels greatly exceed expectations based on the relative abundance of ChAT activity at this age (Coyle and Yamamura, 1976). It is possible that developing cholinergic neurons possess abundant CHT-independent mechanisms for choline uptake to support phosphatidylcholine synthesis that could also contribute to ACh production. Indeed, in the newborn brain, we measured a sizable pool of HC-3-insensitive ACh synthesis (Fig. 6F). Nonetheless, both electrophysiological and morphological analysis of CHT-/- NMJs demonstrate a defect in the availability of releasable ACh, indicating that the CHT-dependent choline supply is intimately linked to the generation of synaptically releasable pools of ACh. These results are particularly intriguing in light of my findings of significantly diminished total ACh levels in the brains of adult CHT+/- mice, which appear to be sufficient to sustain baseline ACh releaseable pools and cholinergically-

mediated behaviors, but likely render the CHT+/- mice vulnerable to direct and sustained challenges to cholinergic signaling (Chapter III).

In summary, the generation and initial characterization of CHT knockout mice reported here demonstrates that choline transported by CHT contributes to ACh synthesis and is essential for sustaining cholinergic neurotransmission at levels required to support life. The recent report of a relatively common, nonsynonymous, single nucleotide polymorphism (SNP) in the coding region of human CHT that results in diminished choline transport (Okuda et al., 2002), as well as the identification of nonsynonymous ChAT SNPs with clinical phenotypes (Maselli et al., 2003; Ohno et al., 2001), predicts that variations in absolute levels of cholinergic capacity might be relatively common across human populations and set risk thresholds for a variety of disorders or their onset severity. In addition to the well recognized deficits in cholinergic function in myasthenic syndromes, defects in the capacity for ACh synthesis in the CNS may contribute to cognitive dysfunction and dementia and may place demands on the regulatory mechanisms revealed by our studies that control CHT function. Further characterization of CHT+/- mice (Chapter III), especially with respect to their responses to behavioral or pharmacological challenges, should identify distinct functions that are sensitive to diminished CHT reserve.

CHAPTER III

CHOLINE TRANSPORTER DEFICIENT MICE DISPLAY BASAL CHOLINERGIC DEFICITS AND MOTOR ABNORMALITIES IN RESPONSE TO PHYSICAL AND PHARMACOLOGICAL CHALLENGE

Introduction

ACh is a neurotransmitter of key importance in both central and peripheral nervous systems. Cholinergic neurotransmission maintains vital biological functions such as movement, autonomic regulation, and cognitive processes including attention and learning and memory (Kaneko et al., 2000; Misgeld et al., 2002; Perry et al., 1999a; Winkler et al., 1995) via both nicotinic (Dani, 2001) and muscarinic (Wess, 2004) receptors. CHT activity is believed to be the rate-limiting step for ACh synthesis and release, particularly under conditions of elevated cholinergic tone (Birks and Macintosh, 1957; Jope, 1979a; Simon and Kuhar, 1975). Consistent with this idea, in vitro inhibition of CHT by the competitive CHT antagonist HC-3 impairs ACh synthesis and release (Guyenet et al., 1973; Maire and Wurtman, 1985; Murrin et al., 1977), whereas *in vivo* pharmacological challenge with sublethal doses of HC-3 impairs learning and memory as measured in the Morris water maze and passive avoidance tasks (Boccia et al., 2004; Franklin et al., 1986; Hagan et al., 1989). Complete pharmacological blockade of CHT (Schueler, 1955) or homozygous deletion of the CHT gene in mice (Chapter II) results in death associated with reduced ACh release at central and peripheral cholinergic synapses that support respiration, including the neuromuscular junction (NMJ).

We identified the murine CHT (mCHT) (Apparsundaram et al., 2001a) with the express purpose of establishing novel in vivo models of cholinergic hypofunction derived from genetically-determined changes in CHT protein levels. As indicated above, CHT-/- newborn mice are apneic and hypoxic, largely immobile, and die within an hour birth (Chapter II). In contrast, CHT+/- mice survive, are grossly indistinguishable from CHT+/+ mice and exhibit levels of forebrain choline uptake equivalent to that of CHT +/+ littermates despite a 50% reduction in CHT protein levels (Ferguson et al., 2004). These latter findings are consistent with the existence of efficient, post-translational regulation of HACU (Apparsundaram et al., 2005; Ferguson and Blakely, 2004) and/or changes in ACh synthesis, release or response. Importantly, CHT +/- mice appear more sensitive to HC-3 (Ferguson et al., 2004), suggesting the existence of underlying compensatory changes beyond CHT that may be engaged to sustain normal behavior.

In the experiments described below, I sought to elucidate basal behavioral and biochemical phenotypes of CHT+/- mice, and initiate an exploration of altered sensitivity in CHT+/- mice to physical and pharmacological challenges. I establish that whereas CHT hemizygosity does not result in overt behavioral phenotypes, this condition leads to significantly reduced bulk ACh brain levels and renders animals vulnerable to behavioral and pharmacological challenges of cholinergically-mediated behaviors. Moreover, I identify changes in M1 and M2 muscarinic receptor densities that I hypothesize arise to compensate for loss of CHT, but which ultimately alter the dynamic range of cholinergic signaling. I discuss my findings in relation to CHT regulation in response to genetic and pharmacological challenges and loss-of-function alleles evident in humans.

Materials and Methods

Drugs

Scopolamine hydrochloride (S-1013) and oxotremorine sesquifumarate salt (O-9126) were obtained from Sigma-Aldrich (St Loius, MO) and dissolved in sterile saline (0.9% NaCl). Both drugs were injected intraperitoneally at a volume of 10 ml/kg.

Mice

All animal procedures were approved by the Vanderbilt University Institutional Animal Care and Use Committee. Mice were housed up to five per cage on a 12-hour light/dark cycle (lights on at 0600 am), and behavioral testing was performed during the light part of the cycle. Food (Purina Rodent Chow #5001) and water were provided ad libitum. All mice were back-crossed at least 7 generations to the C57Bl/6 background except in the rotarod, elevated plus maze, and scopolamine-induced locomotion experiments, where CHT+/- mice back-crossed for 2 generations were used. In all cases, CHT+/+ littermates were used as controls. All behavioral tests were carried out in the Murine Neurobehavioral Laboratory of the Center for Molecular Neuroscience, managed by Dr. John D. Allison. Mice naive to behavioral testing were used in each behavioral task. Mice were acclimated to the testing location at least 12 hours before the start of behavioral testing.

Irwin Screen

At 12 weeks of age, 7 mice from each genotype were subjected to a modified Irwin screen (Irwin, 1968), to assess basic sensory-motor performance. Specifically, the following factors were evaluated on a numerical scale of 0-3: gross appearance (presence of whiskers, fur, wounds, and body weight); behavior in a novel environment (mice were removed from their home cage, placed in a new, clean cage devoid of bedding and evaluated for spontaneous activity, tremor, piloerection, tail elevation, urination, and defecation); and reflexes (touch escape, reaching reflex, pinna reflex).

Exploratory locomotor activity

Locomotion was evaluated in 9- to 12-week-old mice (CHT+/-, n=18; CHT+/+, n=19) using a commercially-available activity monitors measuring 27.9 x 27.9 cm (MED Associates, Georgia, VT). Each apparatus contained 16 photocells in each horizontal direction, as well as 16 photocells elevated 4.0 cm to measure rearing. Mice were placed in the monitors for 30 min and allowed to explore freely. Horizontal beam breaks and rearing were automatically recorded and represented as distance traveled and vertical counts respectively. Data were analyzed in 5-min time bins.

Rotarod

Motor coordination and balance were measured in 3-month-old mice (CHT+/-, n=7; CHT+/+, n=5), using a commercially-available accelerating rotarod apparatus (Model 7650, Ugo Basile, Napoli, Italy). Mice were placed on the rotating cylinder (3 cm in diameter) and confined to a section approximately 6.0 cm long by grey plastic dividers.

The rotational speed of the cylinder was increased from 5 to 40 r.p.m. over a 5-min period. Latency at which mice fell off the rotating cylinder was measured. Each mouse was given 3 trials per day over a period of 3 days.

Elevated plus maze

Anxiety was evaluated using the elevated plus maze. The home-made plus maze consisted of four arms, approximately 10 x 30 cm, connected in a plus configuration and elevated approximately 40 cm above the floor. Two of the arms had walls, approximately 15 cm high ("closed arms"), and two walls had no arms ("open arms"). Mice were placed gently in the center of the four arms at the beginning of the session. The number of entries onto the open arms, and amount of time spent in open arms were recorded.

Light-dark exploration

Anxiety responses were also assessed in 2- to 3-month-old mice (n=8 per genotype), using the activity monitors (MED Associates, Georgia, VT). Half of the chamber was made opaque with a black acrylic insert, while the other half remained transparent. Photocells recorded the movement of the mice between compartments. Mice were placed individually into the dark compartment at the beginning of the session. Total time spent in the dark versus light compartments were recorded. Each mouse was given one 5-minute session.

Morris water maze

Spatial learning and memory were evaluated in CHT+/- (n=11) and CHT+/+ (n=12) mice using the hidden-platform water-maze paradigm. The water maze pool was 92-cm in diameter and filled with water made opaque with non-toxic tempura paint. An acrylic platform (10x10 cm) was submerged approximately 0.5 cm below the surface of the water to allow relief from swimming. The mice were given six spaced trials per day. The hidden platform remained in a fixed location throughout the experiment, but starting positions were different on each trial. Each trial continued for a maximum of 60 sec or until the mouse reached the platform, whichever occurred first. If a mouse did not reach the platform in 60 sec it was captured by the experimenter and placed gently on the platform for 15 sec. Sessions were captured by an overhead camera and analyzed in real time using an NIH Image macro on a Macintosh computer. Parameters measured included latency (time to reach platform), swimming velocity, and path length. Data were analyzed immediately following each set of trials, and once each group of mice reached criterion or 8 sec average latency, they were given a probe test 2 hours after their last training session. Both genotypes reached criterion on the same day, and therefore all mice received the same number of trials.

In the probe trial, the platform was removed, and mice were allowed 60 sec to explore the water maze. The amount of time spent in each quadrant of the pool and platform location crossings were measured for the 60-sec probe trial. A second probe trial was performed 48 hours after the initial probe trial. Following this, mice were re-trained using a new platform location. Platform location was constant across days, and each mouse was ran for 6 spaced trials (6 different starting locations) each day until target

latency to reach the platform (8 sec average for each genotype) was reached. Probe trials were ran 2 hours and 48 hours after the last reverse platform training trial.

Treadmill

Eight- to 10-week-old mice (n=11 per genotype) were run on a motorized, 6-lane treadmill (Columbus Instruments, Columbus, OH) equipped with an adjustable-speed belt (6-100 M/min), and an electric shock grid at one end. On day 1 (training) the mice were exposed to the treadmill without running or shock for 10 min. They were then exposed to gradually-increasing speeds (10 m/min maximum) for 15-30 min in the presence of electric shock (2 mA, 4 min^{-1} frequency) activated by physical contact with the shock grid. This trial was used purely for training purposes and to familiarize the mice with the apparatus. On day 2 (gradual increase in speed**)** the mice were started at 10 m/min and the speed was increased by 1.5 m/min every 2 min. The maximal speed achieved by each mouse and the maximal time a mouse could keep running were recorded and interpreted as measures of motor fatigue. Exhaustion was defined as resting on the electric grid for more than 15 sec/min or falling back onto the grid more than 15 times/min. On day 3 (constant speed) the initial running speed was 6 m/min, and was increased every 30 sec by 2 m/min until a speed of 17 m/min was reached after 2.5 min. At this point the speed was maintained at 17 m/min and the mice were run until exhaustion. To exclude the possibility that the phenotype was due to learning difficulties, the mice were tested in the same paradigm on 2 additional consecutive days, and similar results were obtained. As a control for pain sensitivity, I tested a separate group of experimentally-naive littermates (n=7 per genotype). I exposed the individual mice to shock of increasing current

amplitude, with rest periods between shocks of varying amplitudes, and recorded the current amplitudes at which the mouse first jumped and/or vocalized, as a readout of sensitivity to shock.

Scopolamine-induced locomotor activity

On drug test days the mice were acclimated to the activity monitors (MED Associates, Georgia, VT) for 1 hour, removed and injected i.p. with vehicle or scopolamine, and returned to the activity monitors for 2 hours for activity measurements. Naïve mice were used for each drug concentration. N=8, n=12, and n=5 mice from each genotype were used for the 1mg/kg, 0.5 mg/kg, and 0.1 mg/kg doses respectively.

Oxotremorine-induced tremor

Mice were taken from their home cages and placed in new, individual (one mouse/cage) transparent cages devoid of bedding, and allowed to acclimate for 15 minutes. Each mouse was injected i.p. with vehicle or oxotremorine, and returned to the cage for observation. Naïve mice were used for each drug concentration, and the observer was blind to the genotypes. N=5 mice from each genotype were used for the 0.125 mg/kg and 0.031 mg/kg doses, and n=17 mice from each genotype were used for the 0.062 mg/kg dose. Tremor was scored every 5 minutes on a scale of 0-2 (0 = no tremor, 1 = head and body tremor, 2 = continuous tremor whole body tremor). The data were expressed as percent of the maximal possible tremor (for example a score of 1 was represented as (1 (actual score)/2 (maximum possible score)*100=%tremor) (Li et al., 2003).

Synaptosomal Biotinylation.

I evaluated plasma membrane CHT protein density in crude synaptosomes using the membrane-impermeant biotinylating reagent, sulfosuccinimidobiotin (NHS-biotin) (Pierce Chemical, Rockford, IL). Crude synaptosomes (150 µg of protein/reaction) were incubated with NHS-biotin (3 mg/ml) for 45 min at 4°C, after which ice-cold 1M Tris buffer (pH 7.8) was added, and the reactions were spun at 11k rpm for 5 min at 4°C. The pellet was resuspended in KRH/Tris buffer, spun down again, and lysed with 500 µl of radioimmunoprecipitation assay (RIPA) buffer (10 mM Tris, pH 7.4, 150 mM NaCl, 1 mM EDTA, 0.1% SDS, 1% Triton, and 1% sodium deoxycholate) supplemented with protease inhibitors (1 µg/ml leupeptin, 1 µg/ml pepstatin, 1 µg/ml aprotinin, and 250 µM phenylmethylsulfonyl fluoride). The extracts were incubated with streptavidin beads (Pierce Chemical, Rockford, IL) in the same buffer for 1 h at 4°C. Following the incubation, the biotinylated fractions bound to the beads were separated by centrifugation, washed in RIPA lysis buffer three times, and eluted by washing in Laemmli buffer (62.5 mM Tris, pH 6.8, 20% glycerol, 2% SDS, and 5% bromphenol blue, supplemented with 5% -mercaptoethanol) for 30 min at room temperature. Aliqots of total extract (10% of crude synaptosomal preps) and bead eluents were used in SDS-PAGE for protein separation as described in Immunoblotting methods section (Chapter II). Calnexin immunoblotting was used as a negative control to monitor biotinylation of intracellular proteins by membrane-impermeant NHS biotin, whereas transferin receptor immnoblotting was used as a positive control for plasma membrane protein biotinylation. CHT protein band densities were normalized to transferin receptor band densities.

ACh levels, ChAT and AChE Activity

ACh levels in brain tissue were quantified by previously described high performance liquid chromatography (HPLC) electrochemical detection methods (CHT+/-, n=7; CHT+/+, n=7) (Vanderbilt Neurochemistry Core Resource) (Damsma et al., 1985). Briefly, brain tissue was microwaved for acetylcholinesterase (Bertrand et al., 1994), followed by homogenization in acetonitrile, lipid removal with heptane, and vacuum drying. Activity of ChAT was measured by the synthesis of [14C]ACh from [acetyl-1-14C]acetyl-CoA and choline (CHT+/-, n=4; CHT+/+, n=4) (Frick et al., 2002). AChE activity was determined by colorimetric measurements following the method of Ellman (CHT+/-, n=5; CHT+/+, n=5) (Ellman et al., 1961).

Immunoblot analysis of mAChR expression

Freshly dissected brain tissue (n=4 mice per genotype) was frozen in tubes on dry ice and stored at -80°C. As needed, tubes were removed from -80°C and placed on ice. Protease inhibitor (Sigma, St. Louis, MO, #2714) was dissolved in 10 mM Tris, 1 mM EDTA, pH 7.5, and 500 ul was added to each tube. The tissue was homogenized with a Brinkman Polytron PT3000 using a PT-DA 3007/2 tip at 20k rpm for 10 seconds and the tip was rinsed with dH2O between each sample. After determining and adjusting protein concentration, the homogenate was diluted with sample buffer to yield 1% sodium dodecyl sulfate (SDS), 31.25 mM TRIS pH 6.8, 5% glycerol, 200mM 2-mercaptoethanol. The samples were then resolved on a 10% gel by SDS-polyacrylamide gel electrophoresis (PAGE), transferred to polyvinylidine difluoride membranes and subjected to immunoblot analyses with M1 and M2 polyclonal antibodies (Li et al., 2003;

Volpicelli-Daley et al., 2003b), as well as an EF1a monoclonal antibody for loading control, using an Odyssey imager (Li-Cor, Lincoln, NE). Blot densitometry was performed using ImageJ software (Wayne Rasband, NIH) and the muscarinic receptor band densities were normalized to the EF1a band densities (Volpicelli-Daley et al., 2003b).

Statistical analyses

Two-way repeated measures ANOVA and two-tailed, unpaired Student's t tests were used to analyze the data. The specific statistical analyses used are noted in the text and legends with respect to individual test design.

Results

CHT+/- mice exhibit wild-type levels of overall locomotor activity, but altered patterns of movement in the open field chamber paradigm

Basal exploratory locomotor activity was evaluated in CHT+/- mice and CHT+/+ siblings in the open field activity monitors. CHT+/- mice consistently traveled shorter distances during their first 30 minute exposure to the open field chambers (CHT+/-, 3081 ± 171.8 cm; CHT+/+, 3658 ± 217.7 cm) (Fig 11A). This difference was statistically significant ($F_{(1, 180)} = 4.33$; $P < .05$). In preliminary studies, we also observed diminished motor activity upon initial, but not continued exposure to a running wheel setup in the home cage (data not shown), suggesting a novelty effect may be responsible for the CHT+/- hypolocomotive phenotype. Intriguingly, vertical movement was higher in the CHT+/- mice (711.4 ± 79.0 counts) compared to their CHT+/+ siblings (463.5 ± 90.3

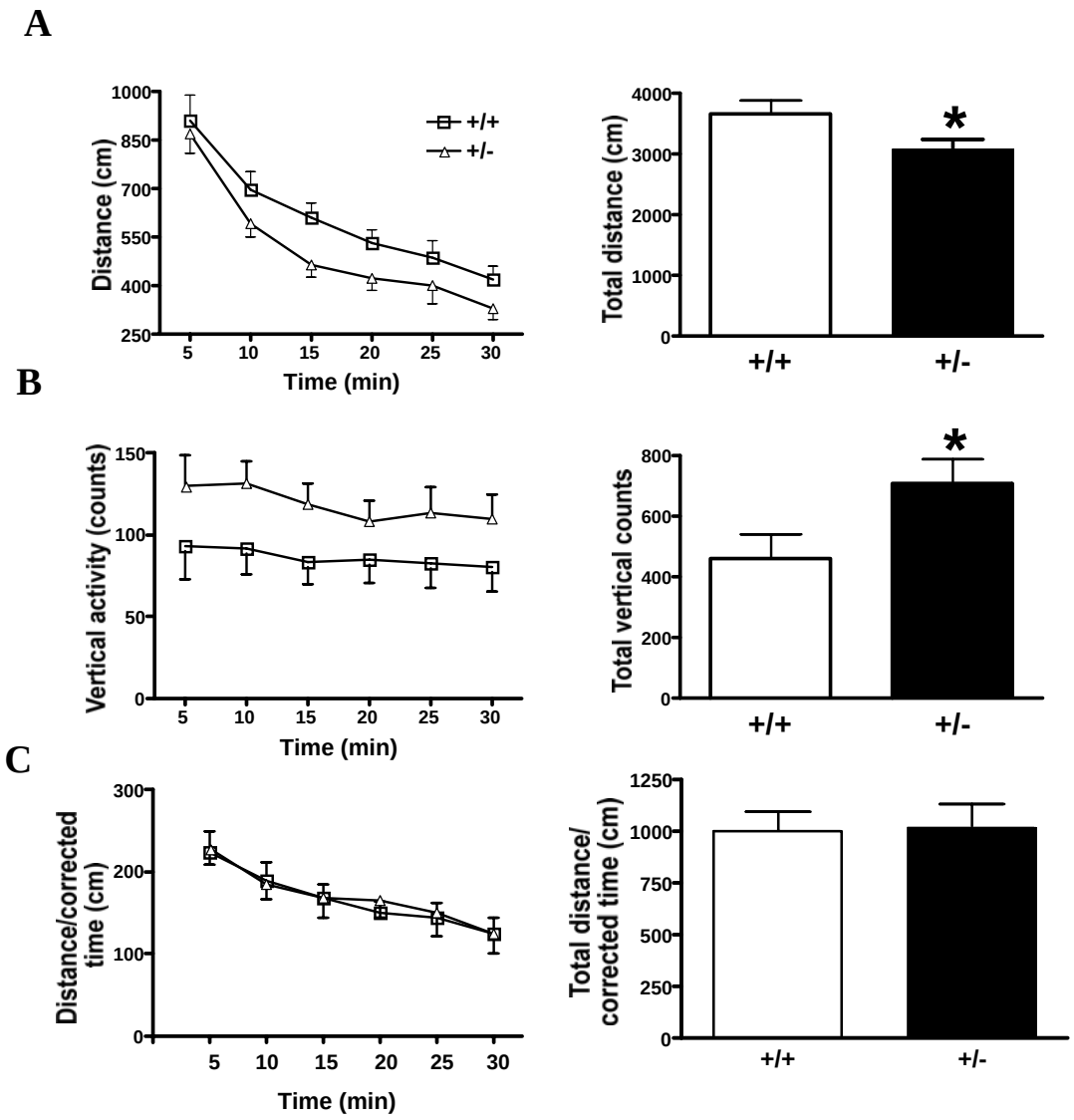

Figure 11. CHT+/- mice display altered basal locomotion in the open field paradigm. CHT+/- mice display reduced horizontal locomotion **(A)**, and increased vertical activity **(B)** in the novel open field environment compared to CHT+/+ littermates. When horizontal activity is corrected for the additional time spent rearing, activity levels are not significantly different between the genotypes **(C)**. Filled triangles, CHT+/- (n=18); open squares, CHT+/+ (n=19). Mean (±SEM) values are indicated (*$p<0.05$).

counts) ($F_{(1,\ 175)} = 5.04$; $P < 0.05$) (Fig. 11B). The inverse relationship between ambulatory and rearing counts suggests that lower levels of horizontal activity by the CHT+/- mice may be due to increased vertical activity, possibly due to increased exploratory drive, rather than impairments in sensory-motor ability. Indeed, when time spent in vertical motion was eliminated from recordings, CHT+/- and CHT+/+ mice showed equivalent distance traveled (Fig. 11C).

Basal sensory-motor performance is intact in CHT+/- mice

A modified Irwin screen (Irwin, 1968) failed to reveal any difference in basal sensory-motor phenotypes between genotypes (data not shown). In addition, the mice were tested on a rotarod test. Both genotypes learned the task at the same rate and demonstrated equivalent performance, as indicated by increases in similar average latencies before falling off the accelerating rod over a period of 3 consecutive trial days (Day 1 latencies: CHT+/-, 66.4 ± 13.4 sec vs CHT+/+, 63.2 ± 22.7 sec; Day 2 latencies: CHT+/-, 188.6 ± 27.1 sec vs CHT+/+, 169.1 ± 39.0 sec; Day 3 latencies: CHT+/-, 245.6 ± 26.0 sec vs CHT+/+, 194.5 ± 35.0 sec (Fig. 12A). There was also no significant difference in the amount of time CHT+/+ and CHT+/- littermates were able to hold onto an inverted screen (data not shown). These results suggest that a single functional CHT allele is sufficient to support overall motor balance and coordination as well as muscle strength.

CHT+/- mice do not show elevated anxiety

One possible explanation for the changes in vertical activity observed in the open

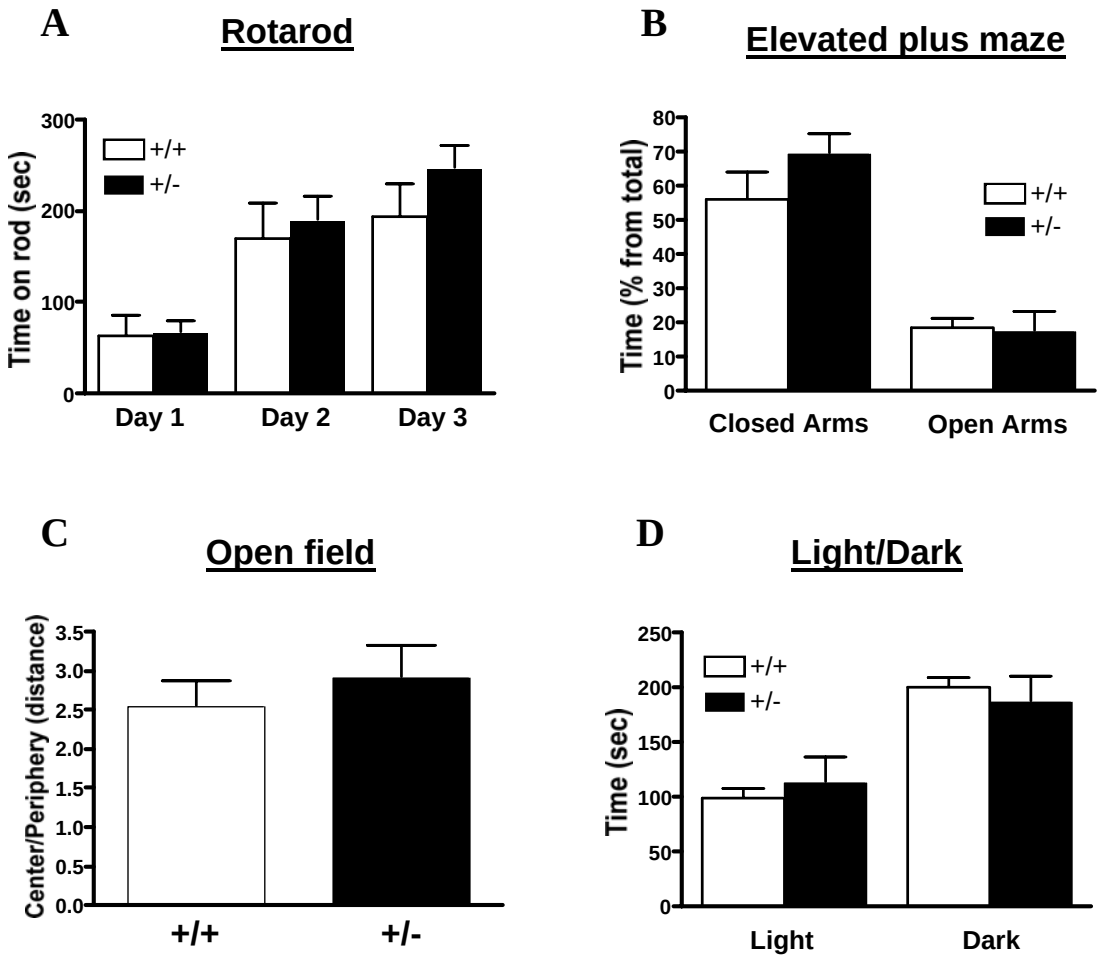

Figure 12. Basal sensory-motor and anxiety behaviors are normal in the CHT+/- mice. Motor coordination, balance, and learning are similar between CHT+/- (n=7) and CHT+/+ (n=5) littermates in the rotarod paradigm (average latencies of 3 trials/day) **(A)**. Anxiety levels are similar between CHT+/- mice and CHT+/+ littermates as indicated by same amount of time spent in open versus closed arms in the elevated plus maze (n=5/genotype) **(B)**, in center vs periphery in open field/novel environment paradigm (CHT+/-, n=18; CHT+/+, n=19) **(C)**, and in light vs dark section of the light/dark paradigm (CHT+/-, n=6; CHT+/+, n=8) **(D)**. Mean (±SEM) values are indicated.

field paradigm is elevation in anxiety. To test this hypothesis, the distance traveled in the center versus the periphery of the open field was evaluated in the same open field trials used to quantify locomotor movement. I found no significant genotype difference in the ratio between distance traveled in the center versus periphery (arbitrary units: CHT+/-, 2.92 ± 0.41; CHT+/+, 2.53 ± 0.34) (Fig. 12C). For an additional evaluation of anxiety, a separate, naïve group of mice was given a 5-min trial in the light/dark paradigm. Again, there was no significant difference between genotypes in the amount of time they spent in the light (CHT+/-, 112.8 ± 23.4 sec; CHT+/+, 99.2 ± 9.0 sec), versus the dark (CHT+/-, 186.2 ± 23.4 sec; CHT+/+, 199.8 ± 9.0 sec) part of the field and, as expected, both genotypes spent more time in the dark part of the field (Fig. 12D). In a final evaluation of anxiety, mice were tested on the elevated plus maze. Consistent with other anxiety measures noted above, the percent time spent in open arms (CHT+/-, 17.4 ± 5.7%; CHT+/+, 18.5 ± 2.7%) versus closed arms (Fig. 12B) (CHT+/-, 69.2 ± 5.9%; CHT+/+, 56.1 ± 8.0 %), and percent entries into open (CHT+/-, 25.3 ± 6.7%; CHT+/+, 31.5 ± 7.6%) versus closed (CHT+/-, 58.7 ± 7.6%; CHT+/+, 60.5 ± 10.8%) arms were not different between the genotypes.

CHT+/- mice display normal performance in the Morris water maze

With findings of normal baseline sensory-motor performance in the CHT+/- mice, I next evaluated CHT genotype effects on spatial learning and memory using the Morris water maze (Winkler et al., 1995). CHT+/- mice did not differ from CHT+/+ littermates in any aspect of the task. Both genotypes learned the Morris water maze task equally well as indicated by similar latencies to reach the platform (Fig. 13A) ($F_{(1,147)} = 0.01$; $P = 0.31$)

and decreasing latencies over 8 days of training ($F_{(7,147)} = 31.02$; $P < 0.0001$). CHT+/- mice were also unimpaired in acquisition of a novel platform location ($F_{(1,60)} = 0.09$; $P = 0.91$) (Fig. 13B) and had similar swim speeds (data not shown). On the probe trial, both CHT+/- and CHT+/+ mice spent significantly greater periods of time in the target quadrant (CHT+/-, 44.5 ± 1.3% of total time ($F_{(3,30)} = 37.19$; $P < 0.0001$); CHT+/+, 41.3 ± 1.8% of total time ($F_{(3,33)} = 13.59$; $P < 0.0001$) (Fig. 13C), indicating intact memory for the platform location. Similarly, mice of both genotypes were more likely to swim over the former platform location, compared to equivalent locations in the other three quadrants (CHT+/-, 3.3 ± 0.9 and CHT+/+, 2.2 ± 0.5 number of crossings over former platform location) (Fig. 13D). No differences in any of the above parameters were observed upon repeating the probe trial 48 hours after the last training session (data not shown) or upon reversing the platform location and repeating the learning and probe trials. To evaluate the effects of aging on spatial learning, a group of naïve 1.5-year-old mice of identical genetic background were tested in the same water maze paradigm using the same test parameters, with results similar to those obtained with younger animals (data not shown).

CHT+/- Mice Are Hypersensitive to the Effects of HC-3

The wild type behavior by the CHT+/- mice in the above assays leads to the question – while CHT hemizygosity appears to be sufficient to support baseline physiology, do challenges directed at CHT function compromise CHT+/- performance? Intraperitoneal injection of the CHT inhibitor, HC-3, results in hypocholinergic function and death (Schueler, 1955). Furthermore, inhibition of choline uptake into synaptosomes

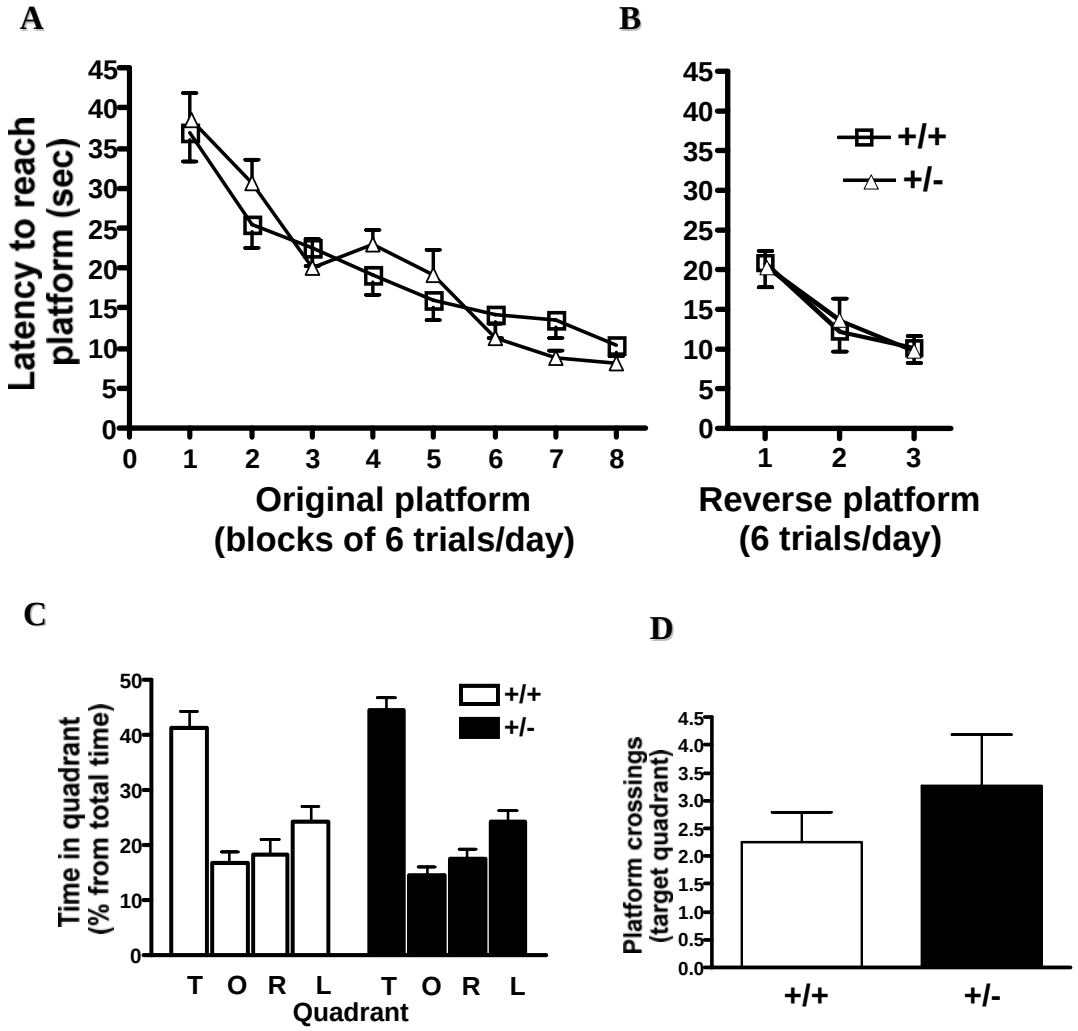

Figure 13. CHT+/- baseline spatial learning and memory performance are normal in Morris water maze paradigm. 3-month-old CHT+/- (n=11) and CHT+/+ (n=12) mice were run in the hidden platform version of the Morris water maze. The CHT+/- mice did not differ on latency to reach the platform during learning trials with original **(A)** and reversed **(B)** platform locations. Both genotypes spent similar amounts of time in the target quadrant on probe trials on the last day of training **(C)** as well as a delayed probe trial (48 hours later, data not shown), and did not differ in number of platform location crossings **(D)**. T = target (platform), O=opposite, R=right, L=left quadrant.

with HC-3 evokes a subsequent increase in choline uptake after the inhibitor is washed away, suggesting that the CHT reserve can be recruited by inhibiting choline uptake (Rylett et al., 1993). If the CHT+/- mice have already functionally compensated for diminished CHT levels, perhaps in part by depleting their vesicular reserves, then they might exhibit greater sensitivity to the lethal *in vivo* effects of HC-3. Therefore, I next tested the HC-3 sensitivity of adult male CHT+/- mice (Fig. 14D). The behavior of the mice after HC-3 administration was similar to that in the original reports of the toxicity of this drug and included labored breathing and convulsions (Schueler, 1955). At a HC-3 dose of 46 µg/kg, wild-type mice displayed labored breathing but then recovered normal function with 100% survival (n = 9), whereas the majority (60%) of the CHT+/- mice did not survive. Likewise, at a dose of 175 µg/kg, all CHT+/- mice died (n = 6) but 50% of wild-type mice still survived (n = 6). At the highest dose examined (655 µg/kg) I observed no survival for the CHT+/- animals (n = 9), whereas only 1 of 6 CHT+/+ mice survived. In comparing the animals of the two genotypes that did not survive the 655 µg/kg HC-3 challenge, the time required for death to occur was significantly less for the CHT+/- mice compared with their +/+ littermates (Fig. 14B) (7.6 ± 0.8 min versus 12 ± 1.2 min, $P < 0.05$, Student's t test).

Physical challenge unmasks a locomotor phenotype in the CHT+/-s

The lack of impairment in the behavioral tasks described previously suggests that cholinergically-supported motor function and spatial learning and memory are normal in the CHT+/- mice under standard measurement conditions. However, the HC-3 lethality studies clearly uncover altered CHT+/- susceptibility to challenge directed at

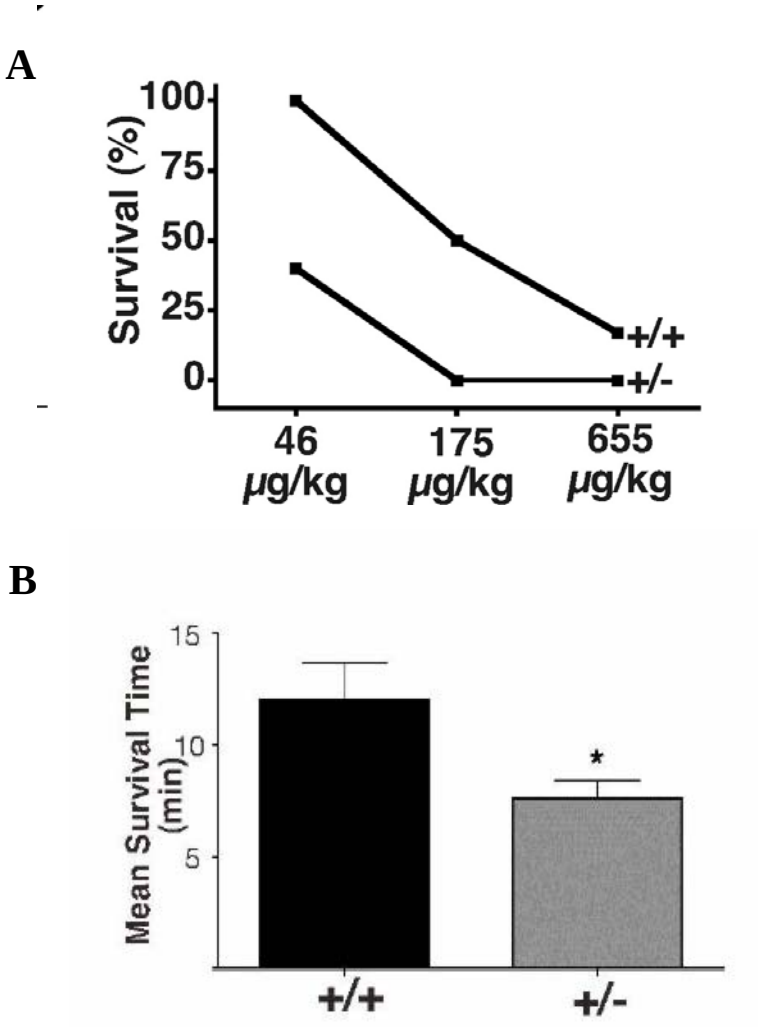

Figure 14. CHT+/- mice are hypersensitive to the effects of HC-3. (A) CHT+/- mice are more sensitive to the lethal effects of HC-3 (i.p. injection) than their +/+ littermates: 100% (n = 9), 50% (n = 6), and 17% (n = 6) survival were observed in CHT+/+ mice with increasing HC-3 doses, whereas the same HC-3 doses resulted in lower survival rates, 40% (n = 10), 0% (n = 6), and 0% (n = 9) in CHT+/- littermates. **(B)** At the highest HC-3 dose (655 µg/kg) the mean survival time was significantly decreased in the CHT+/- mice (7.6+/-0.8 versus 12+/-1.2 minutes, *$p<0.05$, t test).

cholinergically-supported behaviors. Therefore, I next focused on locomotor performance of the CHT+/- animals, and used the treadmill paradigm in order to introduce graded physical demands. My hypothesis was that under conditions of sustained physical challenge – such as continuously increasing treadmill speed (gradual challenge) and/or sustained high speed (acute challenge) – motor performance would be interrupted sooner in the CHT+/- mice compared to their CHT+/+ littermates. Quantitative predictions were that the CHT+/- mice would be unable to reach treadmill speeds as high as those attained by CHT+/+ littermates, and that at a constant treadmill speed the CHT+/- mice would fatigue sooner than the CHT+/+ littermates. Both predictions were confirmed experimentally: whereas both genotypes were able to sustain activity on the treadmill initially, the average time spent running in the gradual acceleration version of the task was significantly lower in the CHT+/- mice (772 ± 60.6 sec) compared to CHT+/+ mice (1089 ± 55.8 sec) ($t_{(12)} = 3.85$, $P < 0.001$) (Fig. 15A). In addition, 18% of CHT+/+'s reached maximal speeds of 25 m/min, while none of the CHT+/-'s exceeded 22 m/min, and only 9% CHT+/- mice reached 22 m/min, versus 45% of CHT+/+'s (Fig. 15B).

In the acute challenge paradigm, the average time spent running was again significantly lower in the CHT+/- mice (1169 ± 139.5 sec) as compared to CHT+/+ littermates (1743 ± 146.3 sec) ($t_{(12)} = 2.84$, $P < 0.01$) (Fig. 15C). Whereas both genotypes performed similarly initially (100% of both genotypes remained on the treadmill at 10 min), only 45.4% of CHT+/- mice, compared to 81.8% of CHT+/+ mice remained on the treadmill by 20 min, only 18.2% of CHT+/- mice but 72.7% of CHT+/+ littermates remained by 30 min, and 0% of CHT+/- mice versus 64.6% of CHT+/+ animals remained longer than 35 min (Fig. 15B). It is unlikely that the differences were due to lack of

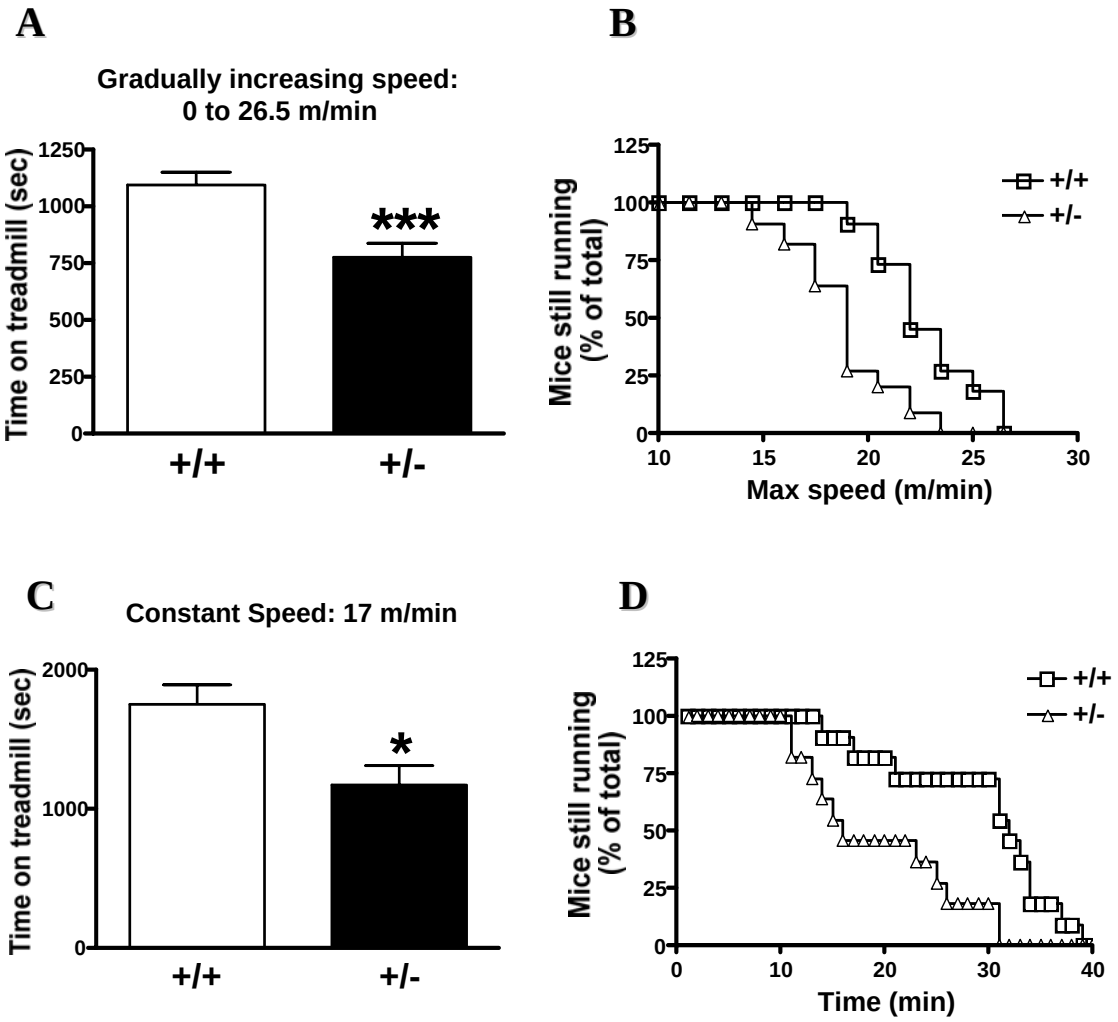

Figure 15. **Physical challenge unmasks a locomotor phenotype in the CHT+/- mice.** CHT+/- mice (n=11) remained on the treadmill for significantly shorter periods of time in both gradual **(A)** and acute **(C)** challenge versions of the treadmill paradigm compared to CHT+/+ littermates (n=11). In addition, while both genotypes performed similarly initially, CHT+/- mice displayed motor fatigue sooner **(D)**, and none of the CHT+/- mice reached the maximal speed reached by the CHT+/+ littermates (**B)**. Mean (±SEM) values are indicated (*p<0.01,***p<0.001).

sensory feedback in the mice, as all mice vocalized and/or jumped when exposed to the electric grid, and immediately resumed running either voluntarily or in response to gentle prodding, unless they were completely exhausted. In addition, a separate experimentally-naïve group of mice was tested for responses to increasing shock amplitudes, and no significant differences in shock sensitivity were evident between genotypes: CHT+/- mice first vocalized at 0.33 ± 0.02 mA of current, while CHT+/+ mice vocalized at 0.35 ± 0.04 mA of current.

Locomotor phenotype in CHT+/- mice is induced by muscarinic challenge

To complement studies of physical stress on cholinergic systems, I investigated pharmacological challenges known to impact ACh signaling and ensuing locomotor performance. Challenge with muscarinic antagonists has a well-known stimulatory effect on locomotor activity, mediated by increased ACh release (Gerber et al., 2001; Gomeza et al., 1999b; Miyakawa et al., 2001; Sipos et al., 1999). I constructed a dose-response profile for CHT+/- mice and CHT+/+ littermates, using open field locomotor behavior as a measure of motor activity (Fig. 16). In both genotypes, locomotion was not affected or increased equally at low (0.1 mg/kg) ($F_{(1,72)} = 1.26$, $P = 0.29$) (Fig. 16A) and high (1 g/kg) ($F_{(1,169)} = 0.26$, $P = 0.62$) (Fig. 16C) doses of scopolamine, respectively.

However, at an intermediate dose (0.5 mg/kg), the CHT+/- mice were significantly less active than their CHT+/+ littermates (Fig. 16B) ($F_{(1,308)} = 4.94$, $P < .05$) (Fig. 16D). The difference in sensitivity to scopolamine was evident in measurements of distance traveled only, as both genotypes displayed equal increases in vertical counts following scopolamine injection (data not shown).

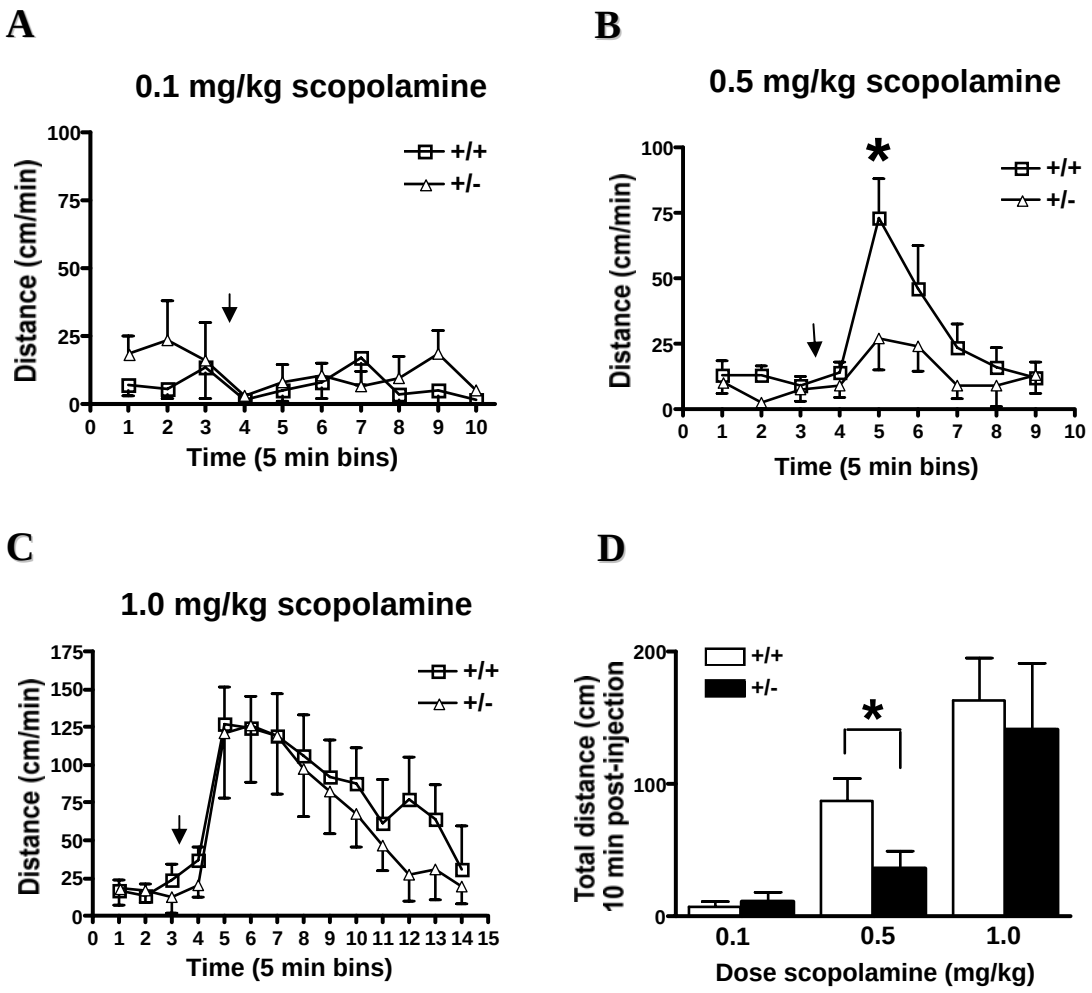

Figure 16. **Locomotor phenotype in CHT+/- mice is induced by muscarinic challenge.** In both genotypes (CHT+/-, n=11; CHT+/+, n=12), locomotion was not affected or increased equally at low (0.1 mg/kg) **(A)** and high (1 mg/kg) **(C)** doses of scopolamine respectively. However, at an intermediate dose (0.5 mg/kg) **(B)**, the CHT+/- mice were significantly less active than the CHT+/+ littermates, showing a decreased sensitivity to the muscarinic antagonist scopolamine **(D).** Arrow = point of drug administration (*$p<0.05$).

In contrast to their hyposensitivity to scopolamine challenge, the CHT+/- mice displayed a dose-dependent increased sensitivity to the muscarinic agonist oxotremorine. Similar to the effects of scopolamine, oxotremorine induced dose-dependent increases in tremor response of the CHT+/- compared to CHT+/+ littermates. There was no difference between the genotypes at low (0.031 mg/kg) and high (0.125 mg/kg) doses of oxotremorine. However, 15 min after injection of an intermediate dose (0.062 mg/kg), the CHT+/- mice displayed a higher degree of tremor (29.4 ± 6.1%) compared to the CHT+/+'s (11.8 ± 5.3%) ($t_{(31)} = 2.17$, $P < 0.05$ by non-parametric unpaired t-test). This hypersensitivity trend persisted as long as 25 min post-injection (CHT+/-, 41.2 ± 4.8%; CHT+/+, 20.6 ± 6.1%; $t_{(30)} = 2.65$, $P < 0.01$ by non-parametric unpaired t-test).

Posttranslational Compensation Maintains Cholinergic Function in CHT+/- Mice

Having investigated basal and challenge-induced behavioral phenotypes, I next turned to biochemical characterization of the CHT+/- mice. As evident from the successful generation of CHT-/- mice, heterozygotes are viable and fertile, yet they exhibit only half the wild-type levels of CHT protein (Fig. 18A). Interestingly, although CHT protein levels are diminished, the rate of choline uptake into synaptosomes from CHT+/- mice was equivalent to that of their +/+ littermates (Fig. 17A), and had an identical dose-response profile to HC-3 inhibition as wild type (Fig. 17B). Analysis of saturation kinetics revealed no difference in either the Kd or the Vmax of whole-brain synaptosomal [3H]choline transport. Furthermore, in additional choline uptake experiments in whole-brain synaptosome preparations that used a single concentration of [3H]choline (50 or 100 nM) no significant difference (t test, $P > 0.05$) was detected

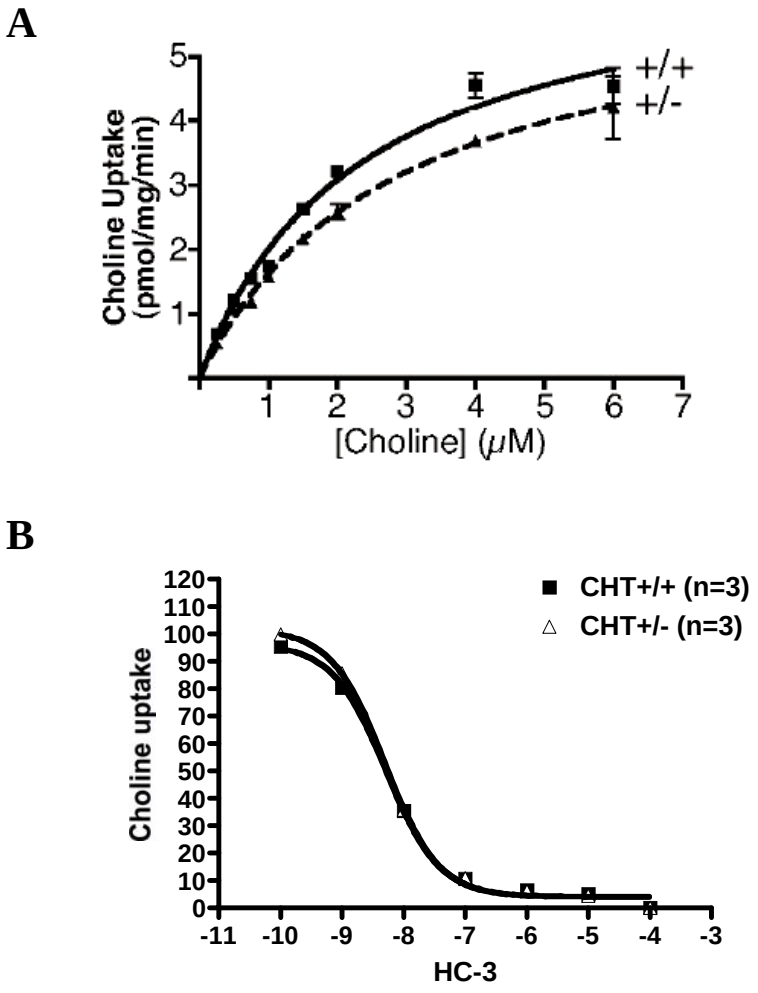

Figure 17. Functional compensation of CHT function in adult CHT+/- mice. (A) In whole brain synaptosome preparations, CHT+/- levels of HC-3-sensitive choline uptake are indistinguishable from wildtype levels. This example of saturation kinetics analysis demonstrates no significant difference in either Kd or Vmax between CHT+/+ mice and their +/- littermates. From three independent experiments (+/+ and +/- littermates aged 7-37 weeks old) performed in triplicate the Kd values were 2.9+/-0.3 µM and 3.3+/-0.3 µM and the Vmax values were 4.2+/-1.2 and 3.9+/-1.2 pmol/mg protein/minute for CHT+/+ and +/- respectively (mean+/-SEM). **(B)** In parallel with the compensations in HC-3-sensitive choline uptake, IC-50 values of HC-3 inhibition of HACU were not different between genotypes (CHT+/+, IC50=5.1x10-9; CHT+/-, IC50=5.0x10-9) (uptake was performed in forebrain synaptosomes,in the presence of 50 nM 3H choline, and 0-100 uM HC-3; n=3, mean+/-SEM of assays performed in triplicate). Shawn Ferguson contributed to this figure.

between CHT+/- and +/+ littermates (CHT+/- = 107 ± 11% of wild-type choline uptake, mean SEM, n = 8 pairs of male littermates, mean age = 12 weeks, range 5–37 weeks). Consistent with these findings, choline clearance rates monitored with ceramic-based choline-sensitive electrodes in the striatum of CHT+/- mice were also indistinguishable from clearance dynamics observed in the striatum of +/+ littermates (Subbu Apparsundaram, personal communication).

Notably, when we measured [3H]HC-3 binding to whole-brain membrane fractions, binding levels exceeded the 50% predicted by genotype and total CHT protein levels and were not significantly different (t test, $P > 0.05$) from the wild-type littermates (Fig. 18B). However, synaptosomal biotinylation and immunoblotting revealed CHT plasma membrane levels in CHT+/- synaptosomes close to half of those in CHT+/+ preparations (Fig. 18A, 18C) (t test, $P < 0.05$). The complete compensation of CHT activity in synaptosomes from CHT+/- mice with only half total and plasma membrane wildtype CHT protein expression suggests that cholinergic neurons can use posttranslational regulatory mechanisms, such as catalytic activation, to control the rate of presynaptic choline uptake.

ACh levels are significantly diminished and muscarinic receptor expression selectively altered in the CHT+/- brain

Do compensatory mechanisms in the CHT+/- brain involve additional participants in cholinergic signaling, such as enzymes or receptors present at the cholinergic synapse? I based my inquiries into this question on the pharmacological phenotypes of the CHT+/- mice described above. The altered CHT+/- sensitivity to muscarinic agents could be due to genotype-dependent alterations in ACh levels, as dictated by compensatory changes in

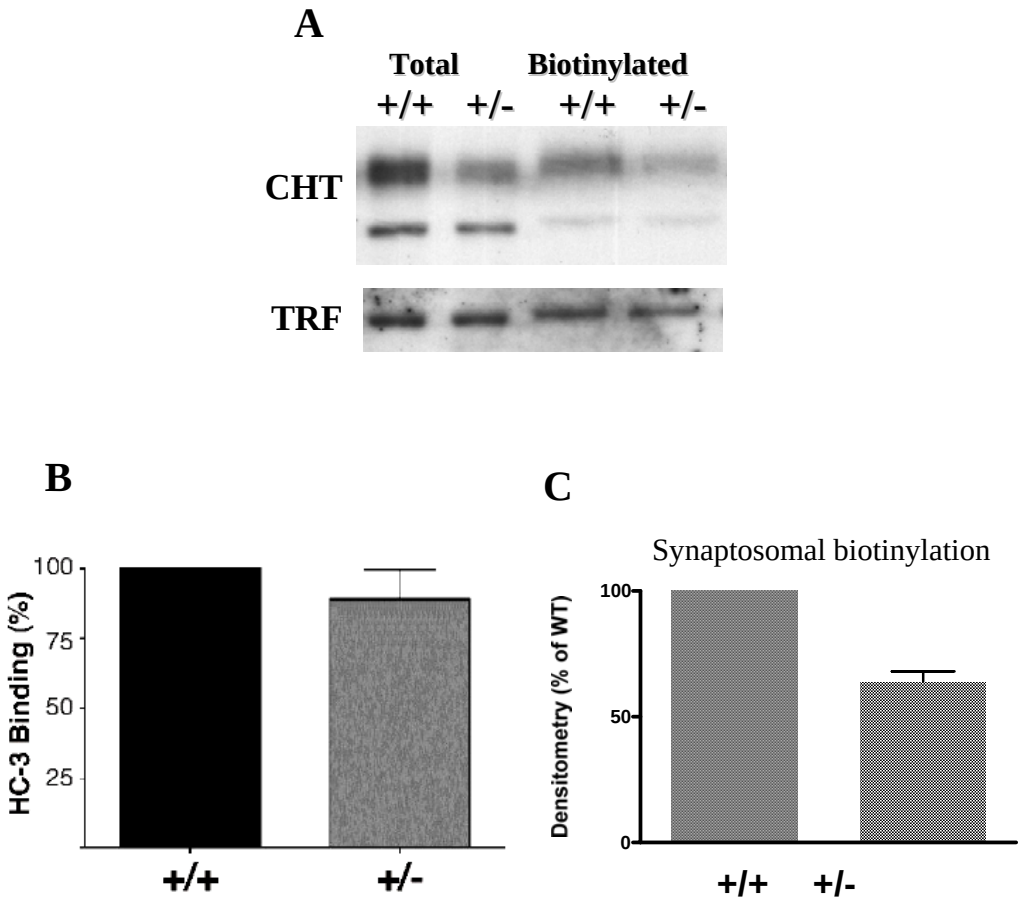

Figure 18. Post-translational CHT regulation in adult CHT+/- brain. (A) CHT protein levels are diminished in whole brain extracts of CHT+/- mice compared to samples from +/+ littermates while TRF protein levels are unchanged. **(B)** [3H]-HC-3 binding to whole brain membrane preparations was not different between CHT+/+ and +/- mice. **(C)** However, synaptosomal biotinylation revealed significantly lower CHT protein density at the CHT+/- plasma membrane (63.1+/-4.8% of +/+), while biotinylation signal for the positive control plasma membrane protein transferin did not differ between genotypes (A); (n=3, mean+/-SEM of assays performed in triplicate); TRF, transferin receptor. Shawn Ferguson cotrnibuted to this figure.

biosynthetic/catabolic pathways, or could arise from changes in muscarinic receptor expression. I examined the former possibility by evaluating bulk ACh and choline levels, as well as ChAT and AChE activities in various brain regions. Bulk ACh levels were significantly lower (Fig. 19A) in the CHT+/- cortex (CHT+/-, 6.9 ± 1.5; CHT+/+, 15.8 ± 2.3 nmol/g wet tissue), hippocampus (CHT+/-, 9.0 ± 2.1; CHT+/+, 20.6 ± 2.2 nmol/g), and striatum (CHT+/-, 24.1 ± 5.2; CHT+/+, 61.7 ± 8.0 nmol/g) ($F_{(1, 3931)} = 16.28$, $P < 0.001$). Conversely, bulk choline levels were significantly elevated (Fig. 19B) in the CHT+/- cortex (CHT+/-, 53.0 ± 6.2; CHT+/+, 31.0 ± 2.6 nmol/g wet tissue), hippocampus (CHT+/-, 37.7 ± 5.0; CHT+/+, 27.6 ± 1.4 nmol/g), and striatum (CHT+/-, 66.9 ± 5.0; CHT+/+, 46.9 ± 4.9 nmol/g) ($F_{(1, 3151)} = 10.74$, $P < 0.01$). There were no significant differences in ChAT activity (cortex, CHT+/-, 52.0 ± 1.9; CHT+/+, 51.3 ± 8.3; hippocampus, CHT+/-, 60.2 ± 4.6; CHT+/+, 61.8 ± 4.4; striatum, CHT+/-, 123.8 ± 27.8; CHT+/+, 130.2 ± 9.9 nmol/hr/mg protein) ($F_{(1, 470)} = 0.05$, $P = 0.83$) or AChE activity (cortex, CHT+/-, 51.8 ± 4.3; CHT+/+, 51.5 ± 4.3; hippocampus, CHT+/-, 54.7 ± 13.9; CHT+/+, 44.8 ± 7.4; striatum, CHT+/-, 288.0 ± 51.0; CHT+/+, 288.2 ± 16.2 nmol/hr/mg protein; ($F_{(1, 126)} = 0.13$, $P = 0.72$).

To test whether alterations were evident in central muscarinic receptors, we performed Western blotting for the M1 and M2 receptor on brain homogenates from CHT+/- and CHT+/+ littermates, using blot densitometry to quantify receptor expression in the cortex, hippocampus, and striatum regions. I focused on these receptors as M2 receptors represent the predominant presynaptic subtype in cortex and hippocampus, but are also expressed in striatum (Rouse et al., 1997) and M1 receptors are widely distributed and participate in both motor and cognitive circuits in the cortex,

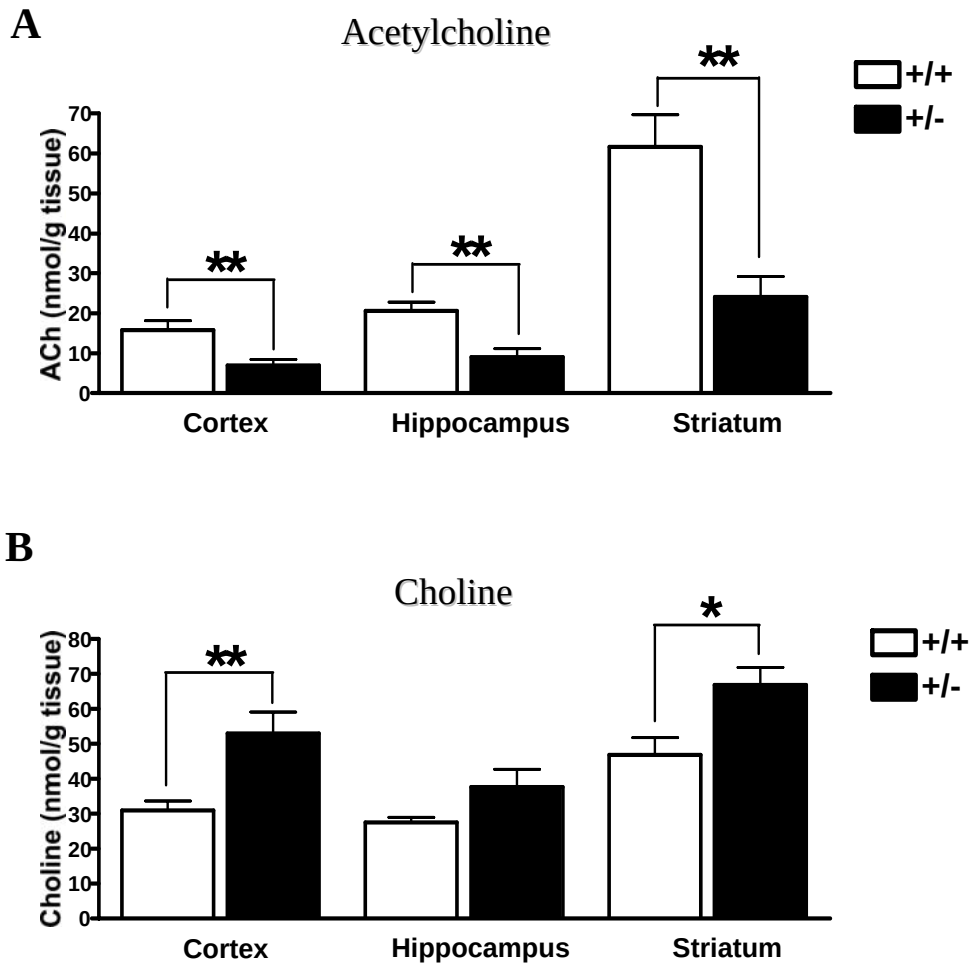

Figure 19. ACh and choline levels are significantly altered in the CHT+/- brain. Tissue ACh levels measured by HPLC are significantly lower in CHT+/- cortex, hippocampus, and striatum **(A)**, whereas choline levels are elevated in the same regions **(B)** (CHT+/-, n=7; CHT+/+, n=7) (*$p<0.05$, **$p<0.01$).

hippocampus and striatum (Alcantara et al., 2001).

I found M1 expression to be 25.4% lower in the striatum, 31.3% lower in the hippocampus, and 20.8% higher in the cortex of CHT+/- mice compared to CHT+/+ littermates (Fig. 20A). This difference reached statistical significance in the striatum ($t_{(6)} = 3.05$; $P < 0.05$). M2 receptor expression was 47.7% lower in the striatum, 34.9% lower in the cortex, and essentially unchanged in the hippocampi of CHT+/- mice compared to CHT+/+ littermates (Fig. 20B). The decreases in M2 expression reached statistical significance in both striatum ($t_{(6)} = 2.81$; $P < .05$) and cortex ($t_{(6)} = 2.91$; $P < 0.05$).

Discussion

Mouse models featuring genetically-established cholinergic deficits have provided new evidence for a dynamic role of CHT as a critical modulator of cholinergic neurotransmission. For example, CHT protein expression increases in response to decreased turnover of ACh in AChE knockout mice (Volpicelli-Daley et al., 2003b). Conversely, CHT density and function are upregulated in hypocholinergic states, produced by overexpression of AChE in transgenic mice (Beeri et al., 1997). Finally, upregulation of CHT protein and function sustains wild type levels of AChE activity, as well as bulk ACh content and depolarization-evoked ACh release in ChAT heterozygote mice (Brandon et al., 2004). In this context, I hypothesized that partial loss of CHT might represent a unique model of cholinergic hypofunction, one where phenotypes might emerge upon behavioral/ pharmacological challenges. In support of this idea, I previously reported an increase in the sensitivity to the lethal effects of HC-3 in CHT+/- mice compared to wild type littermates (Ferguson et al., 2004). My current studies show that

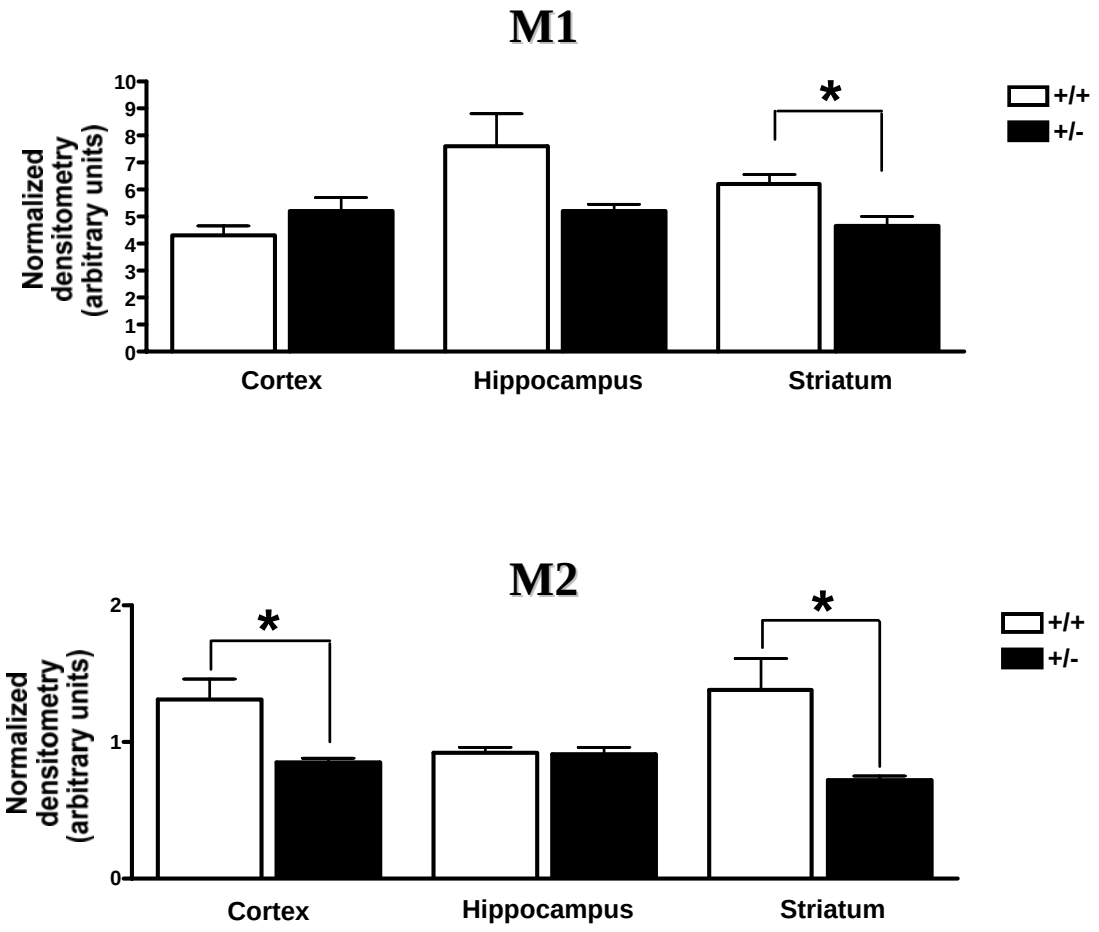

Figure 20. Muscarinic receptor expression is selectively diminished in the CHT+/- brain. Immunoblotting shows that M1 receptor expression is significantly downregulated in the CHT+/- striatum (A), while M2 receptor expression is decreased in both CHT+/- cortex and striatum (B). Mean (+/-SEM) values are indicated (n=4 mice per genotype) (*$p<0.05$). Data obtained through collaborative effort with Allan Levey lab. Craig Heilman contributed to this figure.

CHT+/- mice achieve normal baseline performance on multiple sensorimotor, anxiety and cognitive tasks, consistent with our findings of normal levels of synaptosomal, CHT-mediated HACU (Ferguson et al., 2004). In addition, I demonstrate that physical and/or pharmacological challenges elicit genotype-sensitive phenotypes, consistent with demand-dependent cholinergic hypofunction based on diminished bulk ACh levels.

Cholinergic neurotransmission at the NMJ is essential for movement (Brandon et al., 2003; Misgeld et al., 2002) and ACh modulates extrapyramidal motor function (Borison and Diamond, 1987; Kaneko et al., 2000). Therefore, I began by characterizing motor function in the CHT+/- mice, using the open field chamber paradigm. Whereas overall levels of activity were not different between the genotypes (Fig. 11C), we did observe an interesting pattern of decreased horizontal (Fig. 11A) but increased vertical movement (Fig. 11B) by the CHT+/- mice. This phenotype did not appear to be caused by overt musculoskeletal deficits, as CHT+/- mice travel equivalent distances at swimming velocities similar to CHT+/+ littermates in the Morris water maze (data not shown), perform comparably to CHT+/+ mice at slow speeds and short test intervals on the treadmill (Fig. 15), and are not impaired in the rotarod (Fig. 12A), wire hang, and inverted screen tests (data not shown). Normal basal performance by the CHT+/- mice in the elevated plus maze (Fig. 12B) and light/dark (Fig. 12D) paradigms likely rules out anxiety as an alternative reason for the altered locomotor phenotype. The increased rearing, but preserved overall activity levels, may be interpreted as an altered cognitive response to a novel environment (Sarter and Bruno, 1997), resulting in a unique pattern of exploratory behavior. Additional studies are needed to discern whether altered patterns of autonomic activity may also contribute to this phenotype.

The baseline locomotor data described above not only provide controls for studies of stressed motor function, but also allowed me to proceed with cognitive studies that rely on

normal motor function. Similar to motor activity, cognitive performance in CHT+/- mice appeared grossly normal at baseline in multiple behavioral assays, including spontaneous Y maze and rewarded T maze alternation, conditioned freezing, operant conditioning, and prepulse inhibition (data not shown). CHT+/- mice were also unimpaired in the Morris water maze - a hippocampus-dependent spatial learning and memory task that is sensitive to insults on the cholinergic system, including pharmacological challenges with muscarinic antagonists, aging, and anatomical lesions of cholinergic pathways (Gage et al., 1988). However, Morris water maze performance is unaffected in other models of cholinergic dysfunction, including M1 knockouts (Miyakawa et al., 2001) and ChAT heterozygous (ChAT+/-) mice (Brandon et al., 2004). Interestingly, the normal water maze performance of ChAT+/- mice in particular has been attributed to wild type levels of cholinergic neurotransmission capacity, triggered in part by upregulation of CHT (Brandon et al., 2004). In this context, additional tests, such as those developed in the rat to monitor focused attention (Apparsundaram et al., 2005; Sarter and Bruno, 1997) may be useful in assessing CHT contributions to cognitive performance.

Following observations of normal baseline motor and cognitive performance, I asked whether CHT hemizygosity would render the CHT+/- mice susceptible to challenges directed at cholinergic neurotransmission, specifically stresses that interfere with choline transport or enhance ACh turnover. If cholinergic neurons actively control CHT localization or activity to regulate ACh synthesis and homeostasis, then in response to sublethal *in vivo* concentrations of HC-3 there should be compensatory recruitment of CHTs (Rylett et al., 1993) that may no longer be sustainable in CHT+/- mice. Indeed, I observed lethality in CHT+/- mice at concentrations of HC-3 where all wildtype mice survived (Fig. 14D). These results are functionally consistent with either depleted

intracellular CHT reserve pools, and therefore impaired recruitment to the plasma membrane ("trafficking" hypothesis of CHT regulation, (Ferguson et al., 2003)), or altered availability of active transporters on the plasma membrane independent of trafficking mechanisms ("activation" hypothesis). With respect to functional compensation (wildtype levels of choline uptake in the CHT+/- brain, see below) and *in vivo* antagonist sensitivity in the CHT heterozygotes, I note parallels to the serotonin transporter (SERT) +/- mice. SERT+/- exhibit wild-type rates of serotonin transport in synaptosome preparations but are more sensitive than the SERT+/- mice with respect to their locomotor response to 3,4-methylenedioxymethamphetamine (Bengel et al., 1998).

Having established a pharmacologically induced phenotype in the CHT+/- mice, I next chose motor performance as a readout of challenges directed at cholinergic neurotransmission, as Ie could introduce both physical and pharmacological challenges in multiple paradigms. In treadmill tests of physical strain on locomotion, I found that CHT+/- mice remained on the running belt for significantly shorter periods of time (Fig. 15A) and were not able to reach and sustain the higher speeds attained by age, gender, and weight-matched CHT+/+ littermates (Fig. 15B). Our previous electrophysiological recordings at the NMJ documented normal baseline ACh stores and release in the CHT-/- mice as measured by EPSP magnitude (Ferguson et al., 2004). However, over time, the ACh release diminished to a point where EPSP's as well as mEPPs were no longer observable in the CHT-/- preparations, while CHT+/+ NMJs maintained cholinergic neurotransmission. Although I did not measure neuromuscular signaling per se in these studies, previous studies have shown that reduction in mEPP amplitude, reflecting diminished neurotransmitter release, is significantly greater if the prolonged nerve

stimulation takes place in the presence of the specific CHT inhibitor HC-3, a pharmacological parallel to the genetic deficit induced in the CHT+/- mice (Jones and Kwanbunbumpen, 1970). Therefore, I hypothesize that CHT+/- treadmill performance was impaired due to inability to sustain ACh turnover at the NMJ under conditions of high demand.

Central cholinergic pathways support the motor program both at brainstem and basal ganglia levels. A paradigm that allowed the simultaneous investigation of central cholinergic drive of locomotion and specific challenge to the muscarinic receptor component of ACh turnover, is scopolamine-driven locomotion in the open field paradigm (Sipos et al., 1999). It is well established that scopolamine acts at presynaptic auto-inhibitory muscarinic receptors, resulting in massive ACh release, a corresponding increase in CHT-mediated choline uptake needed to sustain ACh turnover, and hyperlocomotion easily measured as distance traveled in the open field (Douglas et al., 2001; Parikh et al., 2004). My hypothesis was that, under prolonged stimulation, ACh turnover would not be sustainable in the CHT+/- mice, and therefore CHT+/- mice would lack the scopolamine-induced hyperlocomotion evident in their CHT+/+ littermates. Indeed, while a low dose of scopolamine (0.1 mg/kg) failed to elicit a locomotive effect in either genotype, an intermediate dose (0.5 mg/kg) led to significant increases in distance traveled by the CHT+/+ but failed to affect the CHT+/- mice. This finding was particularly interesting in the context of our previous findings with AChE-/- mice, which display normal basal locomotion in the open field chambers, but are hyper-sensitive to challenge at this same intermediate dose of scopolamine (0.5 mg/kg) (Volpicelli-Daley et al., 2003b). The reverse response to scopolamine can be explained if we view the

AChE-/- condition as a potential hypercholinergic state, in contrast with the potential hypocholinergic status of CHT+/- mice. Consistent with this idea, CHT expression is approximately 50% higher in the AChE-/- mice, but 50% lower in the CHT+/- mice (Beeri et al., 1997; Volpicelli-Daley et al., 2003b).

The normal behavioral phenotype of CHT +/- mice in many tasks parallels the wild type levels of synaptosomal HACU activity we previously established (Ferguson et al., 2004). However, the altered sensitivity to cholinergic pharmacological (HC-3, scopolamine, oxotremorine) challenges suggests that other determinants of ACh signaling are altered in the model. Accordingly, I found CHT+/- mice to have normal ChAT and AChE activities (see Results, this chapter), but diminished bulk ACh (Fig. 19A) and increased total choline brain levels (Fig. 19B). Whereas total endogenous ACh levels are significantly lower in the CHT+/- brain, preliminary studies show normal basal 3H-ACh release as measured in an in-vitro slice-perfusion paradigm (D. Lund and M. Bazalakova, unpublished data), suggesting that a redistribution and altered regulation of ACh release and reserve pools (Neher, 1998) may compensate for reduced overall ACh levels.

Decreased bulk ACh and increased total choline brain levels have been observed in several human pathologies and mouse models, including the PDAPP transgenic mouse model of Alzheimer's disease (Bales et al., 2006). Elevated choline levels in the CHT+/- mice likely represent a compensatory attempt to enrich the choline supply pool for ACh synthesis. Unlike the impairments seen in AChE transgenic mice (Meshorer et al., 2005), I have little reason to suspect major blood-brain-barrier dysfunction leading to increased choline flux in the CHT+/- brain. Therefore, elevated choline levels likely represent either a reduction in the recycling and/or ACh-incorporation of HACU-derived choline,

or increased membrane phosphatidyl turnover, resulting from an attempt to increase choline reserves available as precursors for ACh synthesis (Lee et al., 1993). The decreased bulk ACh levels, but normal exogenous 3H-choline conversion and release of 3H-ACh from slices, suggest a possible redistribution of ACh pools (Birks and MacIntosh, 1961), where readily-releasable pools are not different from wild type (possibly sustained by increased choline levels), but reserve pools are compromised. These observations parallel my behavioral findings of normal baseline performance, but challenge-induced deficits in cholinergically-mediated function.

What mechanisms regulate CHT function and lead to compensation for depleted ACh reserves in the CHT+/- brain? My findings of wild-type levels of HC-3-sensitive HACU in whole-brain synaptosomes from CHT+/- mice indicate an unrecognized capacity of cholinergic terminals to compensate for significant reductions in CHT protein levels. Our recent identification of a large pool of CHTs residing on a subset of cholinergic synaptic vesicles (Ferguson et al., 2003) pointed to the presence of a substantial intracellular CHT reserve in wild-type animals. The functional compensation that we observed in [3H]choline uptake and [3H]HC-3 binding is consistent with a redistribution of this vesicular pool of CHTs in CHT+/- neurons. In support of this speculation, the coordinated up-regulation of HACU capacity and HC-3 binding site density in response to stimulation of ACh release is well documented (Ferguson and Blakely, 2004; Lowenstein and Coyle, 1986; Simon et al., 1976).

However, in contrast to this observation, my synaptosomal biotinylation findings suggest an alternative model of CHT regulation, one where levels of CHT at the CHT+/- plasma membrane are halved in comparison to wild type, and thus wildtype levels of

choline uptake are achieved at least in part through activation of plasma membrane resident CHT molecules. Previous studies suggest that HC-3 binding may not accurately reflect protein density, but may instead be influenced by Ca^{2+}-dependent, ATP-induced changes in affinity for the ligand (K_D) (Chatterjee and Bhatnagar, 1990; Saltarelli et al., 1990). Therefore, equal measures of [^{3}H]HC-3 binding, but disparate levels of CHT plasma membrane density assessed by biotinylation, may be the result of conformational changes of the CHT protein already present in the plasma membrane, due to phosophorylation or other protein modifications. Future studies will be needed to determine the exact mechanism of CHT regulation that predominates in the CHT+/- brain.

Functional compensation in the CHT+/- mice may in part be achieved through a region-specific downregulation of M1 (striatum) and M2 (striatum and cortex) receptor expression (Fig. 20). The downregulation of muscarinic receptor expression is consistent with a hyposensitivity to scopolamine challenge in the CHT+/- and is reminiscent of compensatory changes in muscarinic expression and function in another model of cholinergic dysfunction – AChE-/- mice (Volpicelli-Daley et al., 2003b). I was unable to reliably quantify expression of the M3, M4 and M5 receptors, which may also exhibit CHT genotype-dependent modulation. Regardless, the hypo-responsiveness to scopolamine-induced locomotion and mAChR downregulation in the CHT hemizygous state contrasts with enhanced novelty-induced locomotion and M2 striatal overexpression in AChE transgenics, where CHT density and CHT-mediated choline uptake are elevated at baseline (Erb et al., 2001; Svedberg et al., 2003). Together, these findings reinforce an

interplay of CHT with muscarinic receptors in establishing and sustaining cholinergic tone.

In conclusion, I have shown that CHT+/- mice perform comparably to wild type littermates in motor and cognitive tasks, but can display impaired performance when cholinergic neurotransmission is subjected to sustained physical and pharmacological challenge. My findings are particularly relevant in the context of the human CHT single nucleotide polymorphism (SNP) recently identified by Okuda and colleagues (Okuda et al., 2002). The I89V substitution occurs in approximately 6% of the Ashkenazi Jewish population and at similar or higher frequencies in North American Caucasian populations (B. English and R.D. Blakely, unpublished findings) and results in a 40-50% reduction in choline uptake measured in a transfected cell culture system (Okuda et al., 2002). Future studies in the CHT+/- mice can provide insights into the possible impact of the CHT I89V and other hypofunctioning gene variants on human behavior and physiology and provide a valuable new model for testing the theories and therapies related to cholinergic hypofunction.

CHAPTER IV

SYSTEMIC PHYSIOLOGICAL EFFECTS OF CHT HEMIZYGOSITY

Introduction

The cholinergic system has long been implicated as playing an important role in various physiological processes, including cardiovascular (De Biasi, 2002; Gomeza et al., 1999a), circadian rhythm (O'Hara et al., 1998), and dopamine (DA) release regulation (Zhou et al., 2003) affecting drug addiction (Dani, 2003). Pharmacological and genetic studies in mouse models of cholinergic dysfunction that have contributed to our understanding of cholinergic modulation of the aforementioned systemic physiological processes are reviewed below.

Cardiovascular regulation

Acetylcholine is an important regulator of cardiac function, as it mediates the effects of both parasympathetic and sympathetic branches of the autonomic nervous system on the heart. Postganglionic sympathetic innervation to the heart originates from the stellate and middle and superior cervical ganglia (SCG), where synaptic transmission is dependent on postsynaptic nicotinic ACh receptors (nAChR). The positive chronotropic (increased heart rate) effects of sympathetic drive are thought to be mediated by various nAChR subunits, including $\alpha3\beta4$ nAChR heteromers in the mouse and rat SCG (De Biasi, 2002). Consequently, $\alpha3$ and $\beta4$ knockout mice display significant bradycardia and ventricular repolarization defects (Xu et al., 1999; Yu et al.,

2000). α7 is another nAChR subunit, which appears to be essential for baroreflex-mediated activation of sympathetic drive, and consequent increases in heart rate (Franceschini et al., 2000).

The parasympathetic nervous system uses ACh both at ganglionic and target-organ synapses. Cholinergic terminals from the vagus nerve synapse onto nAChR-containing intrinsic cardiac ganglia and cause postganglionic ACh release, thus activating muscarinic ACh receptors (mAChR) in the myocardium. Therefore, muscarinic agonists cause a decrease in heart rate, atrioventricular contraction, and force of contraction in humans in vivo, similar to parasympathetic vagal drive (Dhein et al., 2001). Conversely, muscarinic antagonists increase heart rate. Interestingly, these effects appear to be dose-dependent: high doses of muscarinic agonists can have positive chronotropic effects (Loffelholz and Pappano, 1985), while low doses of muscarinic antagonists can have cholinomimetic, or negative chronotropic effects on heart rate in healthy volunteers (Poller et al., 1997). The latter effect is thought to be mediated by presynaptic muscarinic autoreceptors, which normally inhibit ACh release (Oberhauser et al., 2001).

The predominant mAChR in the mammalian heart is M2 (Peralta et al., 1987), and atria from M2 receptor knockout mice are not responsive to muscarinic stimulation, in contrast with carbachol-induced bradycardia in atria from wild type mice (Gomeza et al., 1999a). In humans, an age-dependent reduction in atrial M2 receptor density appears to underlie decreased responsiveness to muscarinic agents (Brodde et al., 1998). The role of muscarinic receptors in cardiac pathology continues to be the subject of active investigation. While it is known that vagal output decreases in chronic heart failure (Eckberg et al., 1971), the exact mechanisms of this change remain to be elucidated.

As HACU is believed to provide critical precursor support for ACh release, particularly at high rates of cholinergic signaling, I predicted that a genetic perturbation of CHT will limit the ability of animals to sustain cholingergic signaling. With regard to the heart, both the sympathetic and parasympathetic innervation of the heart utilize preganglionic cholinergic signals, whereas postganglionic cholinergic synapses of parasympathetic neurons provide the ACh that slows the heart. CHT dysfunction can thus diminish sympathoexcitation of the heart or diminish cholinergic suppression of adrenergic drive. Moreover, the balance between these two opposing forces may be disrupted, placing the heart at risk for sudden death or drug-induced arrhythmias. Evaluation of the ultimate victor in this chemical tug of war led me to analyses in CHT+/- animals, studies that can lead to a greater awareness of phenotypes likely to be exhibited by human subjects with loss of function mutations in the CHT gene (Okuda et al., 2002).

Dopamine (DA) Release and Addiction

A growing body of evidence describes the importance and mechanisms of ACh regulation in DA release (Zhou et al., 2003) and, consequently, drug addiction (Dani, 2003). It appears that a balance between interrelated but opposing cholinergic and dopaminergic signaling directly modulates basal ganglia-mediated reward (Kaneko et al., 2000). While nigrostriatal dopaminergic projections and DA application inhibit striatal cholinergic neuron activity (Trabucchi et al., 1975), recent studies also suggest that amphetamine pretreatment sensitizes increases in cortical ACh release from nucleus accumbens-cortical projections (Nelson et al., 2000). In addition, cocaine, which prolongs the action of DA, activates cholinergic interneurons (Berlanga et al., 2003) and

increases ACh release measured by microdyalisis (Mark et al., 1999) in the nucleus accumbens of self-administering rats.

Reciprocal studies have shown that striatal cholinergic interneurons in turn regulate DA release from nigrostriatal projections through presynaptic ß2 nicotinic ACh receptors (nAChRs), and that depletion of ACh reduces DA release in the (Zhou et al., 2001). Ventral tegmental area (VTA) dopaminergic neurons are activated by input from pedunculopontine tegmental (PPT) cholinergic projections (Bolam et al., 1991; Oakman et al., 1995), providing yet another example of ACh-induced DA release (Blaha et al., 1996), albeit one mediated by M5 presynaptic receptors (Forster et al., 2002). M5 knockout mice demonstrate reduced response to morphine (Basile et al., 2002) and cocaine (Thomsen et al., 2005) in conditioned place preference and self-administration paradigm, thus leading to the hypothesis that CHT+/- mice may display decreased sensitivity to cocaine or other drugs of abuse.

However, M1 AChR deficiency in M1 knockout (-/-) mice results in increased DA release in the striatum, associated with hyperlocomotion and increased response to amphetamine (Gerber et al., 2001). Ablation of cholinergic cells in the nucleus accumbens, the ventral part of the striatum, also increases sensitivity to cocaine and morphine in the conditioned place preference paradigm (Hikida et al., 2003). While the exact molecular mechanisms are not clear, it is thought that these effects are mediated by dopaminergic hyperactivity due to ACh depletion. This leads to the converse hypothesis that CHT+/- mice may display enhanced sensitivity to cocaine under basal or induced conditions.

CHT+/- mice offer the valuable opportunity to expand our mechanistic understanding of the effects of cholinergic dysfunction on addiction. Our investigations in the whole animal avoid the potential limitations of nonspecific pharmacological and lesion approaches, and offer important insight into the specific contribution of CHT and the effects of its genetic manipulation on DA release and cholinergic modulation of reinforcement behavior.

Cholinergic Modulation of Circadian Rhythms

Acetylcholine is a well-known modulator of mammalian circadian rhythms, and was, in fact, “the first neurotransmitter identified as a regulator of mammalian circadian rhythms“ (Buchanan and Gillette, 2005). Studies show the existence of cholinergic projections from the brainstem and basal forebrain to the suprachiasmatic nucleus (SCN) – a brain region considered essential for circadian rhythm regulation (Bina et al., 1993). The evidence for cholinergic involvement in circadian rhythm modulation includes demonstrations of light-induced ACh release in the SCN (Murakami et al., 1984), carbachol-induced phase shifts of circadian rhythms *in vivo* (Bina and Rusak, 1996; Colwell et al., 1993), and altered SCN neuron firing frequency in slices in response to both muscarinic (Liu and Gillette, 1996) and nicotinic (Miller et al., 1987; O'Hara et al., 1998) stimuli. Based on these previous findings, I hypothesized that CHT+/- mice may display alterations in baseline circadian rhythms and/or light-induced phase-shifts in circadian activity.

Methods

Subcutaneous electrocardiogram recordings (ECG)

All cardiovascular studies were performed in collaboration with the Robertson lab at Vanderbilt, with excellent technical expertise and assistance from Martin Appalsamy, and helpful discussions with Nancy Keller. Mice were anesthesized with 1.5% isoflurane. Three tiny skin needles were fixed on three extremities to record ECG lead II. The ECG signal was amplified with open filter set (GOULD, dx mode, 0-500 Hz) to prevent minimal distortion of QRS complex. The data was recorded using a WINDAQ data acquisition system (DI410, DATAQ, Acron, OH, 14 Bit, 1000Hz) and processed off-line using a custom written software in PV-Wave language (PV-wave, Visual Numerics Inc., Houston, TX).

Placement of Telemetric ECG Device

Recordings were performed following modifications of previously described protocols (Wu et al., 2002). Mice were anesthetized with 2-3% isoflurane (in 100% O2) and placed on an isothermal pad (Deltaphase; Braintree Scientific, Inc., Braintree MA) to maintain body temperature at 36-37 C. Hair in the ventral neck region was removed with a dipilatory agent (Nair, Carter-Wallace, New York NY) and the skin prepared with antiseptic (betadine followed by alcohol). As soon as the animal demonstrated an absence of withdrawal response to nociceptive stimulation of a hindpaw, a 1 cm dorsal midscapular incision was made for placement of the radio transmitter in a subcutaneous pocket formed through the incision site by blunt dissection and sutured (7-0 silk) in place.

Two recording electrodes extending from the transmitter body were inserted into the underlying muscle surface and sutured in place, one in the chest wall and the other in the right axillary region. Care was taken to place the recording electrodes in such a way that no pressure is exerted onto the skin. Animals received an intramuscular injection of prophylactic cefazolin (30 mg/kg) and 1 ml of subcutaneous Lactated Ringer's solution to replenish fluids. The skin was sealed with sutures (5-0 absorbable synthetic) and secured with Nexaband veterinary adhesive. Animals were placed in individual cages on a heated isothermal pad until fully recovered from anesthesia. Mice were allowed at least 7 days to recover before experimentation.

Spectral Analysis

Beat-to-beat values of R-R intervals (Pan and Tompkins, 1985) are interpolated, low pass filtered (cutoff 3 Hz), and re-sampled at 6 Hz. Data segments of 128 seconds are used for spectral analysis. Linear trends were removed and power spectral density are estimated with the Fast Fourier Transform-based Welch algorithm using segments of 256 data points with 50% overlapping and Hanning window. The power in the frequency range of low frequencies (LF=0.250-0.600 Hz) and high frequencies (HF=1.0-3.0 Hz) was calculated in 5 90s segments for recordings obtained between the hours or 8 am-12 pm where the mice were not physically active. The frequency bands were adapted for analysis in mice considering the ranges of heart rate and breathing frequencies.

Vagal Stimulation

Protocols were adapted from previously published studies (Ma et al., 2002; Smith-White et al., 2003; Walker et al., 2004). Briefly, mice were instrumented for subcutaneous ECG recordings, and femoral artery blood pressure readings. The peripheral end of the right vagus nerve was isolated, placed across platinum electrodes, and cut. Two protocols for vagal stiumulation distal to the cut site were used: 1. *frequency-response curve*, where a stimulus of 16V, 2 ms, 30 sec duration was administered at ascending frequencies (5Hz, 10Hz, 15Hz, 20Hz, 25Hz, 50Hz), separated by a 2 min recovery period and 2. *repeated stimulation*, where a stimulus of 25Hz, 16V, 2 ms, 30 sec duration was administered 12 consecutive times with a 10 sec inter-stimulus interval.

Pharmacological Cardiovascular Challenges

Mice were instrumented for telemetry recordings and jugular intravenous (i.v.) catheters, allowing remote administration of drugs during awake, unrestrained behavior. Naïve, 1-1.5 year old, non-backcrossed, male F1 littermates were used for each drug administration. After recording a 15 min ECG baseline, i.v. bolus injections of one of the following drugs were administered: the ganglionic nAChR antagonist hexamethonium (30 µg/kg); the alpha receptor agonist phenylephrine (10 µg/kg); or the. muscarinic antagonist scopolamine (10 µg/kg followed by 25 µg/kg).

Dopamine Microdyalisis

Baseline, nicotine- and cocaine-induced dopamine (DA) release was measured through our collaborative effort with the John Dani lab at Baylor University, using published microdyalisis techniques (Pidoplichko et al., 2004). Briefly, mice were maintained on an isoflurane-gas mixture and the microdialysis CMA/12 (CMA/Microdialysis) guide cannula was aimed at the nucleus accumbens shell (1.7 mm AP; 0.8 mm L; 6.5 mm DV, with the probe at 7.5 mm) and was secured with bone wax reinforced with acrylic cement and three screws into the skull. The mouse was allowed to recover fully for a minimum of 48 h.

CMA/12 probes (diameter, 0.5 mm; length, 1 mm; membrane, polycarbonate; cutoff, 20,000 D) were prepared, and filtered degassed artificial cerebrospinal fluid (aCSF; from ESA) was perfused through the probe at a flow rate of 1 μL/min using a CMA/100 pump. Following a 2-h recovery period, three 20-min fractions were collected to assess the basal output of dopamine in the dialysate. Subsequently, saline and nicotine (1.0 mg/kg i.p.) were injected 1 hour apart, and samples were collected every 20 min for 4 hours following the nicotine injection. At the end of the 4 hours cocaine (10mg/kg) was injected, and samples were collected every 20 min for 1 h. After these experiments, mice were killed with an overdose of anesthetics and trans-cardially perfused with PBS and then 10% formalin. The brain was removed and fixed in 10% formalin. The accuracy of probe placement was later confirmed by histological sectioning.

Dopamine contents of microdialysates were determined using a high-performance liquid chromatography (HPLC) system (model 580 pump, Coulochem II electrochemical detector, model 5014B analytical cell; ESA, Inc.). Separation of dopamine was achieved

on a 150 x 3 mm column with 3 µm particle size (ESA, Inc.; MD-150). An isocratic mobile phase (pH 4.0) containing 75 mM NaH_2PO_4, 2 mM 1-octane sulphonic acid-sodium salt, 20 mM EDTA, 100 µL/L triethylamine, and 18% methanol (from ESA) was used at a flow rate of 0.6 mL/min. This mobile phase and the protocols used produced clearly separable dopamine peaks with a retention time of ~5.6 min. Chromatograms were analyzed with the ESA software. Freshly prepared standards ranging from 0–6 nM DA were used to calibrate the readings.

Cocaine Self-Administration

The self-administration protocol used in our collaboration with the Danny Winder lab at Vanderbilt University has been described in detail (Olsen and Winder, 2006). Briefly, food-restricted, handled, male mice at 7–9 weeks of age were trained to lever press in Med Associates (E. Fairfield, VT) operant chambers on a fixed ratio 1 (FR-1), followed by progressive ratio (PR) schedule of liquid reinforcement (25% Ensure). Mice successfully completing food training were catheterized in the right jugular vein with a SILASTIC catheter. After at least 3 days of recovery with food and water available *ad libitum*, the mice were subjected to a single, overnight, PR session of self-administration, in which pressing of the active lever resulted in delivery of saline or cocaine (0.3 mg/kg or 0.6 mg/kg per infusion in 0.040 ml). Within an hour after the last administration session, catheter patency was verified. Only animals that had patent catheters were included in subsequent data analyses as well as synaptosomal striatal 3H-choline uptake experiments.

Circadian Rhythms and Light Entrainment

Male animals, 11 CHT+/+ and 13 CHT+/-, were placed in wheel-cages with food and water ad libitum. These cages were placed in 12-hr light:12-hr dark cycles (LD) for one week with lights on from 06:00 to 18:00. The light cycle was then phase-shifted 6 hours forward, so that lights-on occurred between 0 and 12:00. This schedule was also maintained for a week. Animals were then subjected to constant darkness for a week and allowed to free-run before being placed back on the original 0600 to 1800 LD cycle. After another week in these LD conditions, animals were removed from the coffins and activity data was analyzed by ClockLab software.

Results and Discussion

Cardiovascular Regulation is Altered in the CHT+/- Mice

All cardiovascular data was obtained through a collaborative effort with the Robertson lab at Vanderbilt University. ECG recordings show that the CHT-/- neonates display two phenotypes: 1. Low average heart rates (Fig. 21): the newborn homozygote average heart rate is significantly lower than wild type (80±15 bpm, (CHT-/-), n=14 vs 220±22 bpm, (CHT+/+), n=4); 2. Prolonged PR intervals: the PR interval was found to be approximately twice as long in the CHT-/- newborns 120-140 ms (vs approximately 60-100 ms long PR interval in +/+ newborns). This may be an interesting finding, since the PR interval depends on AV node conduction, and the AV node receives heavy cholinergic innervation. While these findings may clearly be compromised by the hypoxia induced by increasingly labored breathing in the CHT -/- neonates, in utero

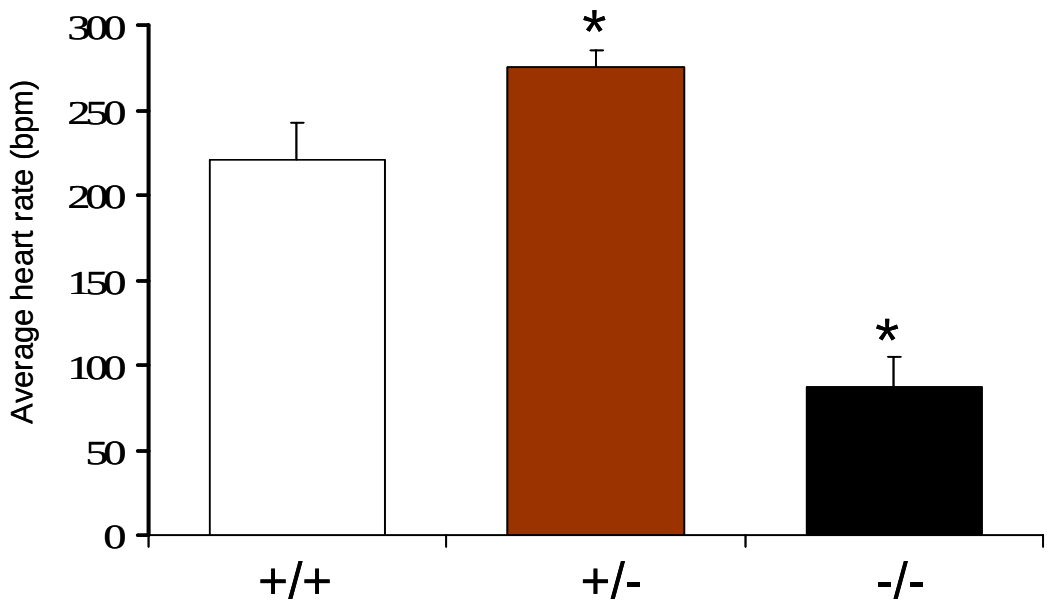

Figure 21. Average heart rates are significantly higher in CHT+/ neonates. ECG recordings were obtained in unanesthetized newborns, using a lead II position Gould Amplifier and WinDaq Acquisition System. Mean heart rate values were 276±9 bpm in the CHT+/- (n=6), 220±22 bpm in the CHT+/+ (n=4), and 80±15 bpm in the CHT-/- (n=12) * $p<0.05$, two-tailed t-test (values +/- SEM).

recordings can be used in the future to determine any intrinsic changes in heart rate. Importantly, the CHT+/- newborns seem to also display a phenotype: the CHT+/- average heart rate (276±9 bpm, n=6) appears to be significantly higher than the wild type average heart rate (220±22 bpm, n=4) (Fig. 21).

In order to avoid the complications of CHT-/- anoxia and lethality, I focused on characterizing basal heart rates in adult CHT+/- animals. I first used subcutaneous ECG electrode recordings in isofluorane-anaesthetized mice, and confirmed the finding of higher basal heart rates in CHT+/- adults compared to wildtype siblings (Fig. 22), which I had also observed in the newborns. To avoid potentially confounding effects of anesthesia we then instrumented mice with telemetric devices, allowing us to record heart rate in freely-moving, awake animals. Preliminary results appear to confirm the higher basal heart rate phenotype in the CHT+/-s (Fig. 23).

Several potential mechanisms could underlie the observed phenotype, including diminished parasympathetic drive or sympathetic overdrive. One approach to investigate possible alterations in autonomic balance is provided by spectral analysis of heart rate variability (HRV). In mice, muscarinic blockade decreases the amplitude of low frequency (LF) (below 1 Hz) oscillations in heart rate, while increases in sympathetic tone increase the prominence of 0.4Hz LF variability. Thus, if CHT+/- mice have decreased parasympathetic drive, I expect to find decreased LF HRV, while sympathetic overdrive would lead to increased LF HRV. Preliminary analyses suggest that the CHT+/- mice display decreased low-to-high frequency heart rate variability ratio, indicative of parasympathetic withdrawal (Fig. 24). These findings are particularly interesting in light of a recent human genotyping study, which showed an association

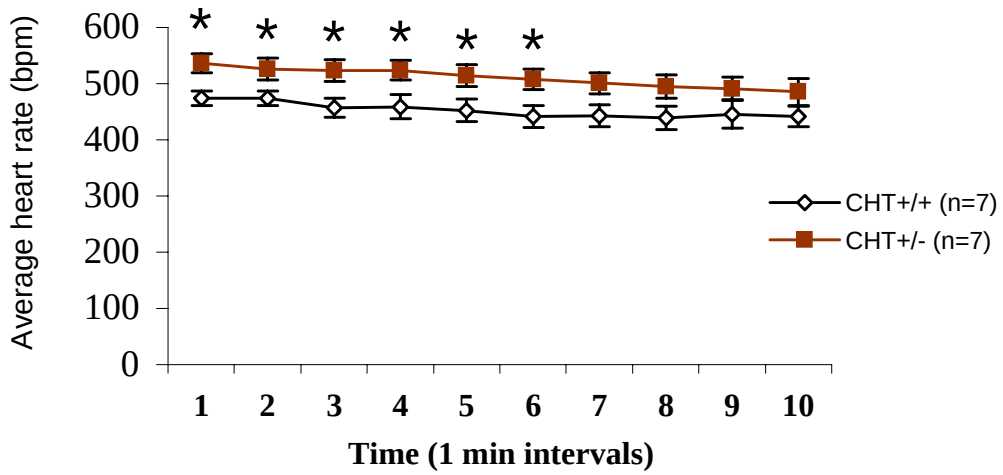

Figure 22. Average heart rates are significantly higher in isofluorane-anaesthetized CHT+/- adults. Subcutaneous ECG recordings were obtained in 1.5 year old, adult, male CHT+/- and CHT+/+ siblings, under 1.5% isofluorane anaesthesia, using a lead II position Gould Amplifier and WinDaq Acquisition System. * $p<0.05$, two-tailed t-test (values +/- SEM).

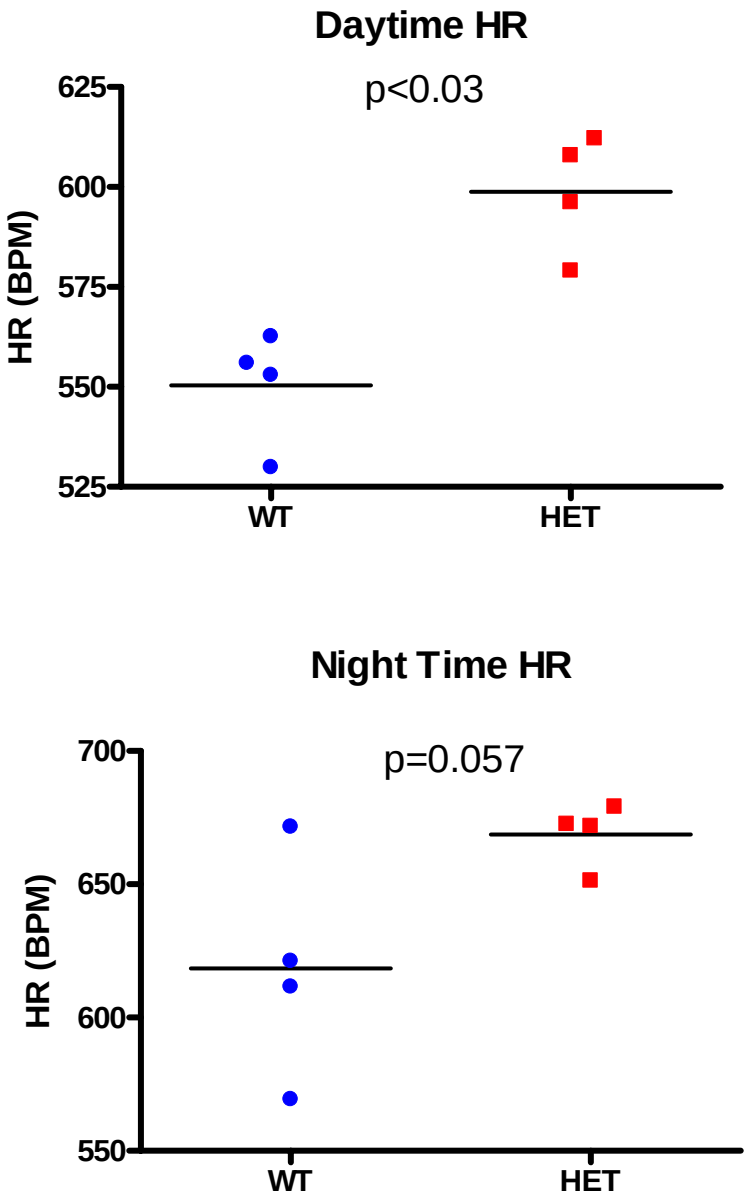

Figure 23. Telemetry recordings confirm significantly higher average heart rates in awake, freely-behaving CHT+/- mice. Telemetry recordings were obtained in freely-behaving, awake, 8-10 weeks old male mice, using implanted telemetry devices; HR = heart rate; WT = CHT+/+ (n=4); HET = CHT+/- (n=4). Data obtained in collaborative effort with David Robertson's lab. Figure contributed by Andre Diedrich.

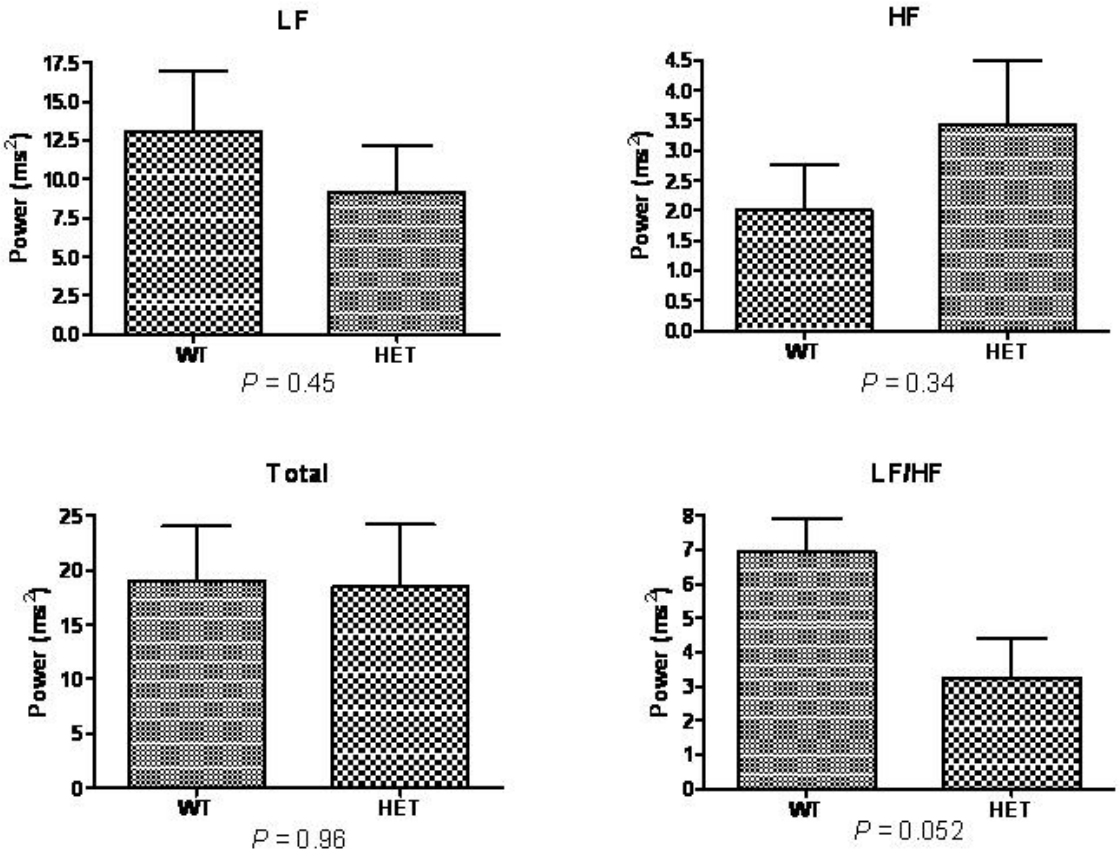

Figure 24. Spectral analysis of heart rate variability suggests parasympathetic withdrawal in CHT+/- mice. The power in the frequency range of low frequencies (LF=0.25-0.60 Hz) and high frequencies (HF=1.0-3.0 Hz) was calculated in 5 90s segments for telemetry recordings obtained between the hours or 8 am-12 pm when the mice were not physically active. WT = CHT+/+ (n=5); HET = CHT+/- (n=4). Laura Miller contributed to this figure through collaborative effort with David Robertson lab.

between lower LF/HF ratios and a single nucleotide polymorphism in the CHT 3' untranslated region (Neumann et al., 2005).

If CHT+/- mice indeed suffer from parasympathetic withdrawal, it is reasonable to hypothesize that their response to vagal stimulation may be compromised. It can also be postulated that CHT+/- mice may not be able to sustain repeated stimulation of the isolated cut vagus by an electrode, as ACh turnover and release may be compromised at the CHT+/- vagal terminal. In order to test these hypotheses I used a vagus stimulation protocol in anaesthetized adult male mice, and recorded bradycardic responses as a readout. CHT+/- mice displayed a frequency-response vagal stimulation curve indistinguishable from wild types (Fig. 25), which was not surprising in light of numerous behavioral and biochemical measures that are unaltered between the genotypes at baseline (Chapter III). However, I was surprised to find CHT+/- mice more, instead of less, responsive to repeated vagal stimulation (Fig. 26). While this finding did not follow my initial experimental predictions, it could potentially be explained in the context of altered sympathetic-parasympathetic balance, mediated by various mechanisms such as hypersensitive ganglionic nicotinic receptors or hyposensitive peripheral presynaptic muscarinic receptors. Pharmacological studies described below address these hypotheses.

Alterations in both sympathetic and parasympathetic innervation could be mediated by changes in sensitivity of cholinergic receptors at the ganglionic or postganglionic level. nAChRs are found at both sympathetic and parasympathetic ganglia, and $\alpha 7$ nAChR's have been implicated in the positive chronotropic effects of sympathetic activation. Target-organ muscarinic AChR's, predominantly of the M2

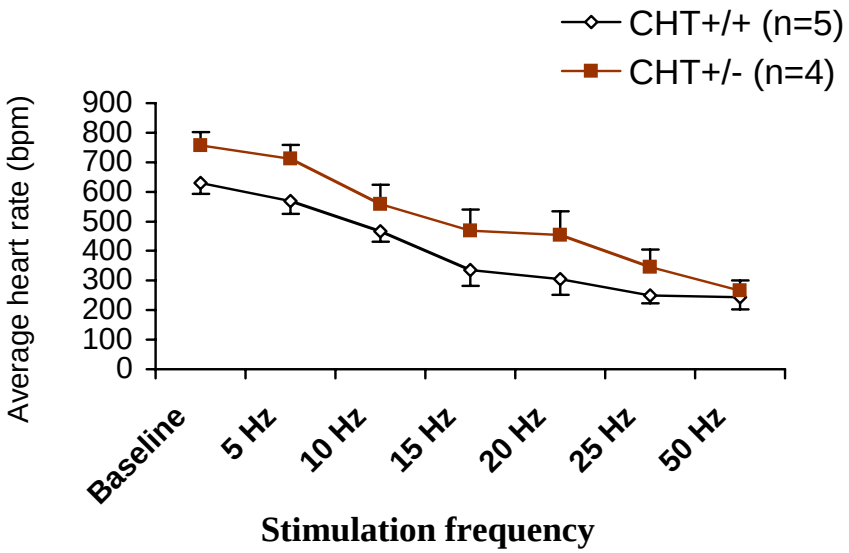

Figure 25. Vagal stimulation decreases heart rate in a frequency-dependent manner in both CHT+/- and CHT+/+ mice. Subcutaneous ECG recordings were used to evaluate bradycardia evoked by right vagal stimulation, using a 2 ms, 16 V, 30 sec duration pulse, in isofluorane-anaesthetized, 1.5 year-old, male mice. The genotypes did not differ in their responses.

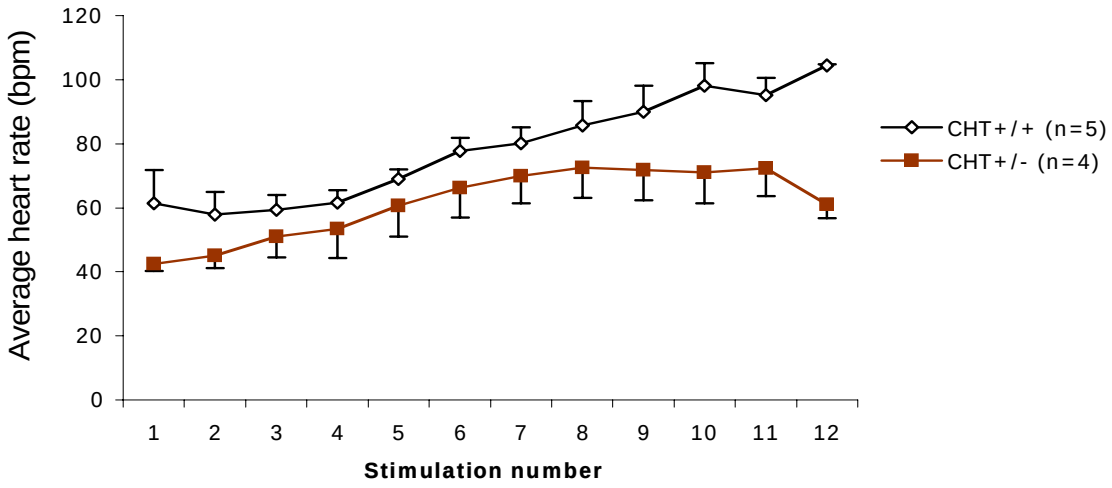

Figure 26. CHT+/- mice display greater bradycardia in response to repeated vagal stimulation. Subcutaneous ECG recordings were used to evaluate bradycardia evoked by right vagal stimulation, using a 25 Hz, 2 ms, 16 V, 30 sec duration pulse, in isofluorane-anaesthetized, 1.5 year-old, male mice. The CHT+/- mice display a trend towards greater capacity for vagally-induced bradycardia.

subtype, mediate vagal innervation of the heart, resulting in bradycardia following parasympathetic activation. In order to investigate possible alterations in nAChR and mAChR function and therefore altered sensitivity to nicotinic and muscarinic agents in the CHT+/- mice, we instrumented CHT+/- and CHT+/+ siblings with ECG telemetry devices and jugular intravenous (IV) ports, allowing the IV administration of drugs in freely moving awake animals, and the subsequent recording of drug effects on heart rate in beats per minute (bpm).

To address nAChR sensitivity in the context of CHT heterozygosity I challenged CHT+/- mice and CHT+/+ siblings with the nicotinic receptor antagonist hexamethonium (30 ug/kg iv). Hexamethonium treatment results in ganglionic blockade, and in mice, where sympathetic tone is predominant, typically lowers heart rate. While at this dose, and within a short term period (less than 30 minutes), heart rates did not change significantly in the CHT+/+ mice and the mice appeared unaffected, heart rates in the CHT+/-s decreased significantly (Fig. 27) and both subjects died. This suggests ganglionic nAChR hypersensitivity in the CHT+/- mice.

To characterize mAChR function, I challenged CHT+/- and CHT+/+ siblings with increasing doses of the muscarinic receptor antagonist metscopolamine (0.1-1 ug/kg iv). Muscarinic blockade blocks vagal innervation to the heart, which in mice is thought to be predominantly mediated by M2, and results in tachycardia, as well as reduced heart rate variability. While increasing doses of metscopolamine led to increases in heart rate in CHT+/+ mice, they did not have a large effect on CHT+/- heart rate (Fig. 28), suggesting a possible mAChR hyposensitivity in the CHT+/- mice. A particularly striking effect was the complete abolition of heart rate variability in the CHT+/- mice.

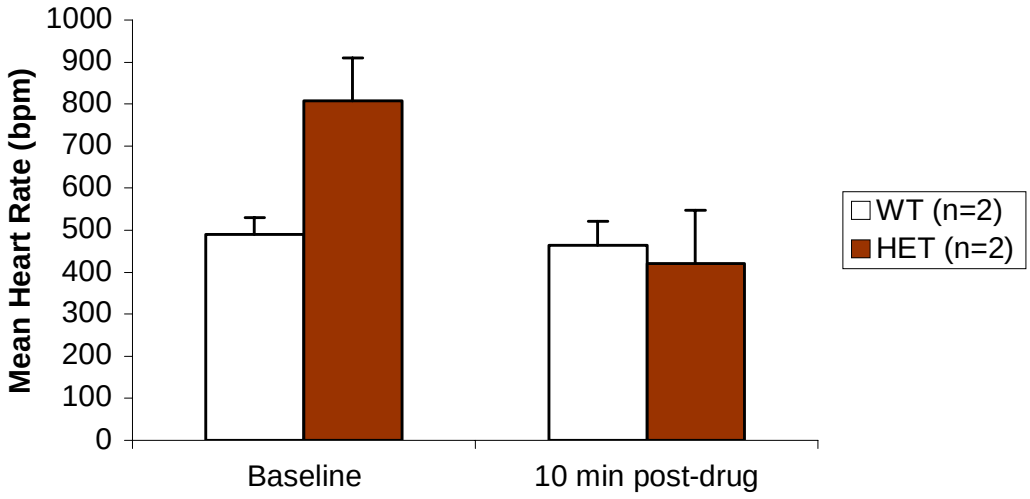

Figure 27. CHT+/- mice appear to be hypersensitive to ganglionic nicotinic receptor blockade. 1.5 year old male mice were instrumented with jugular catheters for intravenous (i.v.) drug administration, and heart rate responses to pharmacological challenge with 30 mg/kg hexamethonium were recorded in awake, freely-behaving mice using implanted telemetry devices. CHT+/- appeared hypersensitive to hexamethonium challenge as measured by heart rate responses, and also by the lethal effect of the drug which left the wild type siblings unaffected. WT = CHT+/+; HET = CHT+/-.

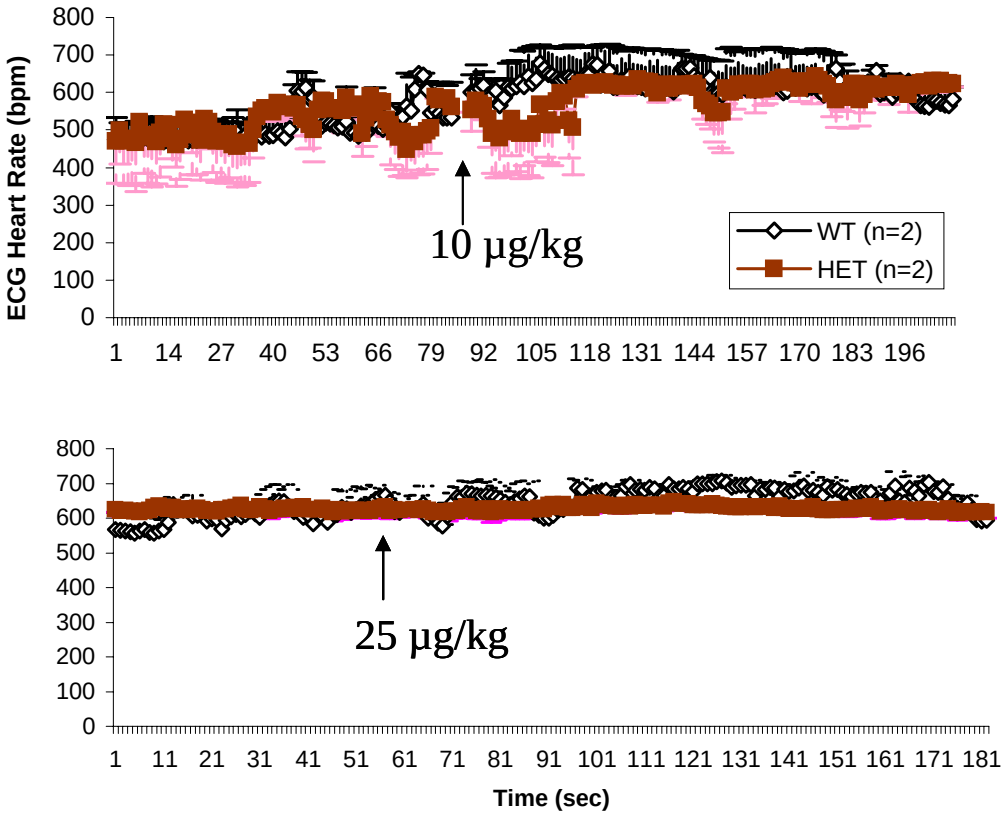

Figure 28. Reduced variability in CHT+/- heart rate in response to peripheral muscarinic blockade. 1.5 year old male mice were instrumented with jugular catheters for intravenous (i.v.) drug administration, and heart rate responses to pharmacological challenge with 10 and 20 µg/kg metscopolamine were recorded in awake, freely-behaving mice using implanted telemetry devices.

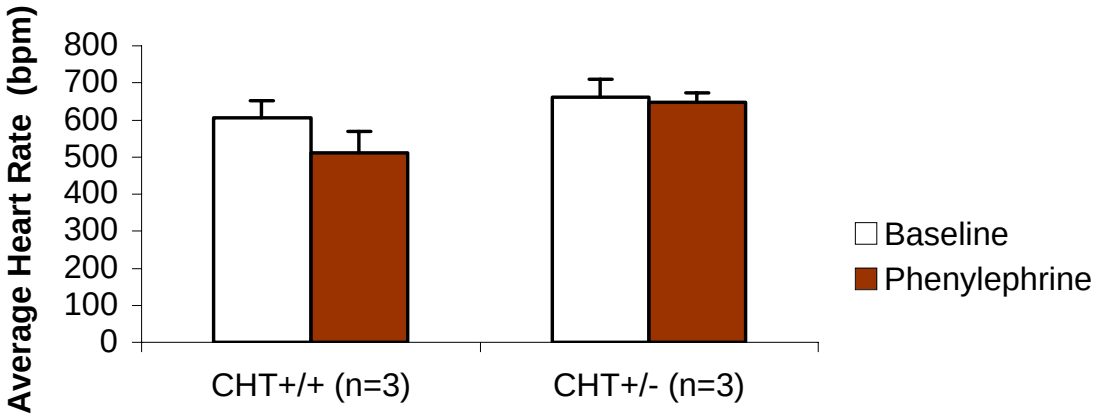

Figure 29. CHT+/- mice may be less responsive to phenylephrine-induced baroreflex bradycardia. 1.5 year old male mice were instrumented with jugular catheters for intravenous (i.v.) drug administration, and heart rate responses to pharmacological challenge with 10 µg/kg phenylephrine (min 46 of recording) following a baseline recording free of drug (min 1-3 of recording) were captured in awake, freely-behaving mice using implanted telemetry devices.

Finally, in order to evaluate the functional responsiveness of the CHT+/- cardiovascular system, I used a phenylephrine challenge to the baroreflex response. Phenylephrine administration results in increased blood pressure and compensatory vagally-mediated bradycardia. I hypothesized that CHT+/- mice may be compromised in their ability to sustain cholinergic signaling underlying a prolonged vagal response, and thus may not be able to mount or maintain a bradycardic baroreflex response to phenylephrine. Indeed, while CHT+/+ animals display reduced heart rates following phenylephrine administration, CHT+/- mice did not seem to respond to the drug challenge (Fig. 29).

Dopamine Release and Cocaine Self-Administration

Preliminary data obtained through collaborative efforts show reduced basal, as well as nicotine- and cocaine- evoked dopamine release in the nucleus accumbens (NAc) of CHT+/- mice (Fig. 31). These results not only support reduced dose-dependent cocaine self-administration (Fig. 32) by the CHT+/- mice (24.0±10.8 cocaine infusions at the 0.3 mg/kg/infusion cocaine dose, compared to 47.0±8.5 infusions by CHT+/+ littermates), but suggest a possible mechanism underlying the phenotype – dysregulated nicotinic receptors. One possible scenario involves hypofunctioning postsynaptic nicotinic receptors NAc on dopaminergic terminals, resulting in reduced DA release. Another potential mechanism may involve hyposensitive presynaptic nicotinic receptors, resulting in reduced ACh release and, consequently, lower DA release. The latter hypothesis is especially important in light of previous demonstrations of increased ACh release in the rat NAc and my findings of increased choline uptake in the striatum of cocaine self-

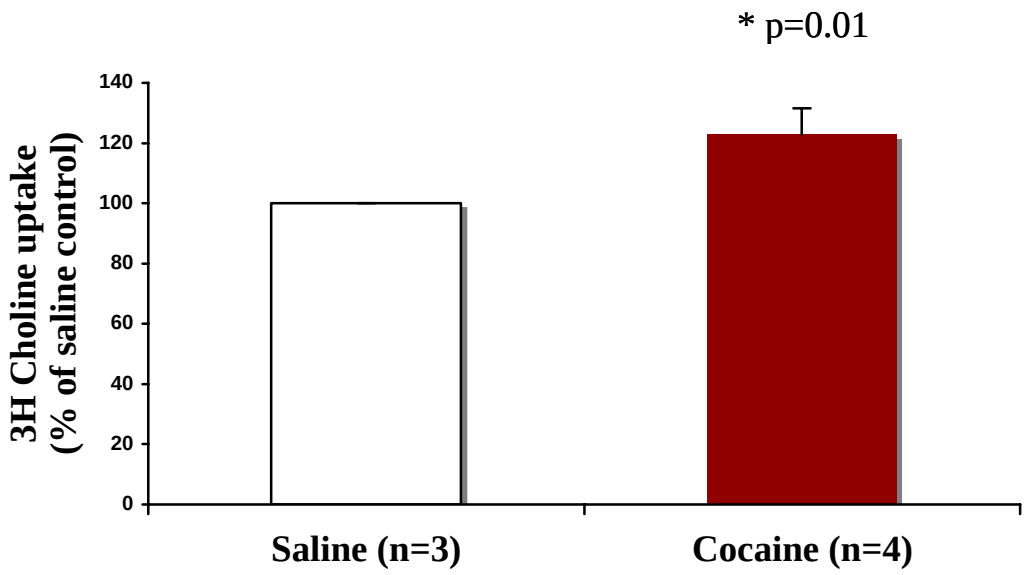

Figure 30. Cocaine self-administration increases HACU in striatum of C57Bl6 mice. HC-3-sensitive 3H choline transport assays were performed in striatal synaptosomes of C57Bl6 wild type mice following saline or cocaine self-administration; one-sample t test against a theoretical value (100% for saline controls). Data obtained through collaborative effort with Chris Olsen, Danny Winder lab.

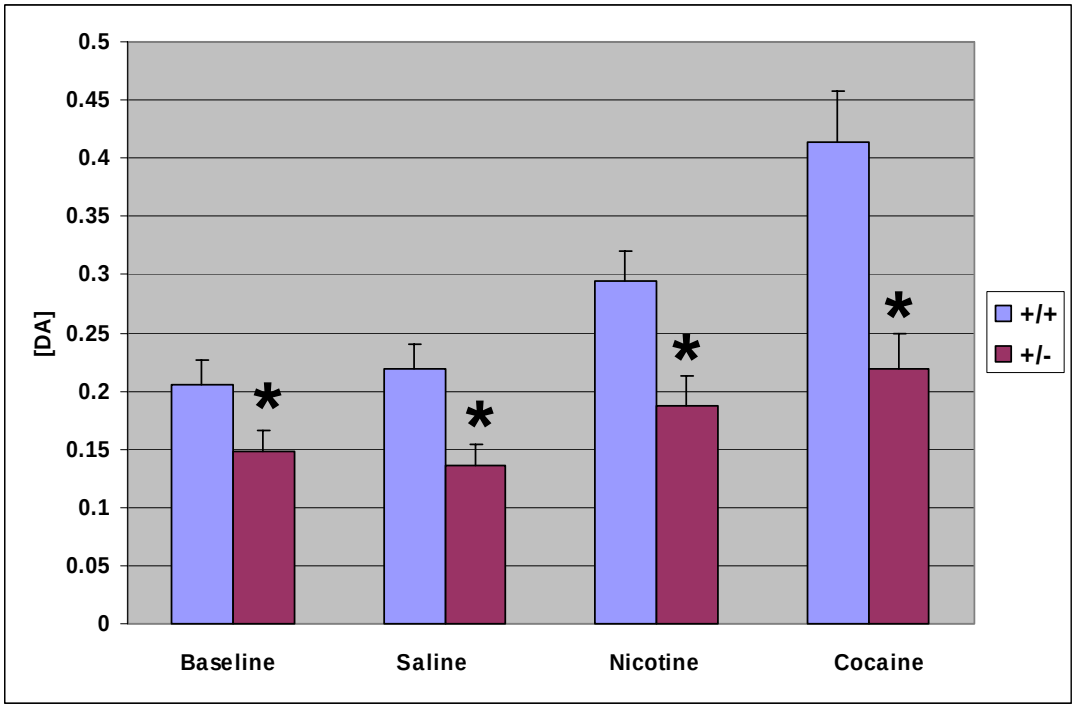

Figure 31. Baseline, nicotine- and cocaine-induced dopamine release is lower in the CHT+/- nucleus accumbens. Microdialysis was used to assess dopamine release in the nucleus accumbens of CHT+/+ (n=30) and CHT+/- (n=33) littermates. Following a baseline dialysate collection, saline and nicotine (1.0 mg/kg i.p.) were injected 1 hour apart. Samples were collected every 20 min for 4 hours following the nicotine injection. At the end of the 4 hours cocaine (10mg/kg) was injected, and samples were collected every 20 min for 1 h. The graph values represent averages of 3 20 min fractions immediately following injections (means ± sem); * $P < 0.05$, t test. Data obtained through collaborative effort with John Dani lab. This figure was contributed by Yu Dong.

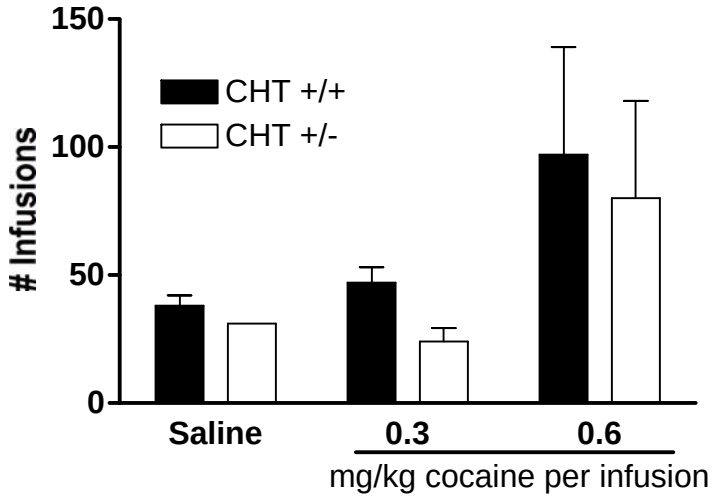

Figure 32. CHT+/- mice appear hyposensitive to low doses of cocaine in self-administration paradigm. Seven to 9 week old male mice were instrumented with jugular catheters to allow intravenous self-administration of cocaine. Whereas genotypes did not differ in the saline or 0.6 mg/kg cocaine conditions, CHT+/- mice self-administered significantly fewer cocaine infusions (24.0±10.8) compared to CHT+/+ littermates (47.0±8.5) at a low, 0.3 mg/kg dose of cocaine. Saline, CHT+/+ (n=2), CHT+/- (n=1); 0.3 mg/kg cocaine CHT+/+ (n=2), CHT+/- (n=4); 0.6 mg/kg cocaine, CHT+/+ (n=2), CHT+/- (n=3). Data obtained through collaborative effort with Danny Winder lab. This figure was contributed by Chris Olsen.

administering wild type mice (Fig. 30). Future studies will pursue these and additional hypothesis to reveal the mechanisms underlying altered DA release and addictive behaviors in conditions of CHT hemizygosity.

Circadian Rhythms

In wheel-running studies, CHT+/- mice show a pattern of reduced running-wheel activity upon initial introduction to a novel environment, with activity gradually increasing to wild type levels as the animals habituate to the surroundings (Bazalakova et al, preliminary findings, data not shown). These data are interesting in the context of our observations of altered patterns of baseline locomotor activity in the open field paradigm (increased vertical rearings, but decreased horizontal counts) (Chapter III), and suggest that novelty-induced exploration may be subtly different in the CHT+/- mice. In addition, circadian rhythm generation is not altered, and CHT+/- mice display wildtype periodicity in 12 hour light-dark, as well as continual darkness, conditions (data not shown). However, a striking difference becomes apparent between genotypes in studies of light-induced phase shifts (Fig. 33A). While only 15% of CHT+/+ mice upregulate their locomotor activity in the first dark period following a 6 hour light phase shift, 85% of CHT+/- mice respond to the phase shift almost immediately. CHT+/- activity levels are indistinguishable from baseline within 2 days post-phase-shift, while CHT+/+ mice require an additional day to recover baseline activity (Fig. 33B). Possible mechanisms underlying this interesting phenotype, including altered cholinergically-modulated retinal function and clock gene regulation, as well as muscarinic and nicotinic receptor expression and function in the SCN, will be investigated in future experiments.

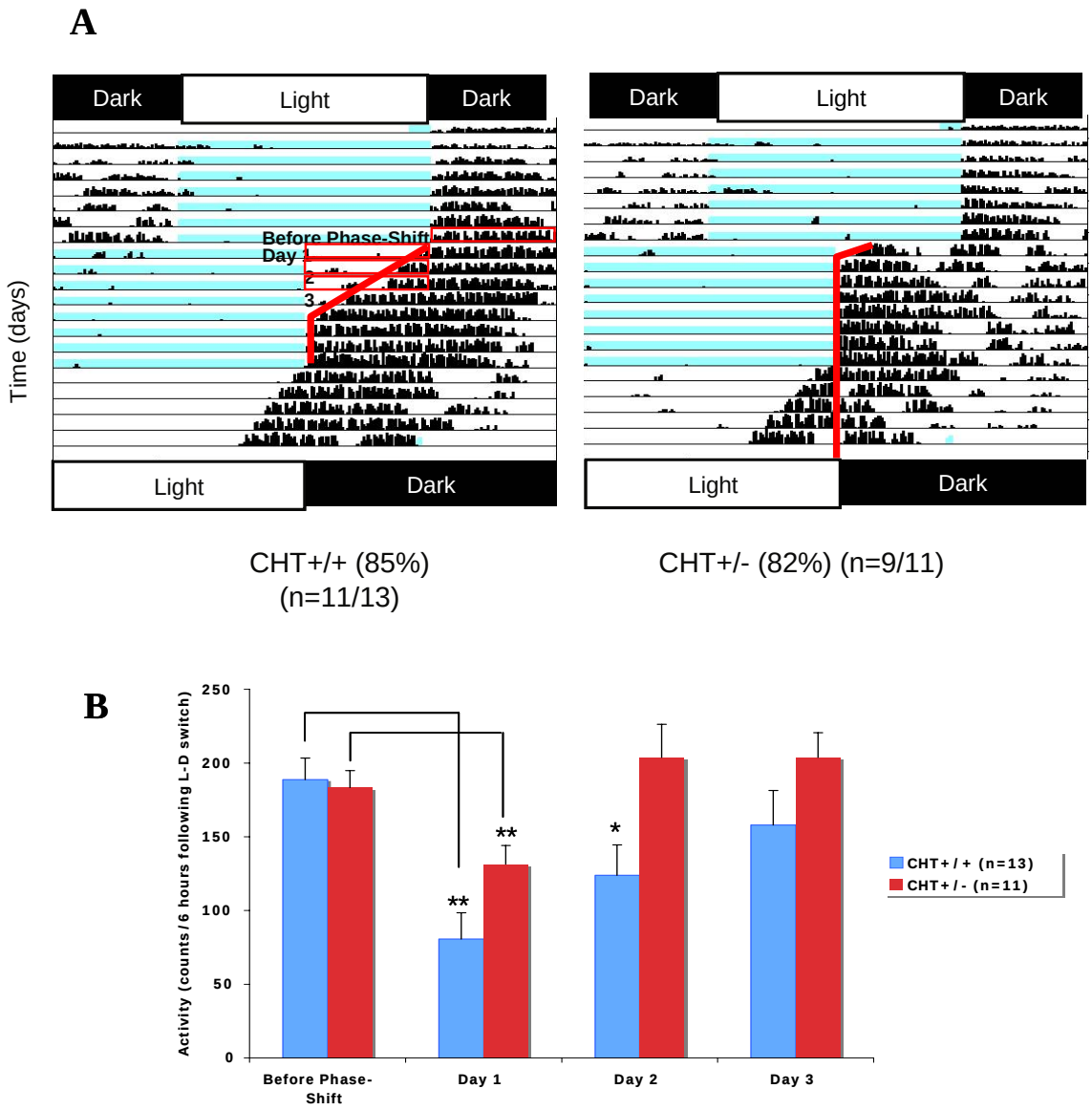

Figure 33. CHT+/- mice are more responsive to phase entrainment. Activity levels were analyzed in 6 hour increments during dark periods immediately preceding (before phase-shift) and on subsequent days (Day 1, 2, 3) following a 6 hour phase-shift in light-dark exposure of adult male mice in a circadian rhythm paradigm **(B).** 82% of CHT+/- mice, but only 15% of CHT+/+ mice adapted to the light phase shift within the first dark period following the phase-shift **(A)**; * $p<0.05$, two-tailed t-test (values +/- SEM). Data obtained through collaborative effort with Hidenobu Ohta and Chris Ciareglio from Doug McMahon lab.

In summary, preliminary studies using small numbers of mice suggest that CHT hemizygosity results in alterations in cardiovascular, dopamine release, drug addiction, and circadian phase shift behaviors. In cardiovascular studies, CHT+/- mice appear to be tachycardic, display reduced LF/HF heart rate variability ratios suggestive of parasympathetic withdrawal, have enhanced responsiveness to repeated vagal stimulation, possibly mediated by hyper-responsive ganglionic nicotinic receptors, and decreased heart rate variability in response to peripheral muscarinic blockade. In preliminary studies of dopaminergic signaling and related behaviors, baseline, as well as nicotine- and cocaine-induced, dopamine release is significantly reduced in the CHT+/- basal forebrain, providing a mechanistic explanation for reduced cocaine self-administration by the CHT+/- mice. Circadian rhythm studies reveal a striking responsiveness to light-induced phase shifting by the CHT+/- mice. Future studies will be needed to extend these intriguing data and elucidate mechanisms underlying the observed phenotypes.

CHAPTER V

CONCLUSIONS AND FUTURE DIRECTIONS

CHT Is Required for Survival: CHT Homozygosity (CHT-/-) is Lethal

The generation of CHT knockout mice via homologous recombination allowed the direct study of CHT's physiological impact *in vivo* (Ferguson et al., 2004). Homozygous (CHT-/-) mice are born at expected Mendelian ratios, and display normal gross anatomy. However, CHT-/- pups appear apneic and hypoxic, are largely immobile, and die within an hour after birth. Electrophysiological recordings at the sternomastoid NMJ show that the CHT-/- animals are born with wild type stores of ACh, but are unable to sustain ACh synthesis and release under high demand for ACh turnover at the NMJ synapse, leading to motor and respiratory paralysis (Ferguson et al., 2004). Detailed immunofluorescence studies of the CHT-/- NMJ reveal a more subtle phenotype of immature NMJ formation, similar to the phenotype observed in another knockout mouse, ChAT-/-, which is incapable of ACh synthesis and is also not viable (Brandon et al., 2003; Misgeld et al., 2002). Although CHT-/- homozygosity is lethal, embryonic neuronal cultures can be used in future studies to investigate the effects of complete lack of CHT on other determinants of cholinergic signaling, including muscarinic and nicotinic receptors, VAChT and other synaptic proteins, and ChAT and AChE enzyme expression and activity.

In addition, efforts are currently underway to rescue the CHT-/- mice. These include the creation of transgenic (CHT-Tg) mice over-expressing CHT under the Hb-9

motor-specific promoter, and the subsequent crossing of CHT-Tg and CHT+/- mice in order to obtain mice with CHT expression restricted to motor neurons. These mice should survive due to restored ACh transmission at the NMJ, yet will allow studies of central and peripheral function in the absence of CHT in any but motor neurons. An alternative approach, also being developed in the lab, is the creation of CHT floxed mice which, when crossed to mice expressing Cre recombinase under a forebrain- or autonomic-specific promoter, will allow the controlled, region-specific ablation of CHT.

Studies in either line of rescue mice will provide invaluable information about the effect of complete loss of CHT in select neuronal populations on ACh turnover and cholinergically-mediated behaviors supported by individual brain regions. Additionally, CHT-Tg mice will allow, for the first time, an investigation of the consequences of CHT over-expression.

CHT Heterozygous (CHT+/-) Mice as Models of Cholinergic Dysfunction

Changes in CHT function and expression have been documented in various mouse models of cholinergic dysfunction, suggesting an active role for CHT regulation in response to insults on ACh neurotransmission (Bazalakova and Blakely, 2006). These observations led to the hypothesis that reduced CHT reserves may result in impairment of cholinergically-mediated behaviors under conditions of physical or pharmacological challenge to cholinergic circuits. In support of this idea, CHT+/- mice display an increase in sensitivity to the lethal effects of HC-3 compared to wild type littermates (Ferguson et al., 2004).

Functional Compensation and Normal Basal Behaviors in CHT+/- Mice

Under normal conditions, CHT+/- mice survive to adulthood, are capable of sustaining basal sensory-motor behaviors, reproduce, and generally appear indistinguishable from their wild type siblings. These observations are supported by the functional compensation evident in biochemical studies: synaptosomal uptake assays show that choline transport in CHT+/- mice is comparable to uptake in CHT+/+ controls (Ferguson et al., 2004). In addition, ChAT and AChE activities are unchanged in the CHT+/- brain (Ferguson et al., 2004); (Bazalakova et al, 2007; Chapter III). In our initial behavioral investigation of this model, CHT+/- performance is indistinguishable from wild type in a wide variety of behavioral tasks, including sensory-motor (Irwin screen, pre-pulse inhibition), motor coordination (rotarod and wire hang), overall locomotor activity (open fields), anxiety (elevated plus maze, light-dark paradigm) and spatial learning and memory tests (Morris water maze, spontaneous Y maze alternation, rewarded T-maze alternation) (Bazalakova et al., 2007).

In light of the alterations in brain ACh and choline levels (possibly in the form of compromised ACh reserve pools and/or precursor choline availability) and challenge-induced phenotypes discussed below, it will be of great interest to repeat the above behavioral studies under physical or pharmacological challenges directed at cholinergic transmission. For example, I would predict dose-dependent impairments in CHT+/- performance in the Morris water maze or T maze in response to scopolamine challenge.

Physical and Pharmacological Challenges Reveal Motor Phenotypes in CHT+/- Mice

As opposed to relatively normal spontaneous behavior, focused challenges reveal that CHT+/- mice are vulnerable to sustained demands on cholinergically-supported behaviors. For example, CHT+/- mice are capable of sustaining running on a treadmill at low speeds or for short periods of time, but they are unable to reach treadmill speeds as high as those attained by CHT+/+ littermates. At a constant high speed, CHT+/- mice fatigue sooner than CHT+/+ controls. Pharmacological challenges also reveal motor phenotypes in CHT+/- mice. Specifically, CHT+/- mice are hyposensitive to muscarinic antagonist (scopolamine)-induced increases in locomotion, and display a trend towards hypersensitivity to muscarinic agonist (oxotremorine)-induced tremor (Bazalakova et al., 2007).

Electrophysiological studies of ACh release at the adult CHT+/- NMJ, as well as detailed morphological examination of muscle anatomy, would be of great value in addressing our hypotheses and ascertaining the exact mechanism underlying motor phenotypes in the CHT+/- mice. Future studies can also examine additional physiological effects of the muscarinic drugs already used, such as salivation in response to oxotremorine, or hypothermia in response to scopolamine, in order to specify the particular cholinergic pathways most affected by hemizygosity in the CHT+/- mice.

ACh Homeostasis and mAChR Expression Are Altered in CHT+/- Mice

The altered sensitivity of CHT+/- mice to muscarinic agents may be explained by region-specific changes in mAChR expression. Indeed, immunoblot studies using mAChR specific antibodies demonstrate decreased M1 (striatum) and M2 (cortex and

striatum) protein expression (Bazalakova et al, 2007). These findings are particularly interesting in light of the alterations of muscarinic receptor expression found in conjunction with changes in CHT protein levels in other mouse models of cholinergic dysfunction, including AChE-/- and AChE-Tg mice (Erb et al., 2001; Svedberg et al., 2003; Volpicelli-Daley et al., 2003b).

It will be of interest to quantify M3, M4, and M5 expression in the CHT+/- brain, as well as evaluate CHT+/- mice performance in behaviors that are known to be altered in various mAChR knockouts. For example, cocaine self-administration is diminished in M5 knockouts, while amphetamine-stimulated locomotion is enhanced in M1 knockout mice (Gerber et al., 2001; Thomsen et al., 2005). Future studies will address these and similar questions, leading to a better understanding of the interplay between CHT and mAChRs in the maintenance of ACh turnover, physiological cholinergic signaling, and psychostimulant action. In particular, functional studies of mAChR, such as carbachol-induced GTPγS stimulation in brain slices, can reveal valuable new information about mAChR function in the CHT+/- brain.

Our findings of reduced ACh and elevated choline levels in the CHT+/- brain have been observed in other mouse models of cholinergic dysfunction, including the PDAPP transgenic mouse model of Alzheimer's disease. PDAPP mice overexpress the human Ab peptide and display behavioral abnormalities, amyloid deposition and plaque formation in the absence of overt cell loss. In vivo microdialysis demonstrates lower basal ACh tissue levels but higher extracellular choline levels in the PDAPP transgenic hippocampus (Bales et al., 2006). Surprisingly, whereas ACh efflux is lower in the hippocampi of scopolamine-treated PDAPP mice compared to scopolamine-treated wild

types, ACh efflux is significantly higher compared to wild type in PDAPP mice exposed to a novel environment, suggesting that a redistribution and altered regulation of ACh release and reserve pools may serve to compensate for reduced overall ACh levels. The authors interpret the elevated extracellular choline levels as another attempt to compensate for decreased ACh levels. Interestingly, HACU Vmax is approximately 50% higher in PDAPP synaptosomes, suggesting that the efficiency of transport and/or targeting of HACU-derived choline is disrupted in the PDAPP brain, possibly by CHT mislocalization on the plasma membrane.

The complementary findings in CHT+/- and PDAPP Tg mice point to the fascinating possibility of creating a new mouse model of cholinergic dysfunction by crossing the two lines of animals. Behavioral, biochemical and pharmacological studies in PDAPP Tg/CHT+/- mice involving the phenotypes and various biochemical determinants of cholinergic signaling described in this work would complement and extend the data obtained in the individual mouse lines. Initial characterizations of variables such as β-amyloid load and rate of plaque formation and/or cell death would inform the relevance of the proposed hybrid line as a potential new model of cholinergically-related disease, specifically Alzheimer's disease.

In summary, CHT plays an important role in the maintenance of ACh turnover and cholinergic neurotransmission. Studies in various mouse models of cholinergic dysfunction demonstrate that CHT actively participates in compensatory pathways aimed at maintaining cholinergic signaling. Initial basic findings suggest that relocalization of vesicular pools to the plasma membrane surface constitutes a likely partial mechanism of CHT regulation. Our synaptosomal biotinylation results (Chapter III) and studies utilizing

genetically modified mouse models may reveal interesting alternatives. For example, if synaptosomal biotinylation or subcellular fractionation techniques demonstrate CHT protein presence on the plasma membrane of α3-/- brain terminals that lack HC-3 sensitive choline uptake, a mechanism of regulation other than vesicular translocation will be indicated. It is also important to address the possible contribution of nAChRs to dysfunction and CHT regulation in the CHT+/- mice. This can be accomplished both through basic characterization of nAChR expression and function in the CHT+/- brain, and also through characterization of the effects of nicotinic agonist and antagonist challenges on select behaviors, such as nicotine-induced locomotion in the open field paradigm.

Preliminary studies point to cardiovascular, dopamine release, drug addiction, and circadian phase shift phenotypes in the CHT+/- mice. In cardiovascular studies, CHT+/- mice appear to be tachycardic, display reduced LF/HF heart rate variability ratios suggestive of parasympathetic withdrawal, have enhanced responsiveness to repeated vagal stimulation, possibly mediated by hyper-responsive ganglionic nicotinic receptors, and decreased heart rate variability in response to peripheral muscarinic blockade. Increased sample sizes and additional experiments, such as assessment of heart rate and blood pressure modulation in response to physical (treadmill) or emotional (shock-induced anxiety) challenge, will provide a clearer understanding of the role of CHT in cardiovascular regulation.

In preliminary characterization of dopaminergic signaling and related behaviors, baseline, as well as nicotine- and cocaine-induced, dopamine release is significantly reduced in the CHT+/- basal forebrain, suggesting one possible mechanistic explanation

for reduced cocaine self-administration by the CHT+/- mice. In light of our muscarinic findings and studies in M5 knockout mice, it would be valuable to characterize muscarinic modulation of DA release and addiction behaviors in the CHT+/- mice and M5 expression in the CHT+/- VTA. In addition, it will be interesting to evaluate CHT+/- responses to other drugs of abuse, such as amphetamine, which would help distinguish the neuroanatomical substrates involved in the observed phenotypes. CHT+/- performance in paradigms such as psychostimulant-evoked hyperlocomotion in the open field, or conditioned place preference (CPP) will facilitate the integration of new findings within pre-existing research and established models of drug abuse.

Circadian rhythm studies reveal a striking responsiveness to light-induced phase shifting by the CHT+/- mice. Future studies will be needed to extend these intriguing data and elucidate mechanisms underlying the observed phenotypes. In the context of previous studies of muscarinic and nicotinic modulation of circadian rhythms in wild type mice, nicotinic and muscarinic pharmacological challenges and analysis of consequent circadian rhythmicity as well as phase shift reponses by CHT+/- mice would be particularly interesting. In addition, characterization of cholinergically-modulated retinal function, as well as clock gene regulation, in the CHT+/- mice will be of importance to understand the neuroanatomical and molecular underpinnings of the phenotypes we have observed.

In summary, the behavioral, biochemical, and pharmacological experiments proposed above will provide further insight into the molecular mechanisms of CHT function and regulation, with the eventual goal of manipulating CHT function in disorders of cholinergic origin.

REFERENCES

Alcantara, A. A., Mrzljak, L., Jakab, R. L., Levey, A. I., Hersch, S. M., and Goldman-Rakic, P. S. (2001). Muscarinic m1 and m2 receptor proteins in local circuit and projection neurons of the primate striatum: anatomical evidence for cholinergic modulation of glutamatergic prefronto-striatal pathways. J Comp Neurol *434*, 445-460.

Apparsundaram, S., Ferguson, S. M., and Blakely, R. D. (2001a). Molecular cloning and characterization of a murine hemicholinium-3- sensitive choline transporter. Biochem Soc Trans *29*, 711-716.

Apparsundaram, S., Ferguson, S. M., George, A. L., Jr., and Blakely, R. D. (2000). Molecular cloning of a human, hemicholinium-3-sensitive choline transporter. BBRC *276*, 862-867.

Apparsundaram, S., Martinez, V., Parikh, V., Kozak, R., and Sarter, M. (2005). Increased capacity and density of choline transporters situated in synaptic membranes of the right medial prefrontal cortex of attentional task-performing rats. J Neurosci *25*, 3851-3856.

Apparsundaram, S., Sung, U., Price, R. D., and Blakely, R. D. (2001b). Trafficking-dependent and -independent pathways of neurotransmitter transporter regulation differentially involving p38 mitogen-activated protein kinase revealed in studies of insulin modulation of norepinephrine transport in SK-N-SH cells. JPET *299*, 666-677.

Arnold, H. M., Burk, J. A., Hodgson, E. M., Sarter, M., and Bruno, J. P. (2002). Differential cortical acetylcholine release in rats performing a sustained attention task versus behavioral control tasks that do not explicitly tax attention. Neuroscience *114*, 451-460.

Bales, K. R., Tzavara, E. T., Wu, S., Wade, M. R., Bymaster, F. P., Paul, S. M., and Nomikos, G. G. (2006). Cholinergic dysfunction in a mouse model of Alzheimer disease is reversed by an anti-A beta antibody. J Clin Invest *116*, 825-832.

Baron, R., and Engler, F. (1996). Postganglionic cholinergic dysautonomia with incomplete recovery: a clinical, neurophysiological and immunological case study. J Neurol *243*, 18-24.

Basile, A. S., Fedorova, I., Zapata, A., Liu, X., Shippenberg, T., Duttaroy, A., Yamada, M., and Wess, J. (2002). Deletion of the M5 muscarinic acetylcholine receptor attenuates

morphine reinforcement and withdrawal but not morphine analgesia. ProcNatlAcadSci *99*, 11452-11457.

Bauerfeind, R., Regnier-Vigouroux, A., Flatmark, T., and Huttner, W. B. (1993). Selective storage of acetylcholine, but not catecholamines, in neuroendocrine synaptic-like microvesicles of early endosomal origin. Neuron *11*, 105-121.

Bazalakova, M., and Blakely, R. D. (2006). The high-affinity choline transporter (CHT) - a critical protein for sustaining choilnergic signaling as revealed in studies of genetically altered mice. Handbook Exp Pharmacol *175*, 525-544.

Bazalakova, M. H., Wright, J., Schneble, E. J., McDonald, M. P., Heilman, C. J., Levey, A. I., and Blakely, R. D. (2007). Deficits in acetylcholine homeostasis, receptors and behaviors in choline transporter heterozygous mice. Genes Brain Behav *6*, 411-424.

Beeri, R., Andres, C., Lev-Lehman, E., Timberg, R., Huberman, T., Shani, M., and Soreq, H. (1995). Transgenic expression of human acetylcholinesterase induces progressive cognitive deterioration in mice. CurOpBiol *5*, 1063-1071.

Beeri, R., Le Novere, N., Mervis, R., Huberman, T., Grauer, E., Changeux, J. P., and Soreq, H. (1997). Enhanced hemicholinium binding and attenuated dendrite branching in cognitively impaired acetylcholinesterase-transgenic mice. J Neurochem *69*, 2441-2451.

Bengel, D., Murphy, D. L., Andrews, A. M., Wichems, C. H., Feltner, D., Heils, A., Mossner, R., Westphal, H., and Lesch, K. P. (1998). Altered brain serotonin homeostasis and locomotor insensitivity to 3,4-methylenedioxymetamphetamine ("ecstasy") in serotonin transporter-deficient mice. Mol Pharmacol *53*, 649-655.

Berlanga, M. L., Olsen, C. M., Chen, V., Ikegami, A., Herring, B. E., Duvauchelle, C. L., and Alcantara, A. A. (2003). Cholinergic interneurons of the nucleus accumbens and dorsal striatum are activated by the self-administration of cocaine. Neuroscience *120*, 1149-1156.

Bertrand, N., Beley, P., and Beley, A. (1994). Brain fixation for acetylcholine measurements. J Neurosci Methods *53*, 81-85.

Bina, K. G., and Rusak, B. (1996). Muscarinic receptors mediate carbachol-induced phase shifts of circadian activity rhythms in Syrian hamsters. Brain Res *743*, 202-211.

Bina, K. G., Rusak, B., and Semba, K. (1993). Localization of cholinergic neurons in the forebrain and brainstem that project to the suprachiasmatic nucleus of the hypothalamus in rat. J Comp Neurol *335*, 295-307.

Birks, R. I., and MacIntosh, F. C. (1957). Acetylcholine metabolism at nerve-endings. Br Med Bull *13*, 157-161.

Birks, R. I., and MacIntosh, F. C. (1961). Acetylcholine metabolism of a sympathetic ganglion. Can J Biochem Physiol *39*, 787-827.

Blaha, C. D., Allen, L. F., Das, S., Inglis, W. L., Latimer, M. P., Vincent, S. R., and Winn, P. (1996). Modulation of dopamine efflux in the nucleus accumbens after cholinergic stimulation of the ventral tegmental area in intact, pedunculopontine tegmental nucleus-lesioned, and laterodorsal tegmental nucleus-lesioned rats. J Neurosci *16*, 714-722.

Blusztajn, J. K. (1998). Choline, a vital amine. Science *281*, 794-795.

Blusztajn, J. K., and Wurtman, R. J. (1981). Choline biosynthesis by a preparation enriched in synaptosomes from rat brain. Nature *290*, 417-418.

Boccia, M. M., Acosta, G. B., Blake, M. G., and Baratti, C. M. (2004). Memory consolidation and reconsolidation of an inhibitory avoidance response in mice: effects of i.c.v. injections of hemicholinium-3. Neuroscience *124*, 735-741.

Bolam, J. P., Francis, C. M., and Henderson, Z. (1991). Cholinergic input to dopaminergic neurons in the substantia nigra: a double immunocytochemical study. Neuroscience *41*, 483-494.

Borison, R. L., and Diamond, B. I. (1987). Neuropharmacology of the extrapyramidal system. J Clin Psychiatry *48 Suppl*, 7-12.

Brandon, E. P., Lin, W., D'Amour, K. A., Pizzo, D. P., Dominguez, B., Sugiura, Y., Thode, S., Ko, C. P., Thal, L. J., Gage, F. H., and Lee, K. F. (2003). Aberrant patterning of neuromuscular synapses in choline acetyltransferase-deficient mice. J Neurosci *23*, 539-549.

Brandon, E. P., Mellott, T., Pizzo, D. P., Coufal, N., D'Amour, K. A., Gobeske, K., Lortie, M., Lopez-Coviella, I., Berse, B., Thal, L. J., *et al.* (2004). Choline transporter 1

maintains cholinergic function in choline acetyltransferase haploinsufficiency. J Neurosci *24*, 5459-5466.

Brodde, O. E., Konschak, U., Becker, K., Ruter, F., Poller, U., Jakubetz, J., Radke, J., and Zerkowski, H. R. (1998). Cardiac muscarinic receptors decrease with age. In vitro and in vivo studies. J Clin Invest *101*, 471-478.

Buchanan, G. F., and Gillette, M. U. (2005). New light on an old paradox: site-dependent effects of carbachol on circadian rhythms. Exp Neurol *193*, 489-496.

Burgel, P., and Rommelspacher, H. (1978). Changes in high affinity choline uptake in behavioral experiments. Life Sci *23*, 2423-2427.

Bussiere, M., Vance, J. E., Campenot, R. B., and Vance, D. E. (2001). Compartmentalization of choline and acetylcholine metabolism in cultured sympathetic neurons. J Biochem (Tokyo) *130*, 561-568.

Calabresi, P., Centonze, D., Gubellini, P., Pisani, A., and Bernardi, G. (2000). Acetylcholine-mediated modulation of striatal function. Trends Neurosci *23*, 120-126.

Cermak, J. M., Holler, T., Jackson, D. A., and Blusztajn, J. K. (1998). Prenatal availability of choline modifies development of the hippocampal cholinergic system. The FASEB Journal *12*, 349-357.

Chatterjee, T. K., and Bhatnagar, R. K. (1990). Ca2(+)-dependent, ATP-induced conversion of the [3H]hemicholinium-3 binding sites from high- to low-affinity states in rat striatum: effect of protein kinase inhibitors on this affinity conversion and synaptosomal choline transport. J Neurochem *54*, 1500-1508.

Colwell, C. S., Kaufman, C. M., and Menaker, M. (1993). Phase-shifting mechanisms in the mammalian circadian system: new light on the carbachol paradox. J Neurosci *13*, 1454-1459.

Coyle, J. T., Price, D. L., and DeLong, M. R. (1983). Alzheimer's disease: a disorder of cortical cholinergic innervation. Science *219*, 1184-1190.

Coyle, J. T., and Yamamura, H. I. (1976). Neurochemical aspects of the ontogenesis of cholinergic neurons in the rat brain. Brain Res *118*, 429-440.

Damsma, G., Westerink, B. H., and Horn, A. S. (1985). A simple, sensitive, and economic assay for choline and acetylcholine using HPLC, an enzyme reactor, and an electrochemical detector. J Neurochem *45*, 1649-1652.

Dani, J. A. (2001). Overview of nicotinic receptors and their roles in the central nervous system. Biol Psychiatry *49*, 166-174.

Dani, J. A. (2003). Roles of dopamine signaling in nicotine addiction. Mol Psychiatry *8*, 255-256.

De Biasi, M. (2002). Nicotinic mechanisms in the autonomic control of organ systems. J Neurobiol *53*, 568-579.

Dhein, S., van Koppen, C. J., and Brodde, O. E. (2001). Muscarinic receptors in the mammalian heart. Pharmacol Res *44*, 161-182.

Doody, R. S. (2003). Current treatments for Alzheimer's disease: cholinesterase inhibitors. J Clin Psychiatry *64 Suppl 9*, 11-17.

Douglas, C. L., Baghdoyan, H. A., and Lydic, R. (2001). M2 muscarinic autoreceptors modulate acetylcholine release in prefrontal cortex of C57BL/6J mouse. JPET *299*, 960-966.

Duysen, E. G., Stribley, J. A., Fry, D. L., Hinrichs, S. H., and Lockridge, O. (2002). Rescue of the acetylcholinesterase knockout mouse by feeding a liquid diet; phenotype of the adult acetylcholinesterase deficient mouse. Brain Res Dev Brain Res *137*, 43-54.

Eckberg, D. L., Drabinsky, M., and Braunwald, E. (1971). Defective cardiac parasympathetic control in patients with heart disease. NEJM *285*, 877-883.

Ellman, G. L., Courtney, K. D., Andres, V., Jr., and Feather-Stone, R. M. (1961). A new and rapid colorimetric determination of acetylcholinesterase activity. Biochem Pharmacol *7*, 88-95.

Engel, A. G., Ohno, K., and Sine, S. M. (2003). Sleuthing molecular targets for neurological diseases at the neuromuscular junction. Nat Rev Neurosci *4*, 339-352.

Erb, C., Troost, J., Kopf, S., Schmitt, U., Loffelholz, K., Soreq, H., and Klein, J. (2001). Compensatory mechanisms enhance hippocampal acetylcholine release in transgenic mice expressing human acetylcholinesterase. J Neurochem *77*, 638-646.

Feng, G., Mellor, R. H., Bernstein, M., Keller-Peck, C., Nguyen, Q. T., Wallace, M., Nerbonne, J. M., Lichtman, J. W., and Sanes, J. R. (2000). Imaging neuronal subsets in transgenic mice expressing multiple spectral variants of GFP. Neuron *28*, 41-51.

Ferguson, S. M., Bazalakova, M., Savchenko, V., Tapia, J. C., Wright, J., and Blakely, R. D. (2004). Lethal impairment of cholinergic neurotransmission in hemicholinium-3-sensitive choline transporter knockout mice. ProcNatlAcadSci *101*, 8762-8767.

Ferguson, S. M., and Blakely, R. D. (2004). The choline transporter resurfaces: new roles for synaptic vesicles? Mol Interv *4*, 22-37.

Ferguson, S. M., Savchenko, V., Apparsundaram, S., Zwick, M., Wright, J., Heilman, C. J., Yi, H., Levey, A. I., and Blakely, R. D. (2003). Vesicular localization and activity-dependent trafficking of presynaptic choline transporters. J Neurosci *23*, 9697-9709.

Fink-Jensen, A., Fedorova, I., Wortwein, G., Woldbye, D. P., Rasmussen, T., Thomsen, M., Bolwig, T. G., Knitowski, K. M., McKinzie, D. L., Yamada, M., *et al.* (2003). Role for M5 muscarinic acetylcholine receptors in cocaine addiction. J Neurosci Res *74*, 91-96.

Forster, G. L., Yeomans, J. S., Takeuchi, J., and Blaha, C. D. (2002). M5 muscarinic receptors are required for prolonged accumbal dopamine release after electrical stimulation of the pons in mice. J Neurosci *22*, RC190.

Franceschini, D., Orr-Urtreger, A., Yu, W., Mackey, L. Y., Bond, R. A., Armstrong, D., Patrick, J. W., Beaudet, A. L., and De Biasi, M. (2000). Altered baroreflex responses in alpha7 deficient mice. Behav Brain Res *113*, 3-10.

Franklin, S. R., Sethy, V. H., and Tang, A. H. (1986). Amnesia produced by intracerebroventricular injections of hemicholinium-3 in mice was prevented by pretreatment with piracetam-like compounds. Pharmacol Biochem Behav *25*, 925-927.

Freeman, J. J., Macri, J. R., Choi, R. L., and Jenden, D. J. (1979). Studies on the behavioral and biochemical effects of hemicholinium in vivo. JPET *210*, 91-97.

Frick, K. M., Burlingame, L. A., Delaney, S. S., and Berger-Sweeney, J. (2002). Sex differences in neurochemical markers that correlate with behavior in aging mice. Neurobiol Aging *23*, 145-158.

Fujii, T., Okuda, T., Haga, T., and Kawashima, K. (2003). Detection of the high-affinity choline transporter in the MOLT-3 human leukemic T-cell line. Life Sci *72*, 2131-2134.

Gage, F. H., Chen, K. S., Buzsaki, G., and Armstrong, D. (1988). Experimental approaches to age-related cognitive impairments. Neurobiol Aging *9*, 645-655.

Garner, S. C., Mar, M. H., and Zeisel, S. H. (1995). Choline distribution and metabolism in pregnant rats and fetuses are influenced by the choline content of the maternal diet. J Nutr *125*, 2851-2858.

Gates, J., Jr., Ferguson, S. M., Blakely, R. D., and Apparsundaram, S. (2004). Regulation of choline transporter surface expression and phosphorylation by protein kinase C and protein phosphatase 1/2A. JPET *310*, 536-545.

Gerber, D. J., Sotnikova, T. D., Gainetdinov, R. R., Huang, S. Y., Caron, M. G., and Tonegawa, S. (2001). Hyperactivity, elevated dopaminergic transmission, and response to amphetamine in M1 muscarinic acetylcholine receptor-deficient mice. ProcNatlAcadSci *98*, 15312-15317.

Goldman, M. E., and Erickson, C. K. (1983). Effects of acute and chronic administration of antidepressant drugs on the central cholinergic nervous system. Comparison with anticholinergic drugs. Neuropharmacology *22*, 1215-1222.

Gomeza, J., Shannon, H., Kostenis, E., Felder, C., Zhang, L., Brodkin, J., Grinberg, A., Sheng, H., and Wess, J. (1999a). Pronounced pharmacologic deficits in M2 muscarinic acetylcholine receptor knockout mice. ProcNatlAcadSci *96*, 1692-1697.

Gomeza, J., Zhang, L., Kostenis, E., Felder, C., Bymaster, F., Brodkin, J., Shannon, H., Xia, B., Deng, C., and Wess, J. (1999b). Enhancement of D1 dopamine receptor-mediated locomotor stimulation in M(4) muscarinic acetylcholine receptor knockout mice. ProcNatlAcadSci *96*, 10483-10488.

Guyenet, P., Lefresne, P., Rossier, J., Beaujouan, J. C., and Glowinski, J. (1973). Inhibition by hemicholinium-3 of (14C)acetylcholine synthesis and (3H)choline high-affinity uptake in rat striatal synaptosomes. Mol Pharmacol *9*, 630-639.

Haga, T. (1971). Synthesis and release of (14C)acetylcholine in synaptosomes. J Neurochem *18*, 781-798.

Haga, T., and Noda, H. (1973). Choline uptake systems of rat brain synaptosomes. Biochim Biophys Acta *291*, 564-575.

Hagan, J. J., Jansen, J. H., and Broekkamp, C. L. (1989). Hemicholinium-3 impairs spatial learning and the deficit is reversed by cholinomimetics. Psychopharmacology (Berl) *98*, 347-356.

Hardman, J. G., and Limbird, L. E. (2001). The Pharmacological Basis of Therapeutics, 10 edn (New York, MgGraw-Hill).

Hikida, T., Kitabatake, Y., Pastan, I., and Nakanishi, S. (2003). Acetylcholine enhancement in the nucleus accumbens prevents addictive behaviors of cocaine and morphine. ProcNatlAcadSci *100*, 6169-6173.

Holden, J. T., Rossier, J., Beaujouan, J. C., Guyenet, P., and Glowinski, J. (1975). Inhibition of high-affinity choline transport in rat striatal synaptosomes by alkyl bisquaternary ammonium compounds. Mol Pharmacol *11*, 19-27.

Irwin, S. (1968). Comprehensive observational assessment: Ia. A systematic, quantitative procedure for assessing the behavioral and physiologic state of the mouse. Psychopharmacologia *13*, 222-257.

Iversen, L. L., Iversen, S. D., and Snyder, S. H. (1975). Biochemistry of Biogenic Amines., Vol 3).

Jones, S. F., and Kwanbunbumpen, S. (1970). Some effects of nerve stimulation andhemicholinium on quantal transmitter release at the mammalian neuromuscular junction. J Physiol *207*, 51-61.

Jope, R. S. (1979a). High affinity choline transport and acetylCoa production in brain and their roles in the regulation of acetylcholine synthesis. Brain Research Reviews *1*, 313-344.

Kaneko, S., Hikida, T., Watanabe, D., Ichinose, H., Nagatsu, T., Kreitman, R. J., Pastan, I., and Nakanishi, S. (2000). Synaptic integration mediated by striatal cholinergic interneurons in basal ganglia function. Science *289*, 633-637.

Karnovsky, M. J., and Roots, L. (1964). A "Direct-Coloring" Thiocholine Method for Cholinesterases. J Histochem Cytochem *12*, 219-221.

Kawashima, K., and Fujii, T. (2003). The lymphocytic cholinergic system and its biological function. Life Sci *72*, 2101-2109.

Kitabatake, Y., Hikida, T., Watanabe, D., Pastan, I., and Nakanishi, S. (2003). Impairment of reward-related learning by cholinergic cell ablation in the striatum. ProcNatlAcadSci *100*, 7965-7970.

Koc, H., Mar, M. H., Ranasinghe, A., Swenberg, J. A., and Zeisel, S. H. (2002). Quantitation of choline and its metabolites in tissues and foods by liquid chromatography/electrospray ionization-isotope dilution mass spectrometry. Anal Chem *74*, 4734-4740.

Kuhar, M. J., and Murrin, L. C. (1978a). Sodium-dependent, high affinity choline uptake. J Neurochem *30*, 15-21.

Kuhar, M. J., Sethy, V. H., Roth, R. H., and Aghajanian, G. K. (1973). Choline: selective accumulation by central cholinergic neurons. J Neurochem *20*, 581-593.

Kus, L., Borys, E., Ping Chu, Y., Ferguson, S. M., Blakely, R. D., Emborg, M. E., Kordower, J. H., Levey, A. I., and Mufson, E. J. (2003). Distribution of high affinity choline transporter immunoreactivity in the primate central nervous system. J Comp Neurol *463*, 341-357.

Lange, K. W., Javoy-Agid, F., Agid, Y., Jenner, P., and Marsden, C. D. (1992). Brain muscarinic cholinergic receptors in Huntington's disease. J Neurol *239*, 103-104.

Laviolette, S. R., and van der Kooy, D. (2004). The neurobiology of nicotine addiction: bridging the gap from molecules to behaviour. Nat Rev Neurosci *5*, 55-65.

Lee, H. C., Fellenz-Maloney, M. P., Liscovitch, M., and Blusztajn, J. K. (1993). Phospholipase D-catalyzed hydrolysis of phosphatidylcholine provides the choline precursor for acetylcholine synthesis in a human neuronal cell line. ProcNatlAcadSci *90*, 10086-10090.

Li, B., Duysen, E. G., Volpicelli-Daley, L. A., Levey, A. I., and Lockridge, O. (2003). Regulation of muscarinic acetylcholine receptor function in acetylcholinesterase knockout mice. Pharmacol Biochem Behav *74*, 977-986.

Li, B., Stribley, J. A., Ticu, A., Xie, W., Schopfer, L. M., Hammond, P., Brimijoin, S., Hinrichs, S. H., and Lockridge, O. (2000). Abundant tissue butyrylcholinesterase and its possible function in the acetylcholinesterase knockout mouse. J Neurochem *75*, 1320-1331.

Lips, K. S., Pfeil, U., Haberberger, R. V., and Kummer, W. (2002). Localisation of the high-affinity choline transporter-1 in the rat skeletal motor unit. Cell Tissue Res *307*, 275-280.

Liu, C., and Gillette, M. U. (1996). Cholinergic regulation of the suprachiasmatic nucleus circadian rhythm via a muscarinic mechanism at night. J Neurosci *16*, 744-751.

Loffelholz, K., and Pappano, A. J. (1985). The parasympathetic neuroeffector junction of the heart. Pharmacol Rev *37*, 1-24.

Lowenstein, P. R., and Coyle, J. T. (1986). Rapid regulation of [3H]hemicholinium-3 binding sites in the rat brain. Brain Res *381*, 191-194.

Ma, X., Abboud, F. M., and Chapleau, M. W. (2002). Analysis of afferent, central, and efferent components of the baroreceptor reflex in mice. Am J Physiol Regul Integr Comp Physiol *283*, R1033-1040.

Macintosh, F. C., Birks, R. I., and Sastry, P. B. (1956). Pharmacological inhibition of acetylcholine sythesis. Nature *4543*, 1181.

Maire, J. C., and Wurtman, R. J. (1985). Effects of electrical stimulation and choline availability on the release and contents of acetylcholine and choline in superfused slices from rat striatum. J Physiol (Paris) *80*, 189-195.

Mark, G. P., Hajnal, A., Kinney, A. E., and Keys, A. S. (1999). Self-administration of cocaine increases the release of acetylcholine to a greater extent than response-independent cocaine in the nucleus accumbens of rats. Psychopharmacology (Berl) *143*, 47-53.

Maselli, R. A., Chen, D., Mo, D., Bowe, C., Fenton, G., and Wollmann, R. L. (2003). Choline acetyltransferase mutations in myasthenic syndrome due to deficient acetylcholine resynthesis. Muscle Nerve *27*, 180-187.

Matthies, D. S., Fleming, P. A., Wilkes, D. M., and Blakely, R. D. (2006). The C. elegans choline transporter CHO-1 sustains acetylcholine synthesis and motor function in an activity-dependent manner. J Neurosci *in press*.

McGaughy, J., Kaiser, T., and Sarter, M. (1996). Behavioral vigilance following infusions of 192 IgG-saporin into the basal forebrain: selectivity of the behavioral impairment and relation to cortical AChE-positive fiber density. Behav Neurosci *110*, 247-265.

Meshorer, E., Biton, I. E., Ben-Shaul, Y., Ben-Ari, S., Assaf, Y., Soreq, H., and Cohen, Y. (2005). Chronic cholinergic imbalances promote brain diffusion and transport abnormalities. Faseb J *19*, 910-922.

Mesulam, M. M., Guillozet, A., Shaw, P., Levey, A., Duysen, E. G., and Lockridge, O. (2002). Acetylcholinesterase knockouts establish central cholinergic pathways and can use butyrylcholinesterase to hydrolyze acetylcholine. Neuroscience *110*, 627-639.

Miller, J. D., Murakami, D. M., and Fuller, C. A. (1987). The response of suprachiasmatic neurons of the rat hypothalamus to photic and nicotinic stimuli. J Neurosci *7*, 978-986.

Misawa, H., Nakata, K., Matsuura, J., Nagao, M., Okuda, T., and Haga, T. (2001). Distribution of the high-affinity choline transporter in the central nervous system of the rat. Neuroscience *105*, 87-98.

Misgeld, T., Burgess, R. W., Lewis, R. M., Cunningham, J. M., Lichtman, J. W., and Sanes, J. R. (2002). Roles of neurotransmitter in synapse formation: development of neuromuscular junctions lacking choline acetyltransferase. Neuron *36*, 635-648.

Miyakawa, T., Yamada, M., Duttaroy, A., and Wess, J. (2001). Hyperactivity and intact hippocampus-dependent learning in mice lacking the M1 muscarinic acetylcholine receptor. J Neurosci *21*, 5239-5250.

Murakami, N., Takahashi, K., and Kawashima, K. (1984). Effect of light on the acetylcholine concentrations of the suprachiasmatic nucleus in the rat. Brain Res *311*, 358-360.

Murrin, L. C., DeHaven, R. N., and Kuhar, M. J. (1977). On the relationship between (3H)choline uptake activation and (3H)acetylcholine release. J Neurochem *29*, 681-687.

Murrin, L. C., and Kuhar, M. J. (1976). Activation of high-affinity choline uptake in vitro by depolarizing agents. Mol Pharmacol *12*, 1082-1090.

Nakata, K., Okuda, T., and Misawa, H. (2004). Ultrastructural localization of high-affinity choline transporter in the rat neuromuscular junction: enrichment on synaptic vesicles. Synapse *53*, 53-56.

Neher, E. (1998). Vesicle pools and Ca2+ microdomains: new tools for understanding their roles in neurotransmitter release. Neuron *20*, 389-399.

Nelson, C. L., Sarter, M., and Bruno, J. P. (2000). Repeated pretreatment with amphetamine sensitizes increases in cortical acetylcholine release. Psychopharmacology (Berl) *151*, 406-415.

Neumann, S. A., Lawrence, E. C., Jennings, J. R., Ferrell, R. E., and Manuck, S. B. (2005). Heart rate variability is associated with polymorphic variation in the choline transporter gene. Psychosom Med *67*, 168-171.

O'Hara, B. F., Edgar, D. M., Cao, V. H., Wiler, S. W., Heller, H. C., Kilduff, T. S., and Miller, J. D. (1998). Nicotine and nicotinic receptors in the circadian system. Psychoneuroendocrinology *23*, 161-173.

O'Regan, S., Traiffort, E., Ruat, M., Cha, N., Compaore, D., and Meunier, F. M. (2000). An electric lobe suppressor for a yeast choline transport mutation belongs to a new family of transporter-like proteins. ProcNatlAcadSci *97*, 1835-1840.

Oakman, S. A., Faris, P. L., Kerr, P. E., Cozzari, C., and Hartman, B. K. (1995). Distribution of pontomesencephalic cholinergic neurons projecting to substantia nigra differs significantly from those projecting to ventral tegmental area. J Neurosci *15*, 5859-5869.

Oberhauser, V., Schwertfeger, E., Rutz, T., Beyersdorf, F., and Rump, L. C. (2001). Acetylcholine release in human heart atrium: influence of muscarinic autoreceptors, diabetes, and age. Circulation *103*, 1638-1643.

Ohno, K., Tsujino, A., Brengman, J. M., Harper, C. M., Bajzer, Z., Udd, B., Beyring, R., Robb, S., Kirkham, F. J., and Engel, A. G. (2001). Choline acetyltransferase mutations cause myasthenic syndrome associated with episodic apnea in humans. ProcNatlAcadSci *98*, 2017-2022.

Okuda, T., and Haga, T. (2000). Functional characterization of the human high-affinity choline transporter. FEBS Lett *484*, 92-97.

Okuda, T., Haga, T., Kanai, Y., Endou, H., Ishihara, T., and Katsura, I. (2000a). Identification and characterization of the high-affinity choline transporter. Nat Neurosci *3*, 120-125.

Okuda, T., Okamura, M., Kaitsuka, C., Haga, T., and Gurwitz, D. (2002). Single nucleotide polymorphism of the human high affinity choline transporter alters transport rate. JBC *277*, 45315-45322.

Olsen, C. M., and Winder, D. G. (2006). A method for single-session cocaine self-administration in the mouse. Psychopharmacology (Berl).

Pan, J., and Tompkins, W. J. (1985). A real-time QRS detection algorithm. IEEE Trans Biomed Eng *32*, 230-236.

Parikh, V., Pomerleau, F., Huettl, P., Gerhardt, G. A., Sarter, M., and Bruno, J. P. (2004). Rapid assessment of in vivo cholinergic transmission by amperometric detection of changes in extracellular choline levels. Eur J Neurosci *20*, 1545-1554.

Peralta, E. G., Ashkenazi, A., Winslow, J. W., Smith, D. H., Ramachandran, J., and Capon, D. J. (1987). Distinct primary structures, ligand-binding properties and tissue-specific expression of four human muscarinic acetylcholine receptors. Embo J *6*, 3923-3929.

Perry, E., Walker, M., Grace, J., and Perry, R. (1999a). Acetylcholine in mind: a neurotransmitter correlate of consciousness? Trends Neurosci *22*, 273-280.

Pfeil, U., Haberberger, R. V., Lips, K. S., Eberling, L., Grau, V., and Kummer, W. (2003a). Expression of the high-affinity choline transporter CHT1 in epithelia. Life Sci *72*, 2087-2090.

Pfeil, U., Lips, K. S., Eberling, L., Grau, V., Haberberger, R. V., and Kummer, W. (2003b). Expression of the high-affinity choline transporter, CHT1, in the rat trachea. Am J Respir Cell Mol Biol *28*, 473-477.

Pham, C. T., MacIvor, D. M., Hug, B. A., Heusel, J. W., and Ley, T. J. (1996). Long-range disruption of gene expression by a selectable marker cassette. ProcNatlAcadSci *93*, 13090-13095.

Pidoplichko, V. I., Noguchi, J., Areola, O. O., Liang, Y., Peterson, J., Zhang, T., and Dani, J. A. (2004). Nicotinic cholinergic synaptic mechanisms in the ventral tegmental area contribute to nicotine addiction. Learn Mem *11*, 60-69.

Poller, U., Nedelka, G., Radke, J., Ponicke, K., and Brodde, O. E. (1997). Age-dependent changes in cardiac muscarinic receptor function in healthy volunteers. J Am Coll Cardiol *29*, 187-193.

Proskocil, B. J., Sekhon, H. S., Jia, Y., Savchenko, V., Blakely, R. D., Lindstrom, J., and Spindel, E. R. (2004). Acetylcholine is an autocrine or paracrine hormone synthesized and secreted by airway bronchial epithelial cells. Endocrinology *145*, 2498-2506.

Rassadi, S., Krishnaswamy, A., Pie, B., McConnell, R., Jacob, M. H., and Cooper, E. (2005). A null mutation for the alpha3 nicotinic acetylcholine (ACh) receptor gene abolishes fast synaptic activity in sympathetic ganglia and reveals that ACh output from developing preganglionic terminals is regulated in an activity-dependent retrograde manner. J Neurosci *25*, 8555-8566.

Ribeiro, F. M., Alves-Silva, J., Volknandt, W., Martins-Silva, C., Mahmud, H., Wilhelm, A., Gomez, M. V., Rylett, R. J., Ferguson, S. S., Prado, V. F., and Prado, M. A. (2003). The hemicholinium-3 sensitive high affinity choline transporter is internalized by clathrin-mediated endocytosis and is present in endosomes and synaptic vesicles. J Neurochem *87*, 136-146.

Ribeiro, F. M., Black, S. A., Cregan, S. P., Prado, V. F., Prado, M. A., Rylett, R. J., and Ferguson, S. S. (2005). Constitutive high-affinity choline transporter endocytosis is determined by a carboxyl-terminal tail dileucine motif. J Neurochem *94*, 86-96.

Richardson, U. I., Liscovitch, M., and Blusztajn, J. K. (1989). Acetylcholine synthesis and secretion by LA-N-2 human neuroblastoma cells. Brain Res *476*, 323-331.

Rodriguez, C. I., Buchholz, F., Galloway, J., Sequerra, R., Kasper, J., Ayala, R., Stewart, A. F., and Dymecki, S. M. (2000). High-efficiency deleter mice show that FLPe is an alternative to Cre-loxP. Nat Genet *25*, 139-140.

Rouse, S. T., Thomas, T. M., and Levey, A. I. (1997). Muscarinic acetylcholine receptor subtype, m2: diverse functional implications of differential synaptic localization. Life Sci *60*, 1031-1038.

Rylett, R. J., Davis, W., and Walters, S. A. (1993). Modulation of high-affinity choline carrier activity following incubation of rat hippocampal synaptosomes with hemicholinium-3. Brain Res *626*, 184-189.

Saltarelli, M. D., Yamada, K., and Coyle, J. T. (1990). Phospholipase A2 and 3H-hemicholinium-3 binding sites in rat brain: a potential second-messenger role for fatty acids in the regulation of high-affinity choline uptake. J Neurosci *10*, 62-72.

Sandberg, K., and Coyle, J. T. (1985a). Characterization of [^{3}H]hemicholinium-3 binding associated with neuronal choline uptake sites in rat brain membranes. Brain Res *348*, 321-330.

Sanes, J. R., and Lichtman, J. W. (1999). Development of the vertebrate neuromuscular junction. Annu Rev Neurosci *22*, 389-442.

Sarter, M., and Bruno, J. P. (1997). Cognitive functions of cortical acetylcholine: toward a unifying hypothesis. Brain Res Brain Res Rev *23*, 28-46.

Schroeter, S., Apparsundaram, S., Wiley, R. G., Miner, L. H., Sesack, S. R., and Blakely, R. D. (2000). Immunolocalization of the cocaine- and antidepressant-sensitive l-norepinephrine transporter. J Comp Neurol *420*, 211-232.

Schueler, F. W. (1955). A new group of respiratory paralyzants. I. The "hemicholiniums". JPET *115*, 127-143.

Simon, J. R., Atweh, S., and Kuhar, M. J. (1976). Sodium-dependent high affinity choline uptake: a regulatory step in the synthesis of acetylcholine. J Neurochem *26*, 909-922.

Simon, J. R., and Kuhar, M. G. (1975). Impulse-flow regulation of high affinity choline uptake in brain cholinergic nerve terminals. Nature *255*, 162-163.

Simon, J. R., and Kuhar, M. J. (1976). High affinity choline uptake: ionic and energy requirements. J Neurochem *27*, 93-99.

Sipos, M. L., Burchnell, V., and Galbicka, G. (1999). Dose-response curves and time-course effects of selected anticholinergics on locomotor activity in rats. Psychopharmacology (Berl) *147*, 250-256.

Smith-White, M. A., Iismaa, T. P., and Potter, E. K. (2003). Galanin and neuropeptide Y reduce cholinergic transmission in the heart of the anaesthetised mouse. Br J Pharmacol *140*, 170-178.

Svedberg, M. M., Svensson, A. L., Bednar, I., and Nordberg, A. (2003). Neuronal nicotinic and muscarinic receptor subtypes at different ages of transgenic mice overexpressing human acetylcholinesterase. Neurosci Lett *340*, 148-152.

Tandon, R. (1999). Cholinergic aspects of schizophrenia. Br J Psychiatry Suppl, 7-11.

Thomsen, M., Woldbye, D. P., Wortwein, G., Fink-Jensen, A., Wess, J., and Caine, S. B. (2005). Reduced cocaine self-administration in muscarinic M5 acetylcholine receptor-deficient mice. J Neurosci *25*, 8141-8149.

Trabucchi, M., Cheney, D. L., Racagni, G., and Costa, E. (1975). In vivo inhibition of striatal acetycholine turnover by L-DOPA, apomophine and (plus)-amphetamine. Brain Res *85*, 130-134.

Tucek, S. (1985a). Regulation of acetylcholine synthesis in the brain. J Neurochem *44*, 11-24.

Vickroy, T. W., Roeske, W. R., Gehlert, D. R., Wamsley, J. K., and Yamamura, H. I. (1985). Quantitative light microscopic autoradiography of [3H]hemicholinium-3 binding sites in the rat central nervous system: a novel biochemical marker for mapping the distribution of cholinergic nerve terminals. Brain Res *329*, 368-373.

Vickroy, T. W., Roeske, W. R., and Yamamura, H. I. (1984). Sodium-dependent high-affinity binding of [3H]hemicholinium-3 in the rat brain: a potentially selective marker for presynaptic cholinergic sites. Life Sci *35*, 2335-2343.

Volpicelli-Daley, L. A., Duysen, E. G., Lockridge, O., and Levey, A. I. (2003a). Altered hippocampal muscarinic receptors in acetylcholinesterase-deficient mice. Ann Neurol *53*, 788-796.

Volpicelli-Daley, L. A., Hrabovska, A., Duysen, E. G., Ferguson, S. M., Blakely, R. D., Lockridge, O., and Levey, A. I. (2003b). Altered striatal function and muscarinic cholinergic receptors in acetylcholinesterase knockout mice. Mol Pharmacol *64*, 1309-1316.

Walker, J. K., Gainetdinov, R. R., Feldman, D. S., McFawn, P. K., Caron, M. G., Lefkowitz, R. J., Premont, R. T., and Fisher, J. T. (2004). G protein-coupled receptor kinase 5 regulates airway responses induced by muscarinic receptor activation. Am J Physiol Lung Cell Mol Physiol *286*, L312-319.

Wenk, G., Hepler, D., and Olton, D. (1984). Behavior alters the uptake of [3H]choline into acetylcholinergic neurons of the nucleus basalis magnocellularis and medial septal area. Behav Brain Res *13*, 129-138.

Wess, J. (2004). Muscarinic acetylcholine receptor knockout mice: novel phenotypes and clinical implications. Annu Rev Pharmacol Toxicol *44*, 423-450.

Whitehouse, P. J., Price, D. L., Struble, R. G., Clark, A. W., Coyle, J. T., and Delon, M. R. (1982). Alzheimer's disease and senile dementia: loss of neurons in the basal forebrain. Science *215*, 1237-1239.

Winkler, J., Suhr, S. T., Gage, F. H., Thal, L. J., and Fisher, L. J. (1995). Essential role of neocortical acetylcholine in spatial memory. Nature *375*, 484-487.

Wu, Y., Temple, J., Zhang, R., Dzhura, I., Zhang, W., Trimble, R., Roden, D. M., Passier, R., Olson, E. N., Colbran, R. J., and Andersen, M. E. (2002). Calmodulin kinase II and Arrhythmias in a Mouse Model of Cardiac Hypertrophy. Circulation *106*, 1288-1293.

Xie, W., Stribley, J. A., Chatonnet, A., Wilder, P. J., Rizzino, A., McComb, R. D., Taylor, P., Hinrichs, S. H., and Lockridge, O. (2000). Postnatal developmental delay and supersensitivity to organophosphate in gene-targeted mice lacking acetylcholinesterase. J Pharmacol Exp Ther *293*, 896-902.

Xu, W., Orr-Urtreger, A., Nigro, F., Gelber, S., Sutcliffe, C. B., Armstrong, D., Patrick, J. W., Role, L. W., Beaudet, A. L., and De Biasi, M. (1999). Multiorgan autonomic

dysfunction in mice lacking the beta2 and the beta4 subunits of neuronal nicotinic acetylcholine receptors. J Neurosci *19*, 9298-9305.

Yamamura, H. I., and Snyder, S. H. (1972). Choline: high-affinity uptake by rat brain synaptosomes. Science *178*, 626-628.

Yamamura, H. I., and Snyder, S. H. (1973). High affinity transport of choline into synaptosomes of rat brain. J Neurochem *21*, 1355-1374.

Yu, W., Mackey, L., Xu, W., Beaudet, A., and De Biasi, M. (2000). Bradycardia and ventricular repolarization defects in mice lacking the alpha3 subunit of neuronal nicotinic acetylcholine receptors. Lester R, editor The 10th neuropharmacology conference: neuronal nicotinic receptors *New Orleans: Elsevier Science*.

Zahalka, E. A., Seidler, F. J., Lappi, S. E., Yanai, J., and Slotkin, T. A. (1993). Differential development of cholinergic nerve terminal markers in rat brain regions: implications for nerve terminal density, impulse activity and specific gene expression. Brain Res *601*, 221-229.

Zhou, F. M., Liang, Y., and Dani, J. A. (2001). Endogenous nicotinic cholinergic activity regulates dopamine release in the striatum. Nature Neurosci *4*, 1224-1229.

Zhou, F. M., Wilson, C., and Dani, J. A. (2003). Muscarinic and nicotinic cholinergic mechanisms in the mesostriatal dopamine systems. Neuroscientist *9*, 23-36.

Zhu, C. B., Hewlett, W. A., Feoktistov, I., Biaggioni, I., and Blakely, R. D. (2004). Adenosine receptor, protein kinase G, and p38 mitogen-activated protein kinase-dependent up-regulation of serotonin transporters involves both transporter trafficking and activation. Mol Pharmacol *65*, 1462-1474.